NOAA Technical Memorandum GLERL-179
DOI: 10.25923/2hy2-ca15

Development of Coupled Hydrologic-Hydrodynamic-Wave Flood Forecasting System for Lake Champlain

D. Beletsky[1], D. Titze[1], J. Kessler[2], L. Mason[2], L. Fry[2], L. Read[3], W. Saunders[4], P. Y. Chu[2], J. Feyen[2], D. Lee[2], J. G. W. Kelley[5], Yi Chen[5] and A. van der Westhuysen[6]

[1] Cooperative Institute for Great Lakes Research, University of Michigan
[2] NOAA Great Lakes Environmental Research Laboratory
[3] National Corporation for Atmospheric Research
[4] NOAA NWS Northeast River Forecast Center
[5] NOAA NOS Office of Coast Survey Coast Survey Development Laboratory
[6] NOAA NWS NCEP Environmental Modeling Center

December 27, 2022

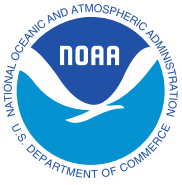

UNITED STATES
DEPARTMENT OF COMMERCE

Gina M. Riamondo
Secretary

NATIONAL OCEANIC AND
ATMOSPHERIC ADMINISTRATION

Dr. Richard W. Spinrad
Administrator

TABLE OF CONTENTS

Abstract **6**

1 Introduction **8**

2 Description of Forecast Models **12**

2.1 Topobathymetric grid development 12

2.2 Hydrodynamic Model (FVCOM) 15

2.3 Wave Model (WAVEWATCH III) 15

2.4 FVCOM-WAVEWATCH III coupling 16

3 National Water Model (NWM) Development and Assessment for the Lake Champlain Basin **16**

3.1 Hydrologic model: NWM 16

3.2 Hydrofabric development for NWM 17

3.3 NWM hindcast validation 18

4 Lake Champlain Model Forcing **21**

4.1 Wind, Overlake Precipitation, Ice 21

4.2 Inflows (NWM) 22

4.3 Outflow (ECCC) 25

4.4 Meteorological and Hydrological Forcing Accuracy Assessment 26

4.4.1 HRRR/GFS 26

4.4.2 National Water Model 28

5 Lake Champlain Model Calibration, Testing, and Skill Assessment **33**

5.1 Observations (Water Level, Waves) 33

5.2 FVCOM 35

5.2.1 Bottom Roughness 35

5.2.2 Storm Surges 36
5.2.3 NWM Coupling 37
5.2.4 Handling Ponding Effects 38
5.2.5 Water Level Nudge 38
5.2.6 Water Level Skill Assessment 39
5.2.7 Baroclinic Temperature Testing 52
5.3 WAVEWATCH III 55
5.3.1 Coupling with FVCOM Water Levels 55
5.3.2 Sensitivity to Water Currents 55
5.3.3 Incorporating Ice Cover 58
5.3.4 Implicit/Explicit Solver Testing 61
5.3.5 Skill Assessment at Buoy 64
6 Nowcast/Forecast System Description 67
6.1 Workflow 67
6.2 Backup forcing 68
7 Future plans 69
7.1 WAVEWATCH III Operational Transition 69
7.2 FVCOM Operational Transition 70
8 Conclusions 71
9 Acknowledgements 72
10 References 72
APPENDIX 75

LIST OF FIGURES

Figure 1.1 Lake Champlain watershed 10

Figure 1.2 Lake Champlain bathymetry (feet)..... 11

Figure 2.1 Lake Champlain FVCOM/WAVEWATCH III grid 13

Figure 2.2 Example of floodplain coverage in Lake Champlain grid (Burlington, VT area)..... 14

Figure 3.1 National Water Model tributary network extent for version 2.0 (a) and version 2.1 (b). 17

Figure 3.2 Map of USGS gages used for validation overlaid on NWM stream network. 19

Figure 3.3 Boxplots showing skill metrics for all gages in the Lake Champlain watershed. 19

Figure 3.4 Scatter plots showing skill metrics for each gage in the Champlain watershed throughout the 3 year hindcast simulation. For each metric, a majority of the stations show improvement (indicated by shaded regions) from NWM 2.0 to 2.1. 20

Figure 3.5 Seasonal correlation based on all gages in the Champlain watershed..... 20

Figure 4.1 Locations of modeled Lake Champlain inflows. 22

Figure 4.2 Locations of Lake Champlain water level gauges. 25

Figure 4.3 Location of FEMC (triangles) and NDBC (circles) wind observations in Lake Champlain 27

Figure 4.4 Rivers used in National Water Model version 2.1 skill assessment. 29

Figure 4.5 National Water Model version 2.1 nowcast skill assessment results. 30

Figure 4.6 National Water Model version 2.1 forecast skill assessment results..... 31

Figure 5.1 Location of Waverider buoy in 2021..... 34

Figure 5.2 Significant wave height observations (ft) in Lake Champlain during one week in 2021; Waverider data. 35

Figure 5.3 FVCOM bottom roughness calibration results. 35

Figure 5.4 Comparison of FVCOM water level results with and without wind forcing 36

Figure 5.5 Locations of USGS and ECCC water-level gauges used to evaluate Lake Champlain water level nowcasts and forecast guidance. 42

Figure 5.6 Surface weather map valid at 7 AM EST, July 18, 2021. Green indicates areas of precipitation. 44

Figure 5.7 Surface weather map valid at 7 AM EST, October 31, 2021. Green indicates regions of precipitation. 44

Figure 5.8 Time series plots of hourly Lake Champlain nowcasts of water level (red) vs. observations (black, converted to NAVD88 (ft)) at USGS and ECCC gauges (From north to south: 1. Philipsburg, QC, ECCC, 2. Rouses Point, NY, USGS, 3. Burlington, VT, USGS, 4. Po 45

Figure 5.9 Time series plots of hourly Lake Champlain nowcasts of water level (red) vs. observations (blue) referenced to model datum of 95.1184 ft at the USGS gauge at Whitehall, NY from March 11 (Day 70) to March 21 (Day 80) in 2021. 46

Figure 5.10 Same as Fig. 5.9 but for the period from March 31 (Day 90) to April 10 (Day 100) in 2021..... 46

Figure 5.11 Same as Fig. 5.9 but for the period from May 20 (Day 140) to June 4 (Day 155) in 2021..... 47

Figure 5.12 Time series plots of hourly Lake Champlain nowcasts of water level (red) vs. observations (blue) referenced to model datum of 95.1184 ft at the ECCC gauge at Philipsburg, QC from March 11 (Day 70) to March 21 (Day 80) in 2021. 47

Figure 5.13 Same as Fig. 5.12 but for the period from March 31 (Day 90) to April 10 (Day 100) in 2021. 48

Figure 5.14 Same as Fig. 5.12 but for the period from but for the period from May 20 (Day 140) to June 4 (Day 155) in 2021..... 48

Figure 5.15 Water level MAE or bias (in, negative values gray, positive values red) by forecast projections at USGS and ECCC gauges (From north to south: 1. Philipsburg, QC, ECCC, 2. Rouses Point, NY, USGS, 3. Burlington, VT, USGS, 4. Port Henry, NY, USGS, and 5. Whitehall, NY, USGS), Lake Champlain during 2021. 51

Figure 5.16 Same as Fig. 5.15 but for water level RMSE (in, blue) by forecast projections. 51

Figure 5.17 FVCOM thermal structure results using bathymetry with reduced depth-variability. 52

Figure 5.18 FVCOM thermal structure results at Valcour Island using a high-resolution grid. .. 53

Figure 5.19 Sensitivity of modeled wave heights to water currents at the location of NDBC Buoy 45166 (difference between model runs with and without current forcing). 55

Figure 5.20 Spatial differences in sensitivity of modeled wave heights to water currents (runs with and without current forcing). 56

Figure 5.21 Creating ice forcing from an ice mask. 58

Figure 5.22 Influence of ice forcing on modeled wave height results. 59

Figure 5.23 WAVEWATCH III explicit and implicit solver convergence. 61

Figure 5.24 WAVEWATCH III model configuration optimization. 62

Figure 5.25 Skill assessment of modeled wave height. 64

Figure 5.26 Skill assessment of modeled wave direction. 65

Figure 5.27 Skill assessment of modeled wave period. 66

LIST OF TABLES

Table 4.1 List of National Water Model inflow features to Lake Champlain. 23

Table 4.2 Rivers used in National Water Model version 2.1 nowcast and forecast skill assessment. 28

Table 5.1 Description of NOS skill assessment statistics (Modified from Hess et al., 2003) along with NOS Acceptance Criterion (targets) used to evaluate nowcasts and forecast guidance. 41

Table 5.2 Information on USGS and ECCC stations whose water level observations were used to evaluate the Lake Champlain nowcasts and forecasts. 43

Table 5.3 Summary of skill assessment statistics evaluating the ability of the Lake Champlain nowcasts to predict hourly water levels at USGS and ECCC gauges in Lake Champlain during 2021. Gray shading, if present, indicates that it did not meet the NOS acceptance criteria. 49

Table 6.1 Backup forcing methods. 68

ABSTRACT

Lake Champlain is a binational lake bordered by New York on the west side, Vermont on the east side, and Quebec in the north. In recent years, severe floods caused by intense rain events and spring runoff caused significant destruction of property and infrastructure in the Lake Champlain Basin. In addition, high lake water levels provided conditions for more shoreline destruction by wind waves and storm surges that build over the long north-south fetch of the lake. In 2016, the International Joint Commission began a $14M, 5-Year study to explore solutions to flooding in the binational Lake Champlain-Richelieu River system. The study was prompted by the record flood of 2011. To improve predictions of future flood events, a flood forecasting system was developed for the Lake Champlain-Richelieu River basin. The system resolves river- and wind-driven spatial variability in water levels, surface waves, and the associated extent of coastal inundation, thus improving upon an existing one-dimensional model that is currently used for forecasting by the NWS Northeast River Forecast Center (NERFC). The modeling framework couples the National Water Model (NWM) configuration of the Weather Research and Forecasting-Hydrologic distributed model (WRF-Hydro) with a hydrodynamic model, the Finite Volume Community Ocean Model (FVCOM). For accurate prediction of water level in Lake Champlain, NWM domain was expanded across the Richelieu River portion of the Lake Champlain basin. A moderate-resolution hydrofabric was developed based on the NHDPlus V2 dataset (1:100,000 scale) and was included in version 2.1 of the NWM.

The horizontal resolution of the Champlain FVCOM model ranges from 160 to 1300 ft. The model grid has 61,355 triangular grid elements, and covers Lake Champlain, upper Richelieu River, and a portion of the floodplain. The model has 20 vertical levels uniformly distributed over the water column. The model is currently run in a 3D barotropic mode without temperature or ice predictions, driven by meteorological forcing (wind and overlake precipitation), river flows, and a single outflow (Richelieu River). The real-time prediction version of the FVCOM-based lake modeling system uses the NWS High-Resolution Rapid Refresh (HRRR) model's winds and precipitation in a nowcast mode. In the forecast mode, HRRR output is used in the first 48 hours, followed by NWS Global Forecast System (GFS) forecast guidance for the rest of the 5-day forecast period. National Water Model output is used as input inflows to FVCOM. 73 NWM features are combined and applied at 14 river inflow points. Water level observations at the St. Jean, Quebec (QC) Environment and Climate Change Canada (ECCC) gauge are used as downstream boundary conditions. In addition, a spatially-uniform water level adjustment is used in the nowcast mode to keep water level aligned with observations. Water level data for this nudging are provided by 5 United States Geological Survey (USGS) or ECCC gauges. Nowcasts and forecast guidance from the real-time Lake Champlain modeling system show strong agreement with water level observations.

As part of the real-time Lake Champlain modeling system, wind waves in the lake are predicted by a new NOAA WAVEWATCH III wave model, with wetting/drying in floodplain areas informed by FVCOM. Model grid and wind forcing (HRRR and GFS) is identical to that of driving FVCOM. The wave model was calibrated and validated with observations collected at

two wave buoys deployed in different parts of the lake in 2020 and 2021. An experimental real-time application of the coupled flood forecasting system began operation in 2020 at NOAA's Great Lakes Environmental Research Laboratory (GLERL) and the system exhibited a high level of robustness and skill during two years of operations.

1 INTRODUCTION

Lake Champlain is a binational lake bordered by New York on the west side, Vermont on the east side, and Quebec to the north (Fig.1.1). Lake Champlain has a length of approximately 125 mi, maximum width of 13 mi, maximum depth of 400 ft (Fig. 1.2) but an average depth of only 62 ft (Manley et al., 1999). Lake Champlain is traditionally divided into different sections: the Main Lake, the Restricted Arm in the northeast portion of the lake, and the riverine South Lake (Myer and Gruendling, 1979). In the Restricted Arm narrow causeways separate several smaller sub-basins and restrict water exchange with the Main Lake. The hydraulic residence time of Lake Champlain is 2.2 years (Shanley and Denner, 1999).

The Lake Champlain watershed is 8,234 mi^2, about 19 times larger than the lake area. About 84% of the watershed is in the US and 16% is in Canada. The U.S. portion of the watershed contains the headwaters and is mountainous (with New York's Adirondack Mountains on the western shore and Vermont's Green Mountains on the eastern shore) while the low-lying Canadian portion is relatively flat. Eleven major rivers (watershed areas > 100 mi^2) and 19 smaller rivers route runoff to the lake. Lake Champlain itself drains north into the Richelieu River across Quebec to the St. Lawrence River.

The lake level fluctuates 3 to 6 ft around the mean lake level (96.5 feet NGVD 29) during its seasonal cycle with the minimum typically occurring in the fall and maximum in spring driven by runoff. Large, mountainous, flashy watersheds that store significant snowpack combined with a relatively small lake volume make the Lake Champlain shoreline conducive to flooding after severe precipitation and/or snowmelt events, especially in the northern low-lying areas. The long north/south fetch of the lake makes possible the development of wind waves that can reach 10 ft during major storms. In addition, the combination of long fetch with small mean depth leads to substantial storm surges (up to 1 foot) and seiches with a period of 4 hours (Hunkins et al., 1998, 1999).

The lake is covered by ice during winter and is thermally stratified from May to October. Stratification leads to existence of large internal seiches (up to 100 ft) in summer with a period of 4 days (Manley et al 1999), upwellings, coastal jets (Manley et al., 2012) and internal bores (Saylor et al 1999).

In recent years, severe floods caused by intense rain events and spring runoff caused significant destruction of property and infrastructure in the Lake Champlain Basin. The record flood of 2011 occurred from April 13 to June 19 (lasting 67 days) and was particularly damaging with 4,000 homes damaged in the U.S. and Canada, and total damages exceeding $110 million (80% of which were in QC; 20% were in NY and VT). Conditions leading to the 2011 flood included near-record snow melt and heavy spring rains. As a result of the high water levels, lake area increased by 12% (Bjerklie et al., 2014). Storm surges and waves led to even higher lake water levels and further damage. The Lake Champlain 2011 flooding resulted in a Reference issued by the US and Canada to the International Joint Commission (IJC) to study the flooding and make recommendations.

Currently, the NWS Northeast River Forecast Center (NERFC) produces deterministic forecasts for the lake based on a 1-D hydraulic Hydrologic Engineering Center-River Analysis System (HEC-RAS) model that does not account for effects of wind or waves along or across the lake. The objective of this project is to develop a real-time flood forecast modeling system for the Lake Champlain-Richelieu River basin. This system will generate operational flood forecasts for the Lake Champlain-Richelieu River (LCRR) system and enable the development of inundation mapping. This project is a part of the International Lake Champlain-Richelieu River Study, https://www.ijc.org/en/lcrr. The resultant LCRR flood forecast system will also support other forecast needs such as for recreational activities and search and rescue efforts. The flood modeling system will serve operational needs of the National Weather Service (NWS; includes Weather Forecast Office in Burlington and the Northeast River Forecast Center in Norton, MA). It will provide input, particularly water levels, for Canadian flood models of the Richelieu River to enable improved flood forecasting in Quebec.

The modeling framework consists of a hydrodynamic lake model, the Finite Volume Community Ocean Model (FVCOM), and a wind wave model based on the WAVEWATCH III model. The hydrodynamic model is driven by hydrologic runoff from the operational National Water Model (NWM) and meteorological forcing (wind and precipitation) that comes from operational NWS numerical weather prediction modeling systems: the HRRR (High-Resolution Rapid Refresh) model and the GFS (Global Forecast System) model. The same meteorological forcing is used by the wave model which is also informed by water levels predicted by the hydrodynamic model (one-way coupling). Throughout the model development process, the models' configuration was adjusted to meet operational requirements for accuracy, timeliness, and robustness.

The hydrodynamic modeling system was developed to be implemented in a manner similar to the Great Lakes Operational Forecast System (GLOFS, Anderson et al., 2010) that runs on NOAA's Weather and Climate Operational Supercomputing System (WCOSS). The resulting models were designed to provide real-time forecast guidance on a sub-daily basis of water levels, waves, and circulation. Following model calibration and validation, a pre-operational demonstration of the hydrodynamic forecast system was implemented at NOAA/GLERL in 2020 with output made available in real-time on GLERL's web site (https://www.glerl.noaa.gov/res/champlain). The forecast modeling system exhibited a high level of robustness during two years of operations.

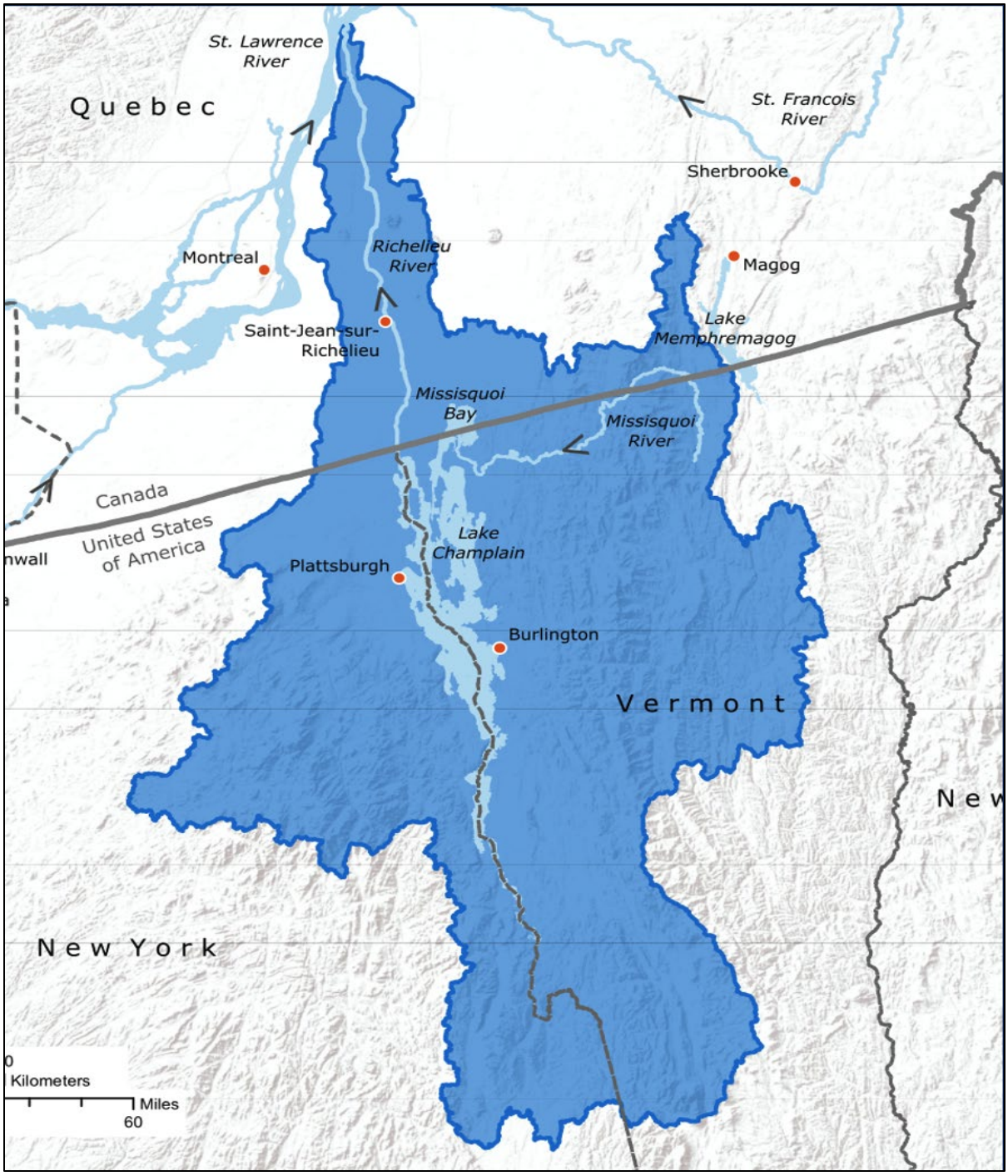

Figure 1.1 Lake Champlain watershed

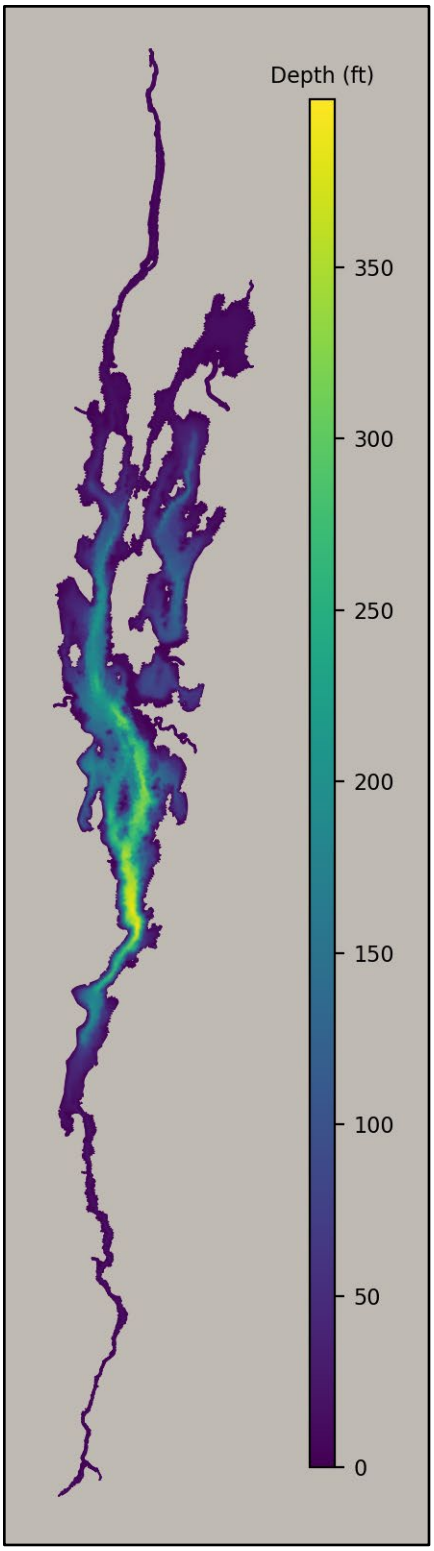

Figure 1.2 Lake Champlain bathymetry (feet)

2 DESCRIPTION OF FORECAST MODELS

2.1 TOPOBATHYMETRIC GRID DEVELOPMENT

The Lake Champlain-Richelieu River model domain covers Lake Champlain, the Upper Richelieu River (Fig. 2.1), and the surrounding floodplain (Fig 2.2). It extends southward to South Bay and the Poultney River at Whitehall NY, and extends northward to Fryers Rapids, just downstream of St Jean QC. The grid is unstructured, and is composed of interlocking triangular grid elements of variable size. The topobathymetric grid used in the Lake Champlain forecast modeling system was derived from the mesh developed by Environment Canada for their 2D hydrodynamic model of Lake Champlain, which is based on a Digital Elevation Model (DEM) compiled from various sources (ECCC 2015).

Due to the computational requirements of FVCOM and WAVEWATCH III, the grid used in the Lake Champlain forecast system was modified and downscaled from this original mesh. The original mesh contained 148,191 triangular elements, ranging in size to as small as a few feet. This was downscaled to a mesh containing 61,332 triangular elements, ranging in size from approximately 160 ft in dynamic coastal regions, to approximately 1300 ft in less-dynamic offshore areas. The grid resolves key morphological features in the domain, while remaining computationally feasible in a real time operational environment. The same unstructured grid is used in both the FVCOM and WAVEWATCH III models.

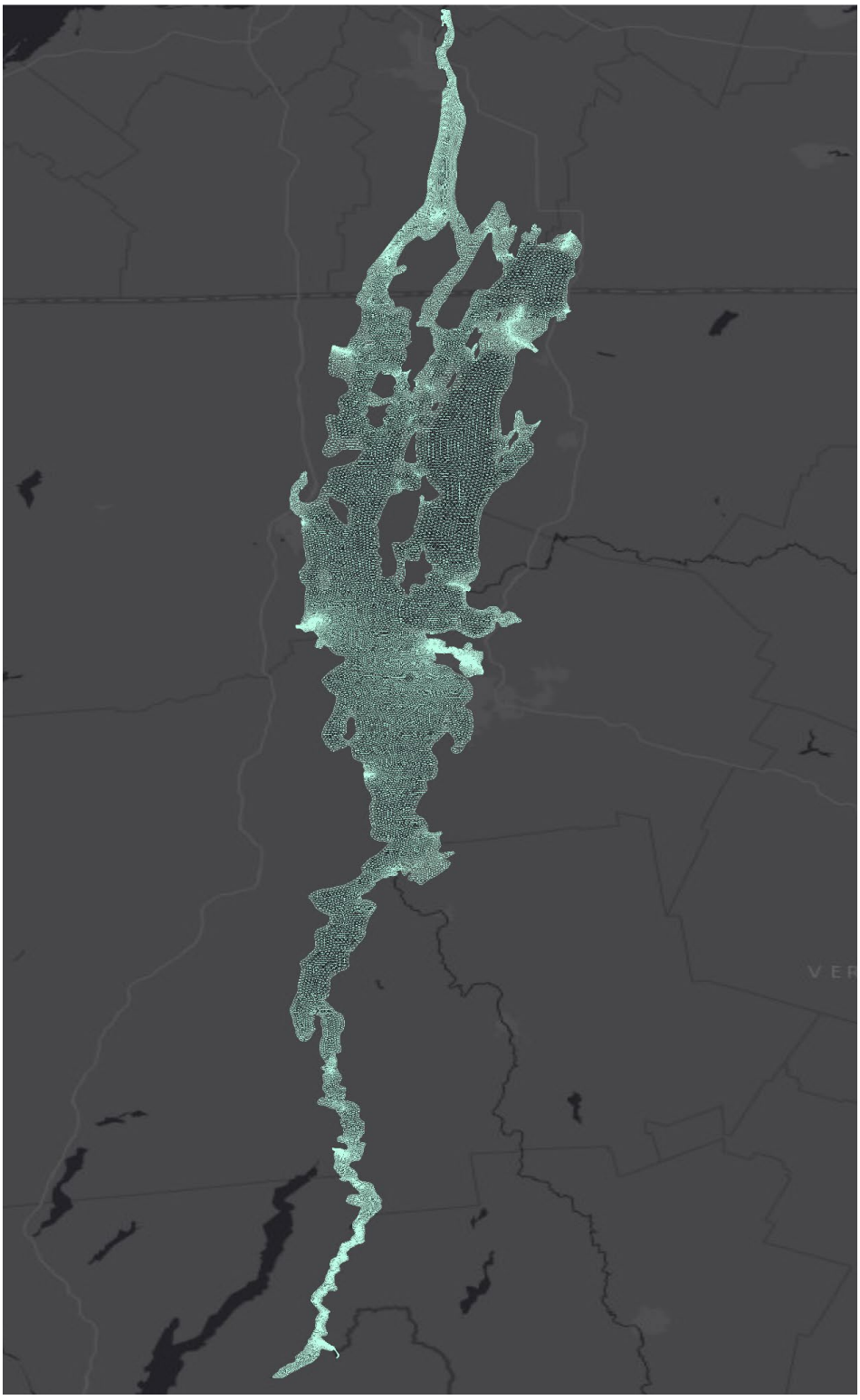

Figure 2.1 Lake Champlain FVCOM/WAVEWATCH III grid

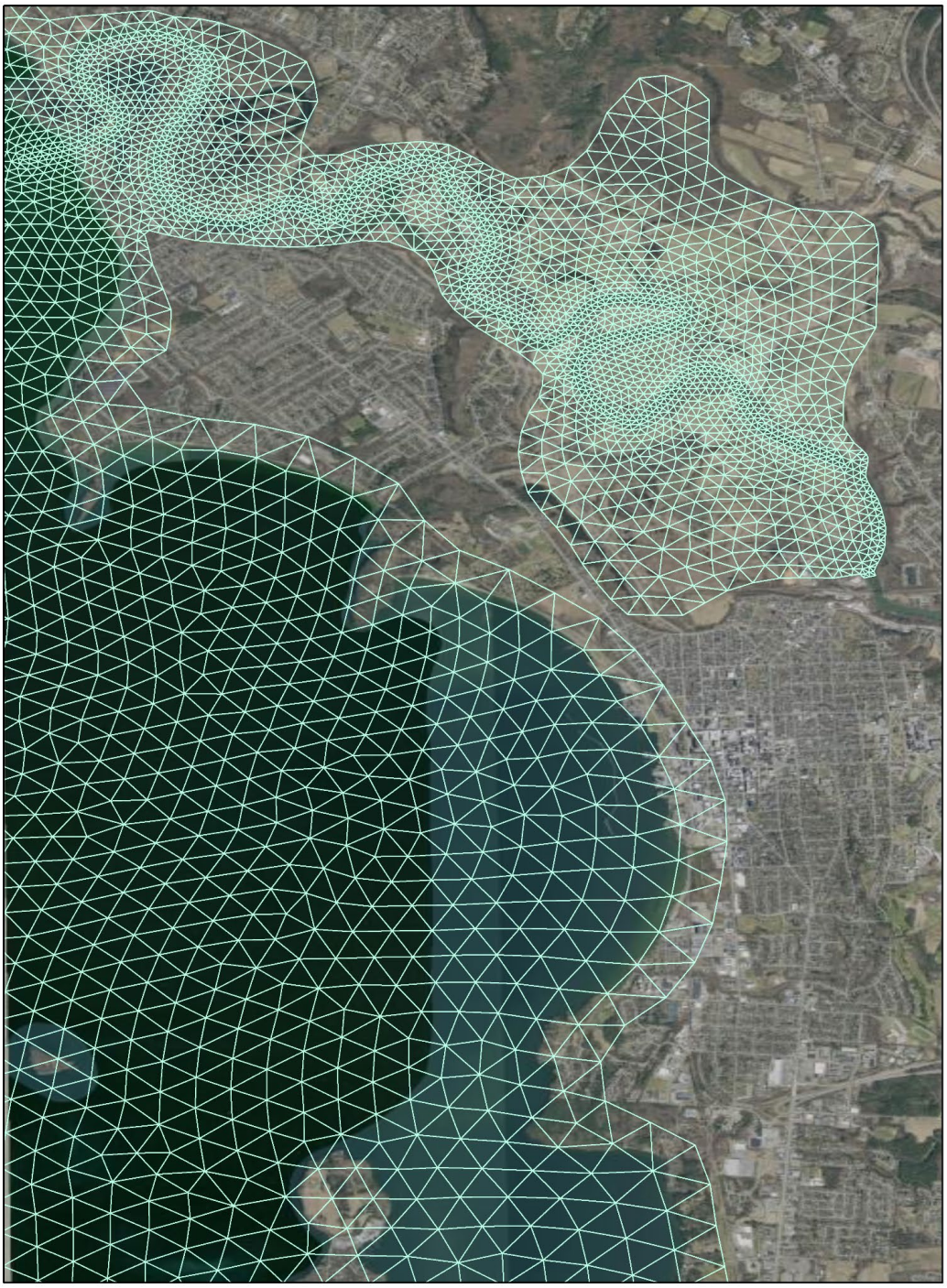

Figure 2.2 Example of floodplain coverage in Lake Champlain grid (Burlington, VT area)

2.2 HYDRODYNAMIC MODEL (FVCOM)

The state-of-the-art hydrodynamic model FVCOM (Chen et al., 2003) is used to predict water levels, wetting/drying areas and lake circulation. FVCOM is a 3D nonlinear Navier-Stokes, unstructured grid, hydrodynamic model with terrain following (sigma) vertical coordinates. The model has a free upper surface with barotropic (external) mode and baroclinic (internal) mode. Vertical turbulence submodel is based on Mellor-Yamada formulation (Mellor and Yamada, 1982). Horizontal turbulence is based on Smagorinsky (1963) formulation. FVCOM has wetting-drying capability which is important for accurate simulation of coastal flooding. Horizontal resolution of Champlain FVCOM ranges from 160 to 1300 ft. The model grid has 61,355 triangular grid elements, 32,709 vertices ("nodes") and covers Lake Champlain, upper Richelieu River, and a portion of the floodplain. The model has 20 vertical levels uniformly distributed over the water column.

The model is currently run as a real-time system using its 3D barotropic mode without ice, driven by meteorological forcing (wind and overlake precipitation), river flows, and single outflow (Richelieu River). The current version of the model uses HRRR winds and precipitation in the nowcast mode. For the forecast, HRRR output is used in the first 48 hours, followed by GFS output for the rest of the 5-day forecast period. National Water Model output is used as FVCOM input (inflows). 73 NWM features are combined and applied at 14 river inflow points. Water level observations at St. Jean, QC ECCC gauge are used as downstream boundary conditions. In addition, spatially-uniform water level adjustment is used in the nowcast mode to keep water level from drifting over time. Water level data for nudging are provided by 5 USGS/ECCC gauges. Time step in the external mode is 0.5 s, and 10 s in the internal mode.

2.3 WAVE MODEL (WAVEWATCH III)

The Lake Champlain forecast modeling system uses WAVEWATCH III version 6.07 to simulate surface gravity waves. WAVEWATCH III is a spectral wave model developed by NOAA/NCEP, which solves the spectral action wave balance equation. It can be run on an unstructured grid, and incorporates parameterization for coastal processes such as refraction and straining due to spatial variations in depth, as well as several growth and decay processes (W3DG 2019).

The Lake Champlain configuration of WAVEWATCH III is run in the unstructured mode using the implicit solver with a time step of 2 minutes. The model uses the same unstructured grid as FVCOM. The model is forced with spatially-variable wind, water level, and ice fields. Wind forcing is from HRRR for the nowcast, and a combination of HRRR (hours 0-48) and GFS (hours 48-120) for the forecast; this is the same source of wind forcing as used in the FVCOM model (Section 2.2). Water levels are variable in space and time, and are based on results of the FVCOM model through a one-way coupling setup (Section 2.4). Ice cover data is forced using a binary simple blocking parameterization, with ice coverage data from the NOAA National

Weather Service Weather Forecast Office in Burlington VT (Section 5.3.3). The model outputs instantaneous hourly results.

2.4 FVCOM-WAVEWATCH III COUPLING

Water level information for WAVEWATCH III is informed by the FVCOM hydrodynamic model through a one-way coupling setup. FVCOM water levels capture the effects of localized storm surges and flooding, in addition to the lake stage. By incorporating this water level information into WAVEWATCH III, the model will produce waves in these inundated areas, and provide critical information on the impacts that storm surges and flooding may have on floodplain areas.

This coupling process requires that FVCOM has first run to completion prior to initiating the corresponding WAVEWATCH III run. There is no feedback from WAVEWATCH III to FVCOM. After an FVCOM run is completed, water level results are then read and reformatted such that they can be ingested into the WAVEWATCH III model. Because FVCOM only produces valid water level results for areas that are wet in the model domain, water level forcing is conveyed to WAVEWATCH III for only these wet areas, with dry areas masked. These masked dry areas in the WAVEWATCH III water level forcing files are subsequently interpreted as dry land areas in the WAVEWATCH III wave model. Because FVCOM and WAVEWATCH III are run on the same unstructured mesh, no interpolation of water level or inundation results is necessary between FVCOM and WAVEWATCH III. Rather, water level data is being directly reformatted from an FVCOM output format to a WAVEWATCH III input format.

3 NATIONAL WATER MODEL (NWM) DEVELOPMENT AND ASSESSMENT FOR THE LAKE CHAMPLAIN BASIN

3.1 HYDROLOGIC MODEL: NWM

The National Oceanic and Atmospheric Administration's (NOAA) National Water Model (NWM) is a hydrological modeling framework that provides forecasts of hourly streamflow across a network of over 2.7 million reaches representing 3.4 million miles of rivers and streams across CONUS. The National Center for Atmospheric Research (NCAR) community Weather Research and Forecasting Hydrologic model (WRF-Hydro, https://ral.ucar.edu/projects/wrf_hydro/overview), configured to use the Noah-MP Land Surface Model (LSM) and separate routing models forms the core of the NWM. In spring of 2021, NWM v2.1 became operational. Among other upgrades, an important advancement for the Great Lakes in this version was the expansion of streamflow forecasts and data assimilation into the Canadian portion of the Great Lakes and Lake Champlain basins. That effort included the development of a hydrofabric that resolved data discontinuities across the border as well as calibration of the model at Canadian gaging stations. Streamflow predictions are now output operationally in the

Canadian portion of the Great Lakes and Lake Champlain basins. The expansion of this model to the full Lake Champlain basin allowed for inclusion of the forecasted contribution of runoff to Lake Champlain from the entire lake basin area.

3.2 HYDROFABRIC DEVELOPMENT FOR NWM

At the beginning of the LCRR Study, the operational version of the NWM version 2.0 did not include the Richelieu River portion of the basin (see Figure 3.1 below). Including the entirety of the basin in the hydrologic model was vital for accurate prediction of the basin's water budget and the corresponding water level in Lake Champlain. To address the need to support the flow of water across the system, the "hydrofabric", which is the geographic description of the land surface, streams, and corresponding data, was expanded to include the Richelieu River portion of the Lake Champlain basin. A moderate-resolution hydrofabric was developed based on the NHDPlus V2 dataset (1:100,000 scale) and was included in the most recent version of the NWM (version 2.1).

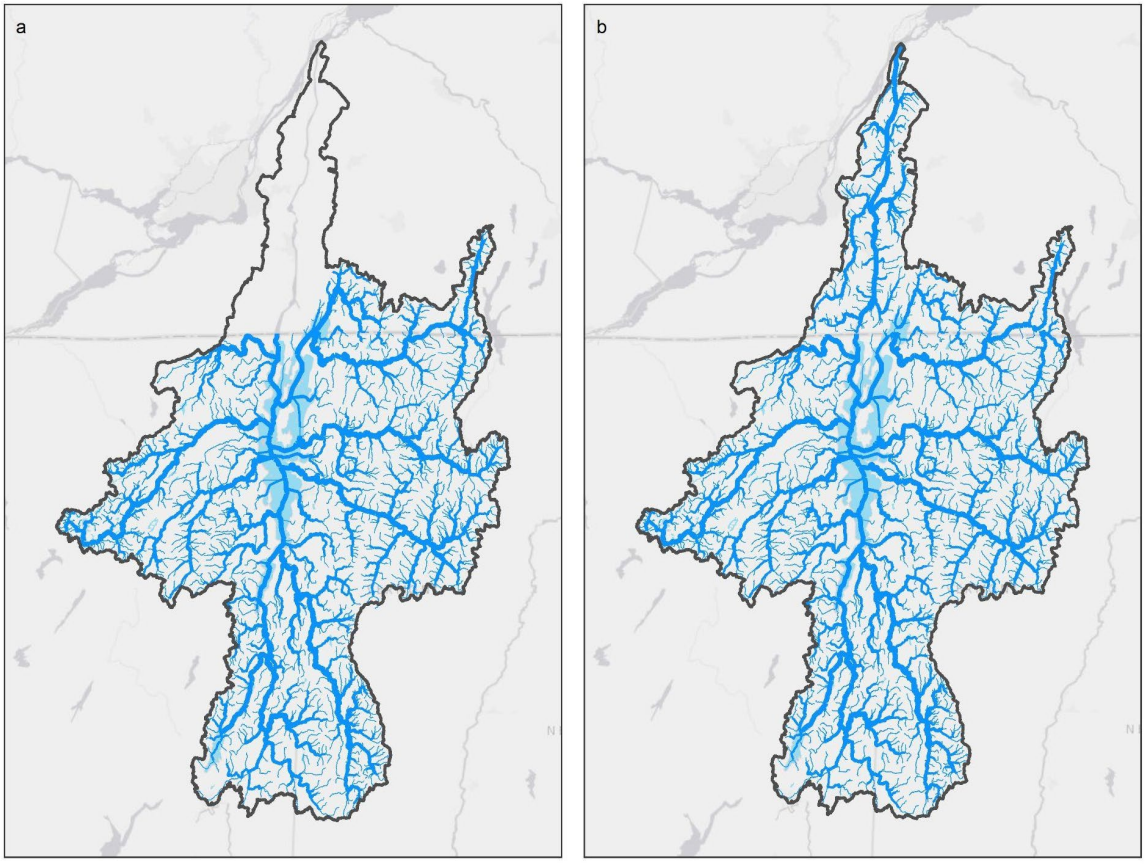

Figure 3.1 National Water Model tributary network extent for version 2.0 (a) and version 2.1 (b).

3.3 NWM HINDCAST VALIDATION

Although the National Water Model has been extensively validated and skill assessed at broad (e.g. CONUS, regional) scales [Gochis et al., 2019], skill in the Champlain watershed has not been specifically addressed, and was also required for the expansion into the Canadian portion of the basin. Section 4.4 includes skill assessment specific to Champlain for the NWM analysis and forecasts, which are heavily dependent on data assimilation and accurate atmospheric forecasts, respectively. Another means to validate the NWM skill is by conducting retrospective hindcasts which use the best available atmospheric data available but apply no data assimilation. This provides additional insight into model performance such as identifying systematic biases that are hidden by data assimilation.

Hindcast skill assessment for Champlain was conducted by closely following NCAR's skill assessment methodology: parallel NWM simulations using two versions of the model (v2.0 and v2.1) were run for only the Lake Champlain watershed for the period 2016-2018 at GLERL using the Analysis of Record for Calibration (AORC) atmospheric forcing, and the results evaluated against observations. The NWM team at NCAR was consulted extensively to confirm that the model version, configuration and inputs on GLERL's HPC matched that of the National Water Model's retrospective simulations.

Data from 34 USGS stream gages were available (see Figure 3.2) and three skill metrics were used to evaluate NWM skill at all 34 available gages for the hindcast: correlation coefficient, bias, and Nash-Sutcliffe Efficiency. Based on these three skill metrics, model skill was assessed for each year of simulation and also for each season (aggregated throughout the years).

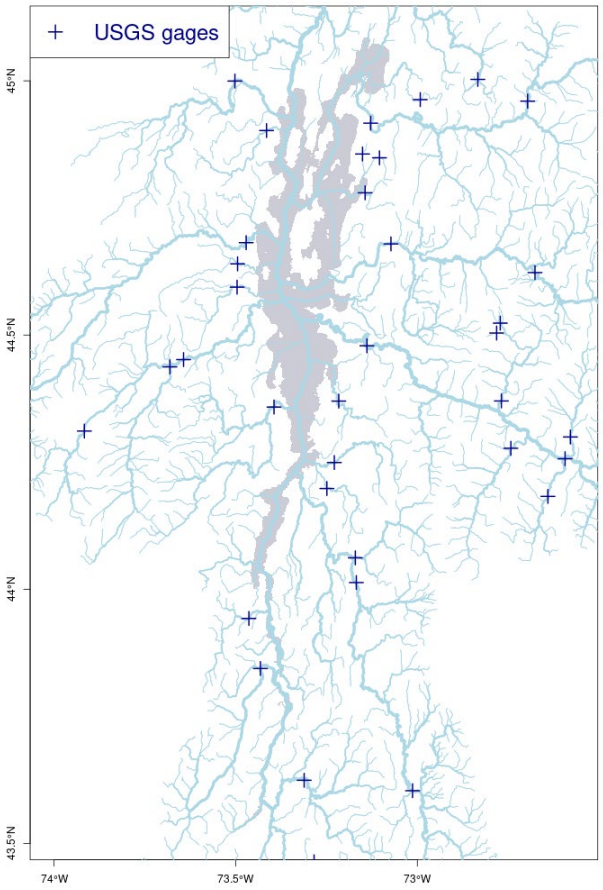

Figure 3.2 Map of USGS gages used for validation overlaid on NWM stream network.

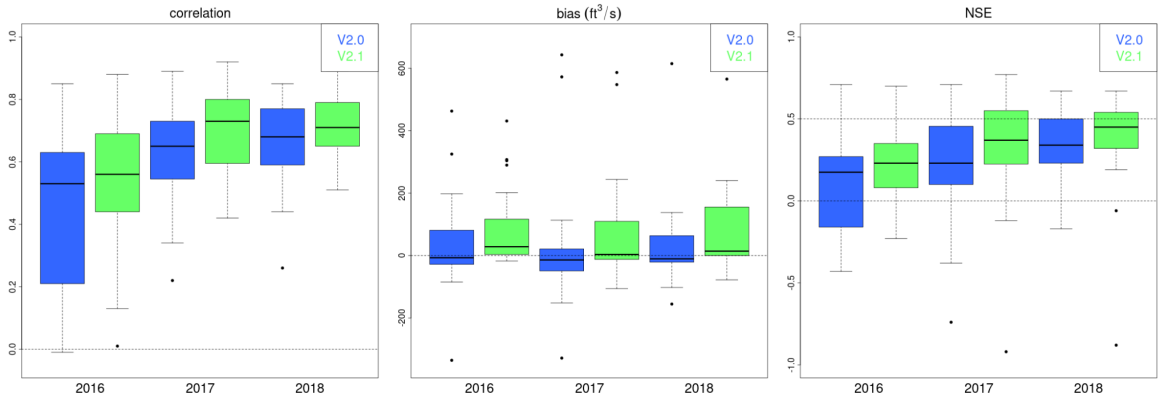

Figure 3.3 Boxplots showing skill metrics for all gages in the Lake Champlain watershed.

In general, NWM performed well in the Lake Champlain region for all three years with marginal to moderate improvement from 2.0 and 2.1. NWM version 2.1 had consistently higher streamflow when compared to version 2.0. The result was a decrease in the mean (absolute) bias during 2017 but actually changed the sign of mean bias for all three years. Correlation coefficient increased (from version 2.0 to 2.1) the most during Spring and Fall but showed little or marginal difference during Summer and Winter.

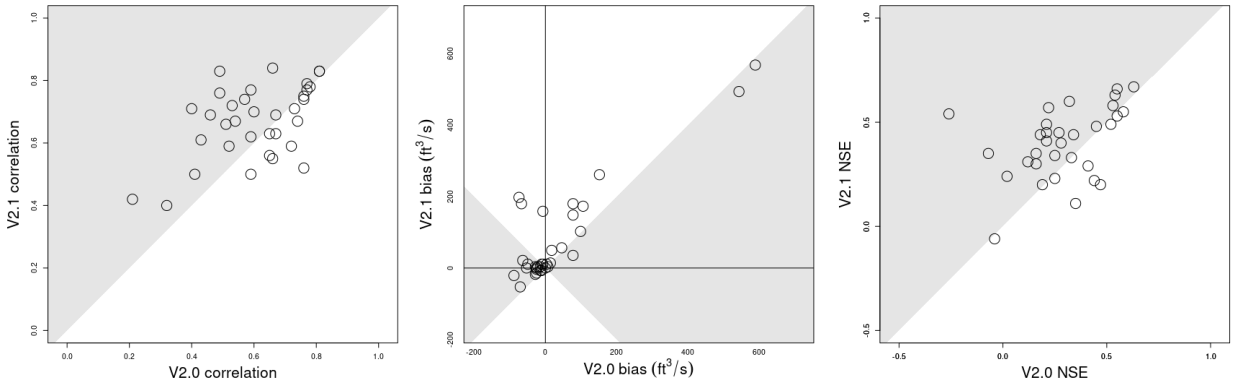

Figure 3.4 Scatter plots showing skill metrics for each gage in the Champlain watershed throughout the 3 year hindcast simulation. For each metric, a majority of the stations show improvement (indicated by shaded regions) from NWM 2.0 to 2.1.

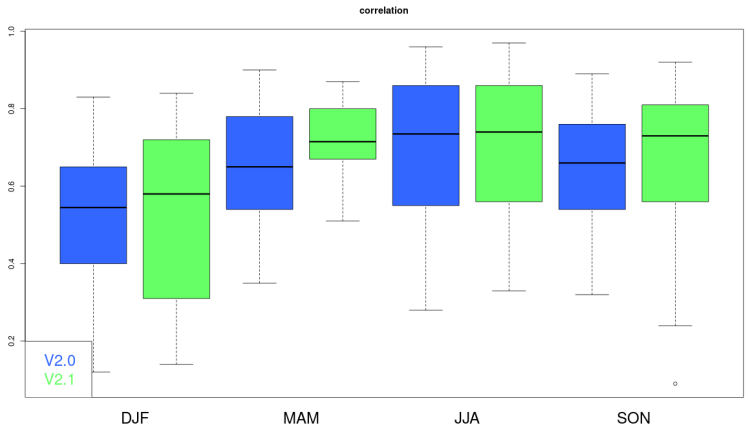

Figure 3.5 Seasonal correlation based on all gages in the Champlain watershed

4 LAKE CHAMPLAIN MODEL FORCING

4.1 WIND, OVERLAKE PRECIPITATION, ICE

Wind forcing (FVCOM and WAVEWATCH III) and overlake precipitation (FVCOM) is based on the output of two operational NOAA NWS National Centers for Environmental Prediction (NCEP) numerical weather prediction modeling systems (HRRR and GFS) linearly interpolated to FVCOM grid. HRRR (version 4) produced output each hour at 3 km (1.875 mi) horizontal resolution. HRRR time horizon is 48 hours and is available at the 00z, 06z, 12z, and 18z cycles. Hourly forcing during the remaining 3 days of the 5-day Lake Champlain forecast cycle is provided by the GFS model also available at the 00z, 06z, 12z, and 18z cycles. Horizontal resolution of the GFS model is 28 km (17.5 mi).

In addition to wind forcing, an ice mask with approximately 2.5 km (~1.6 mi) resolution is applied during WAVEWATCH III runs. The ice mask, produced by NWS Weather Forecast Office (WFO) Burlington, is manually drawn based on clear-sky satellite visual imagery. Data is updated based on availability of clear-sky satellite images (may be multiple weeks between updates). Coverage must be persisted from the previous update until the next update. Data spatial coverage consists of the Main Lake and Restricted Arm and is extrapolated to South Lake and Upper Richelieu River since they are not covered. Ice cover data is binary, showing either presence or absence of ice.

4.2 INFLOWS (NWM)

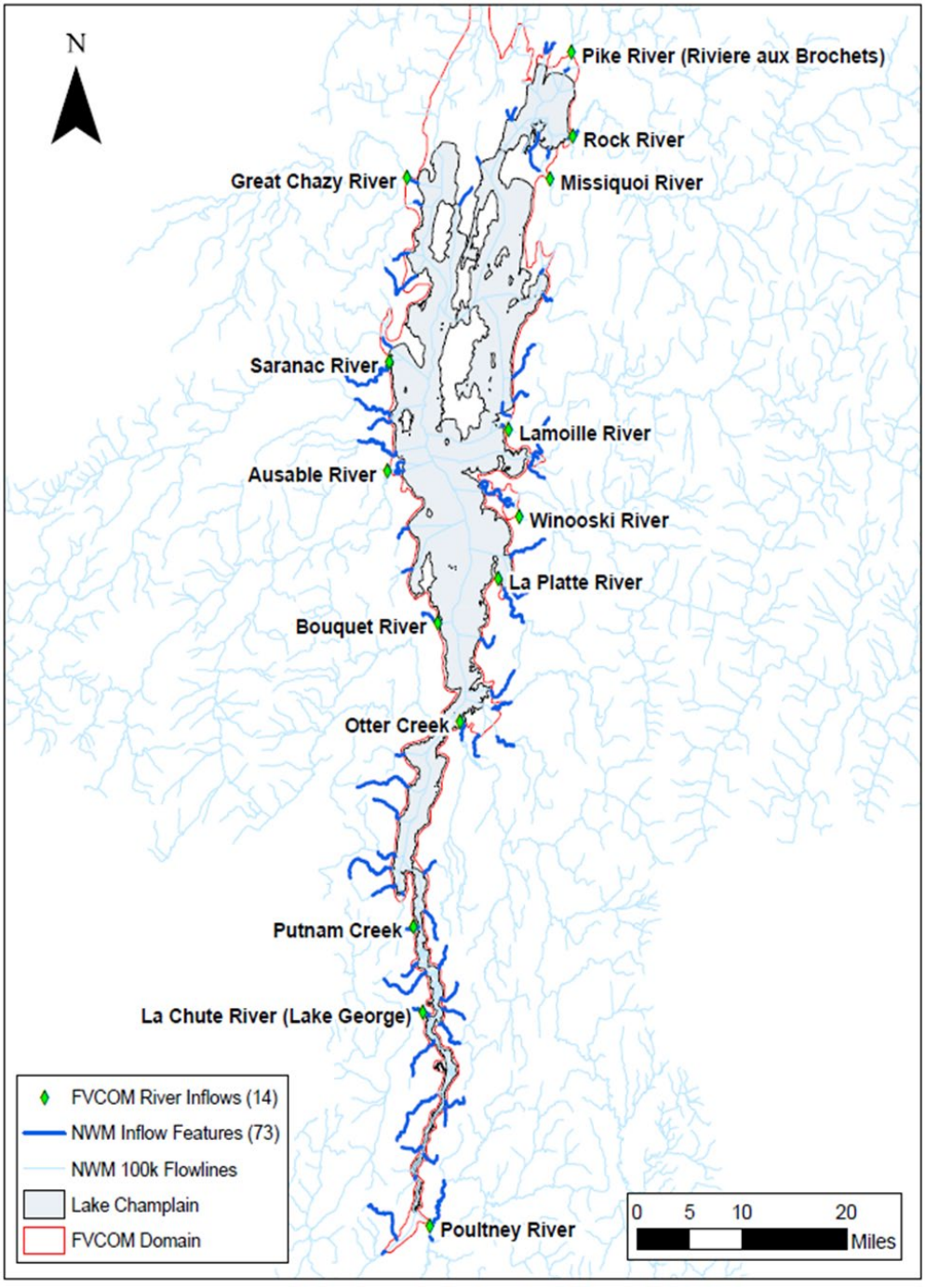

Figure 4.1 Locations of modeled Lake Champlain inflows.

Table 4.1 List of National Water Model inflow features to Lake Champlain.

	Forecast System River ID	NWM Feature ID	NWM Inflow Longitude (ºE)	NWM Inflow Latitude (ºN)	River Name
1	AllenBrk	4587138	-73.16833	44.57550	Allen Brook
2	AusableRiv	9527431	-73.42271	44.56652	Ausable River
3	AusableRivS	9527403	-73.42315	44.55597	Ausable River South
4	BayofVeniceEastTrb	1020000701	-73.13220	45.10017	Unnamed Tributary to Bay of Venice (East)
5	BayofVeniceWestTrb	1020000700	-73.13220	45.10017	Unnamed Tributary to Bay of Venice (West)
6	BeadlesCoveTrb	10312294	-73.36885	43.84945	Unnamed Tributary to Beadles Cove
7	BensonLandingTrb	10312348	-73.36724	43.72908	Unnamed Tributary near Benson Landing
8	BouquetRiv	9528451	-73.35851	44.35545	Bouquet River
9	BraistedBrk	10312266	-73.39910	43.97850	Braisted Brook
10	BrownsBayTrb	10312366	-73.36897	43.72041	Unnamed Tributary to Browns Bay
11	BulwaggaBaySouthTrb	10311432	-73.44266	44.00343	Unnamed Tributary to Bulwagga Bay
12	CarmanBrk	4590969	-73.09134	44.98722	Carman Brook
13	ChamplainCnl	10312474	-73.40081	43.55178	Champlain Canal
14	ChapmanBayEastTrb	1020000778	-73.19932	45.01334	Unnamed Tributary to Chapman Bay (East)
15	ChapmanBayWestTrb	1020000779	-73.19932	45.01334	Unnamed Tributary to Chapman Bay (West)
16	CharterBrk	10312338	-73.38495	43.80862	Charter Brook
17	DeadCrk	9521435	-73.44314	44.71776	Dead Creek
18	DresdenTrib	10312396	-73.41182	43.66933	Unnamed Tributary near Dresden
19	EastCrk	10312708	-73.37548	43.82885	East Creek
20	FivemileCrk	10312610	-73.39809	43.89710	Fivemile Creek
21	GrantBrk	10312602	-73.41454	43.91001	Grant Brook
22	GreatChazyRiv	9521381	-73.38544	44.93231	Great Chazy River
23	GroveBrk	10311328	-73.45413	44.01373	Grove Brook
24	GuayCrk	9521139	-73.40642	44.84100	Guay Creek
25	HandsCoveTrb	10312608	-73.37150	43.86312	Unnamed Tributary to Hands Cove
26	HoisingtonBrk	10311306	-73.43322	44.18485	Hoisington Brook
27	HolmesCrk	4578778	-73.28246	44.33317	Holmes Creek
28	HortonBrk	10312408	-73.41002	43.65979	Horton Brook
29	IndianBrk	4587154	-73.17335	44.57031	Indian Brook
30	JewettBrk	4587228	-73.15176	44.81022	Jewett Brook
31	KimballBrk	4578822	-73.26325	44.26539	Kimball Brook
32	LaChuteRiv	10312290	-73.39494	43.84012	La Chute River
33	LaPlatteRiv	4578818	-73.23439	44.39903	La Platte River
34	LamoilleRiv	4588694	-73.23251	44.61380	Lamoille River
35	LamoilleRivN	4587322	-73.22919	44.64304	Lamoille River North
36	LewisCrk	22220497	-73.26201	44.24153	Lewis Creek
37	LittleAusableRiv	9527387	-73.43827	44.58123	Little Ausable River
38	LittleChazyRiv	9521393	-73.38067	44.90392	Little Chazy River

39	LittleOtterCrk	22220501	-73.25446	44.20487	Little Otter Creek
40	LittleTroutBrk	9527909	-73.41640	44.48165	Little Trout Brook
41	McKenzieBrk	10311368	-73.46072	44.03505	McKenzie Brook
42	MillBayBrk	10312380	-73.38225	43.73690	Mill Bay Brook
43	MillBrk	10311316	-73.45303	44.05045	Mill Brook
44	MillRiv	4587100	-73.14699	44.78315	Mill River
45	MissisquoiRiv	166176983	-73.14899	44.99572	Missisquoi River
46	MissisquoiRivS	4590951	-73.13125	44.97297	Missisquoi River South
47	MudCrk	4587300	-73.26362	44.95615	Mud Creek
48	MullenBrk	10311360	-73.44507	44.09988	Mullen Brook
49	MunroeBrk	4578768	-73.22305	44.40716	Munroe Brook
50	OtterCrk	22220529	-73.32468	44.22552	Otter Creek
51	PikeBrk	10312688	-73.46321	43.54791	Pike Brook
52	PikeRiv	1020000728	-73.09384	45.07490	Pike River
53	PikeRivTrb	1020000727	-73.09384	45.07490	Unnamed Tributary to Pike River
54	PineLakeBrk	932010003	-73.42526	43.63187	Pine Lake Brook
55	PondBrk	4587142	-73.17300	44.57413	Pond Brook
56	PotashBrk	4578758	-73.22020	44.43880	Potash Brook
57	PoultneyRiv	10312692	-73.40028	43.56888	Poultney River
58	PutnamCrk	10312706	-73.41042	43.95771	Putnam Creek
59	RileyBrk	9521343	-73.39302	44.81176	Riley Brook
60	RockRiv	4590933	-73.08378	44.98910	Rock River
61	SalmonRiv	9527383	-73.44876	44.62848	Salmon River
62	SaranacRiv	9521459	-73.44623	44.69981	Saranac River
63	SilverStm	9527301	-73.44619	44.62162	Silver Stream
64	SouthBayCrk	10312504	-73.48466	43.53289	South Bay Creek
65	SouthSlangCrk	22220373	-73.28922	44.20833	South Slang Creek
66	StacyBrk	10311358	-73.42626	44.14075	Stacy Brook
67	StoneBridgeBrk	4587112	-73.20906	44.67520	Stony Bridge Brook
68	StonyCoveTrb	10312278	-73.37453	43.90197	Unnamed Tributary to Stony Cove
69	SuckerBrk	4587090	-73.30555	44.90286	Sucker Brook
70	TroutBrk	4587122	-73.20924	44.64404	Trout Brook
71	WardsCrk	10311402	-73.39973	44.02784	Wards Creek
72	WillsboroBayWestTrb	9527945	-73.41024	44.42660	Unnamed Tributary to Willsboro Bay
73	WinooskiRiv	4576956	-73.27342	44.53089	Winooski River

River inflows to the FVCOM hydrodynamic model are forced using output from the operational version 2.1 of the National Water Model (NWM). Rivers are forced as volumetric flow rates in FVCOM on the edges of cells at the boundary of the domain. A combination of NWM output

from the analysis model (nowcast), short-range forecast (18-hour horizon), and medium-range forecast (10-day horizon) are used to force the FVCOM nowcast/forecast system. The NWM uses data assimilation methods to incorporate observations from available flow gauges throughout the basin into the analysis model.

All 73 NWM inflows into Lake Champlain are incorporated into the FVCOM model (Figure 4.1, Table 4.1). Because many of these inflows are too small to be spatially resolved in the model, inflows are aggregated and applied at 14 fully-resolved major inflow points at the edge of the model domain. A skill assessment of the NWM results is presented in Section 3.3, and details regarding the inclusion of NWM inflows into FVCOM are discussed in Section 5.2.3.

4.3 OUTFLOW (ECCC)

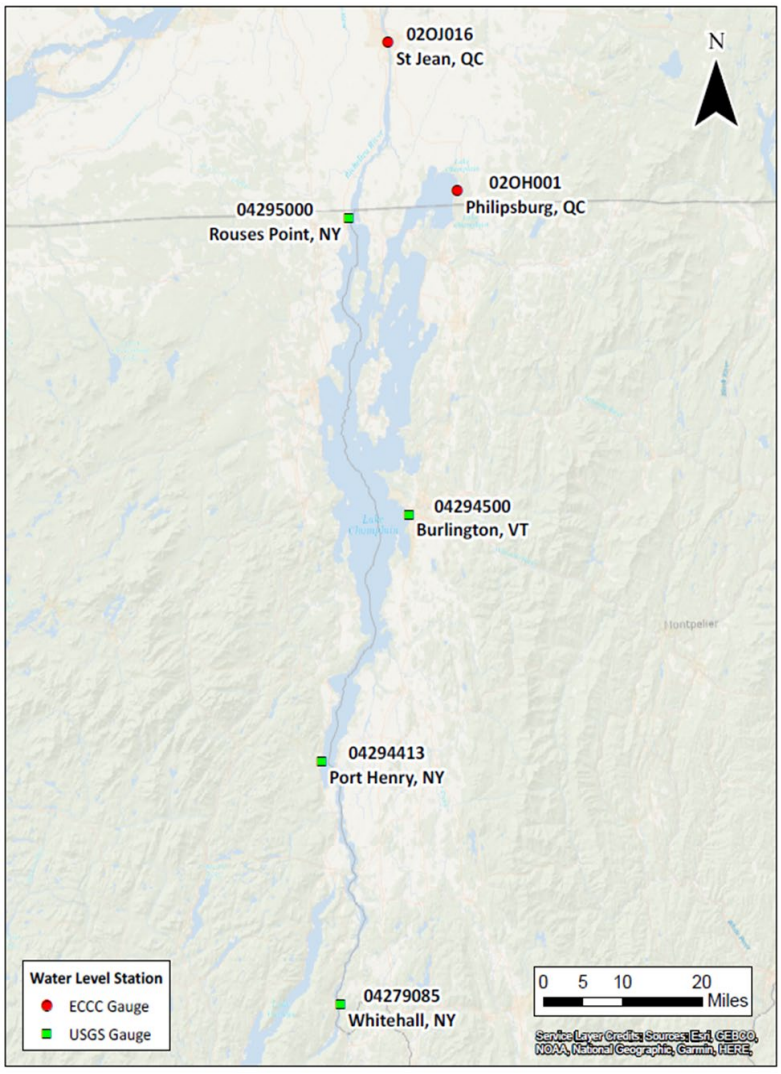

Figure 4.2 Locations of Lake Champlain water level gauges.

The Richelieu River flows northward out of Lake Champlain, and is forced as an elevation open-boundary condition in the FVCOM model. Observations used to force the model are obtained from Environment and Climate Change Canada (ECCC) water level gauge 02OJ016, located on the Richelieu River in St Jean QC (Figure 4.2). The water level open-boundary condition is applied across four FVCOM nodes that span the boundary at the location of the gauge.

ECCC water level observations are published on a delay of up to 6 hours from realtime. Available data are downloaded and archived locally prior to initiating an FVCOM nowcast/forecast run. Because FVCOM nowcast and forecast runs are delayed by only 80 and 140 minutes, respectively (Section 6.1), the most recent outflow water level data is typically not yet available when models are run. In these cases, the most recent hourly water level is persisted as a constant elevation over the portion of the run for which water level data is not yet available.

No data sources have been identified that provided skillful forecasts of the flowrate or elevation of the Richelieu River outflow. Due to this limitation, the outflow for the forecast model is forced using the persistence condition described above, resulting in a constant open boundary condition that is based on the last available observation at the time the forecast model is initiated. The NWM was also assessed as a possible source of outflow information. However, review of NWM results for the Richelieu River demonstrated poor correlation with observations from the ECCC St Jean QC gauge, likely due to the simplified treatment of Lake Champlain hydrodynamics in the NWM. This ultimately precludes the use of the NWM for outflow forcing in the modeling system.

4.4 METEOROLOGICAL AND HYDROLOGICAL FORCING ACCURACY ASSESSMENT

4.4.1 HRRR/GFS

HRRR and GFS surface (10 m, ~32.8 ft Above Ground Level) winds were skill assessed using available overlake observations. Wind observations are routinely collected at three NDBC (National Data Buoy Center) buoys (deployed seasonally) and three FEMC (Forest Ecosystem Monitoring Cooperative) meteorological towers located on small islands in various parts of the lake (Fig 4.3). Careful inspection of data revealed issues with buoy 45188 wind direction and data from that buoy were excluded from analysis. In addition, Burton Island tower data were excluded because of sheltering. All data were scaled to a consistent 10 m (~32.8 ft) height above lake surface using neutral stability assumption. Model skill assessment is conducted based on the 24-hour atmospheric model forecast. Because buoy data is not available during winter, different periods were chosen for skill assessment: October 2019-May 2020 for FEMC towers and July-August 2019 for NDBC buoys.

Results showed that in case of FEMC towers, wind speed bias is slightly negative in HRRR forecasts (-0.5 to -1.6 mph) and although deteriorates somewhat in GFS (-2.0 to -2.5 mph) is still acceptable. Wind direction bias is also relatively small (< 16^{o}) in HRRR but somewhat larger (up to 22 ^{o}) in GFS which does not resolve the lake because of low horizontal resolution. In case of

NDBC buoys, model skill assessment was conducted for HRRR forecasts only and showed results consistent with that of FEMC towers. Wind speed bias was negative (-0.7 to -2.0 mph) and wind direction bias was even smaller (< 10º) than in FEMC case, although we note that validation period is much shorter in buoy case: 2 months versus 8 months in case of towers.

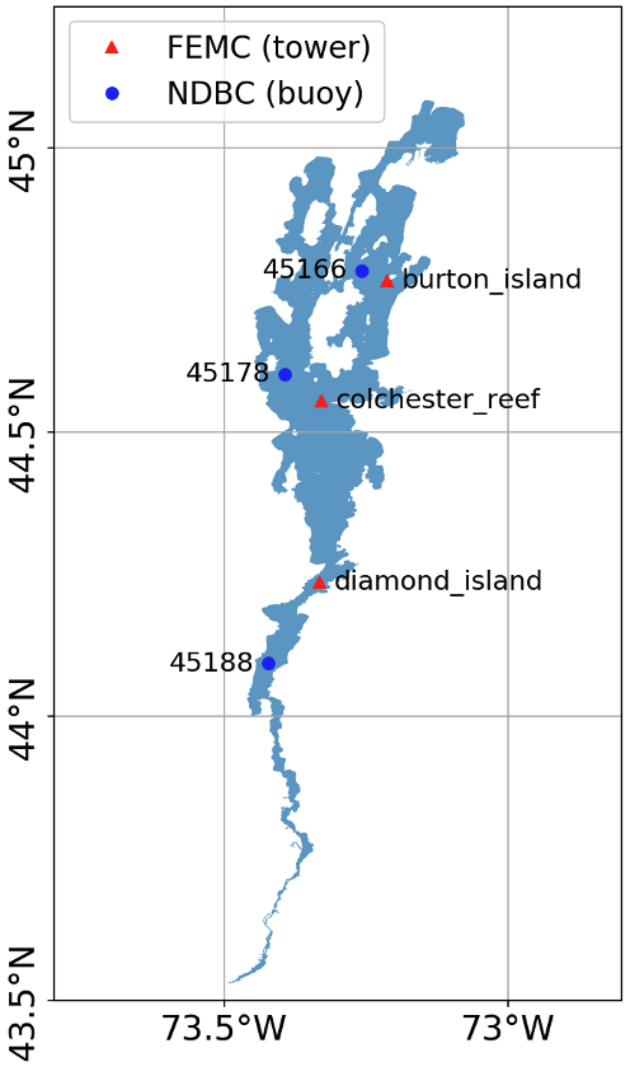

Figure 4.3 Location of FEMC (triangles) and NDBC (circles) wind observations in Lake Champlain

4.4.2 National Water Model

Table 4.2 Rivers used in National Water Model version 2.1 nowcast and forecast skill assessment.

Tributary	Gauge ID	Gauge Latitude (ºN)	Gauge Longitude (ºE)	NWM Feature ID
Ausable River	USGS 4275500	44.4514	-73.6425	9528411
Bouquet River	USGS 4276500	44.3583	-73.4083	9528597
Great Chazy River	USGS 4271500	45.0000	-73.5008	9525609
Jewett Brook	USGS 4292810	44.8561	-73.1508	4587092
La Platte River	USGS 4282795	44.3700	-73.2167	4578818
Lamoille River	USGS 4292500	44.6792	-73.0731	4587250
Lewis Creek	USGS 4282780	44.2492	-73.2289	22220497
Little Ausable River	USGS 4273800	44.5942	-73.4961	9527387
Little Chazy River	USGS 4271815	44.9022	-73.4150	9521395
Little Otter Creek	USGS 4282650	44.1981	-73.2494	22220501
Mettawee River	USGS 4280450	43.4639	-73.2842	10313430
Mill River	USGS 4292750	44.7797	-73.1442	4587100
Missisquoi River	USGS 4294000	44.9167	-73.1289	166176984
Otter Creek	USGS 4282500	44.0131	-73.1683	22220605
Pike River	USGS 4294300	45.0028	-72.8339	4589889
Poultney River	USGS 4280000	43.6242	-73.3119	10312666
Rock River	USGS 4294140	44.9631	-72.9919	4590269
Salmon River	USGS 4273700	44.6400	-73.4947	9527383
Saranac River	USGS 4273500	44.6817	-73.4711	9521459
Winooski River	USGS 4290500	44.4789	-73.1392	4578836

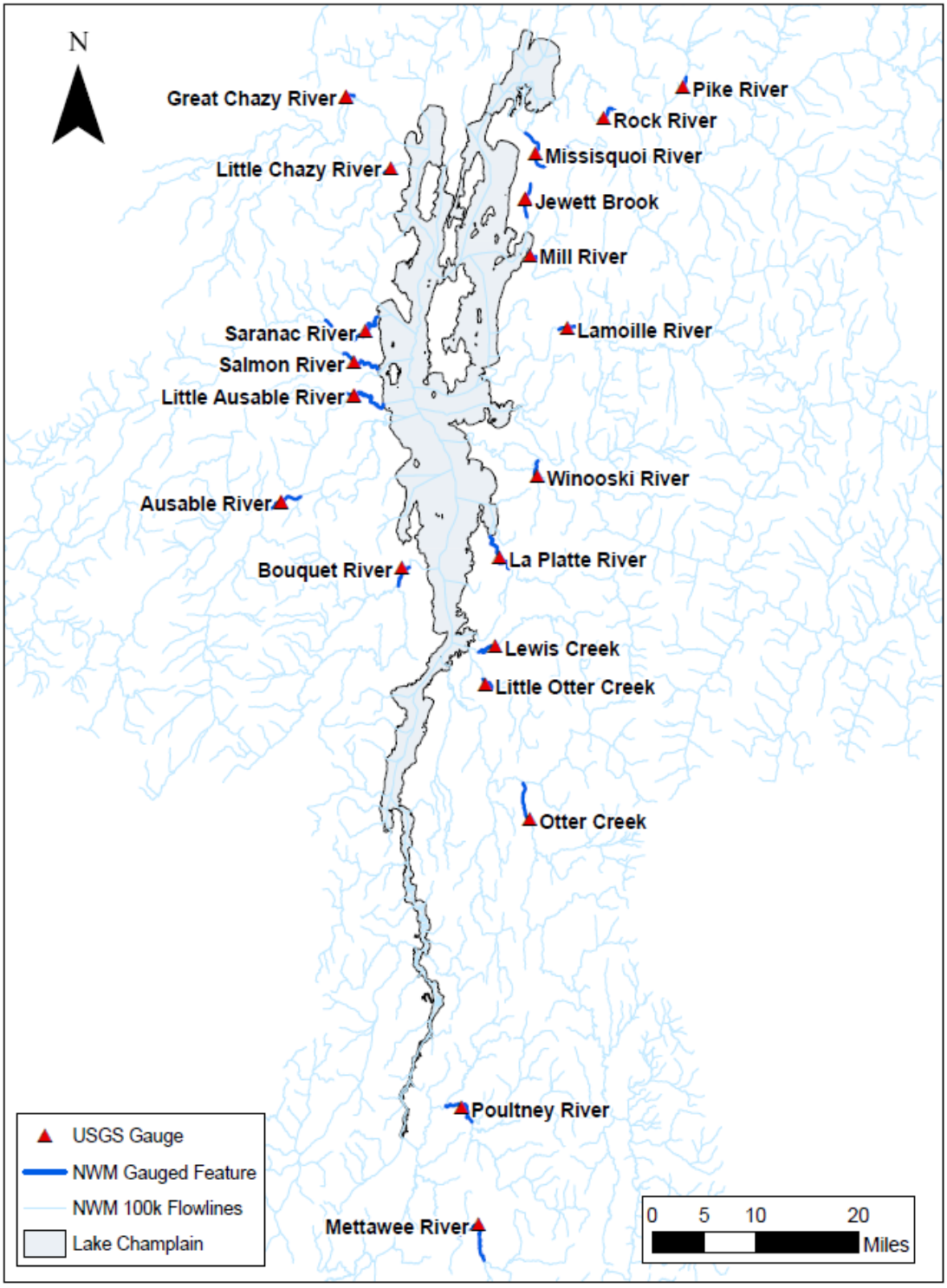

Figure 4.4 Rivers used in National Water Model version 2.1 skill assessment.

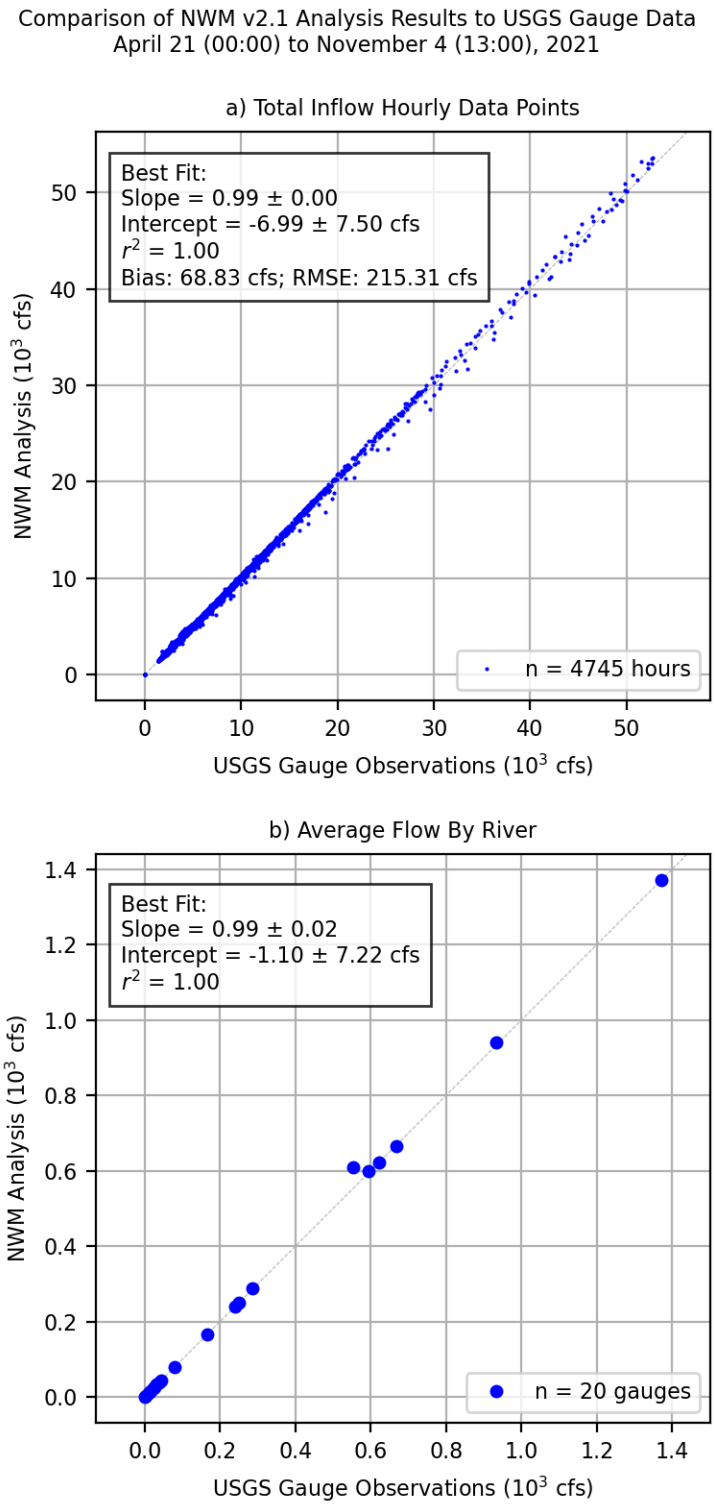

Figure 4.5 National Water Model version 2.1 nowcast skill assessment results.

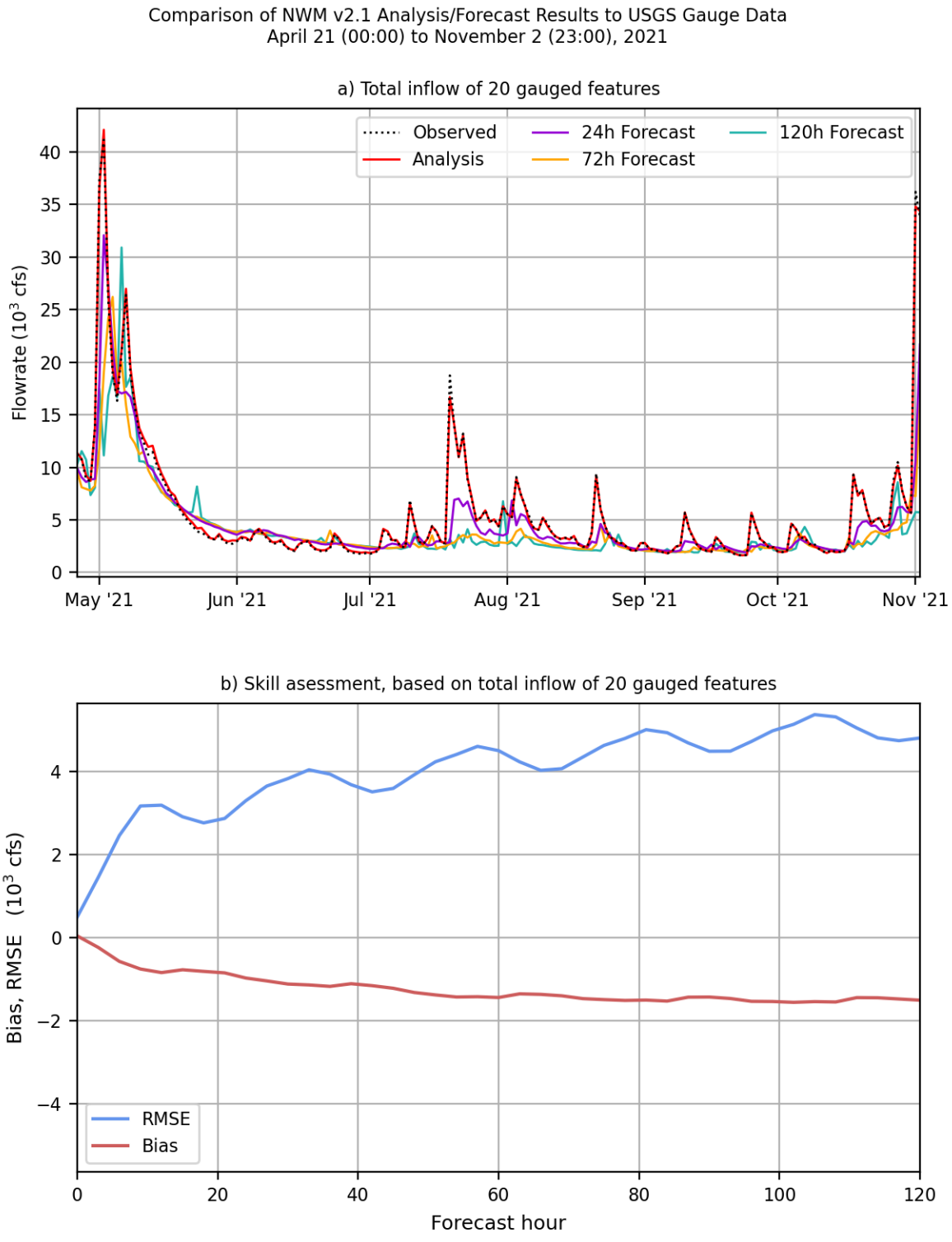

Figure 4.6 National Water Model version 2.1 forecast skill assessment results.

Skill assessments were conducted on results from operational version 2.1 of the National Water Model (NWM) for a subset of stream features that are gauged. The skill assessment uses NWM results from April 21 to November 3, 2021, which covers the time period from when NWM v2.1 became operational to the time the skill assessment was conducted. A total of 20 tributaries to Lake Champlain have gauge observations for this skill assessment period. (Table 4.2; Figure 4.4).

The skill assessment of the NWM v2.1 analysis model uses data from all 20 gauged tributaries, and was analyzed both by time and by river. First, the total inflow from all tributaries with available data was compared to the corresponding total NWM inflow results for the same tributaries (Figure 4.5a). These observed and modeled total inflow values were calculated for each hourly model time step, resulting in a total of 4,744 hourly data points. A linear regression of these points yields a slope of 0.99 +/- 0.00 and an r^2 value of 1.00; skill statistics calculated on the time series show a bias of +68.83 cfs and a RMSE of 215.31 cfs. When scaled to the average observed total inflow of these tributaries over the same period (5,878 cfs), the relative bias is +1.2% and the relative RMSE is 3.7%.

The skill of the NWM v2.1 analysis model was also assessed by river (Figure 4.5b). For each of the 20 tributaries with data during the skill assessment period, the average observed flow was compared to the average modeled flow, aggregated over all times for which both modeled and observed data were available for the tributary. A linear regression was performed on the 20 resulting data points, yielding a slope of 0.99 +/- 0.02 and an r^2 value of 1.00. The Ausable River has a noticeable high bias in the NWM v2.1 average modeled flow (609 cfs), relative to the average observed flow (553 cfs); the reason for this is currently unknown.

There is strong agreement between the NWM analysis model and observations, when analyzed both by time and by river. This high degree of skill in the NWM analysis model is expected, due to the fact that the NWM uses data assimilation techniques to assimilate observations from gauges into the analysis model.

Skill assessments were also conducted for the NWM v2.1 short- and medium- range forecast models. The 5-day NWM forecasts examined in this skill assessment consist of NWM analysis model for hour 0, the NWM short-range forecast for hours 1-18, and the NWM medium-range forecast for hours 19-120. This is consistent with the NWM forecasts used as forcing in FVCOM (Section 5.2.3).

In order to characterize how the NWM forecast skill varies by forecast horizon, time-series of select forecast horizons were plotted (Figure 4.6a) and skill statistics were calculated at three-hourly forecast intervals out to 120 hours (Figure 4.6b). Results from the skill assessment demonstrate a steeper decline in skill over approximately the first 12 hours of the forecast, followed by more gradual declines in skill up to approximately day 2 of the forecast, with minimal declines in skill over the remainder of the 5-day forecast. At a forecast horizon of 120 hours, the forecast has a bias of -1,507 cfs, and a RMSE of 4,807 cfs; when scaled to the average total flow of these rivers at the times analyzed (5,649 cfs), the relative bias is -27% and the

relative RMSE is 85%. As is apparent in the time-series of select forecast horizons, larger streamflow events are typically underpredicted at longer forecast horizons. This is consistent with an increasing negative bias at longer forecast horizons in the skill statistics.

5 LAKE CHAMPLAIN MODEL CALIBRATION, TESTING, AND SKILL ASSESSMENT

5.1 OBSERVATIONS (WATER LEVEL, WAVES)

For hydrodynamic model calibration, validation and assimilation, Lake Champlain water level observations are routinely available at four USGS gauges (Whitehall, NY, Port Henry, NY, Burlington, VT and Rouses Point, NY) and at the ECCC gauge at Philipsburg, QC (Fig. 4.2). Water level observations are taken every 15 min. Wave observations, on the other hand, are spatially sparse, seasonal, and available only during ice-free conditions. To obtain wave data suitable for WAVEWATCH III calibration and validation, NOAA GLERL acquired a Waverider buoy in 2020 with intent to conduct observations during two consecutive years of this project. Waverider deployment was initially scheduled for 2020, but was delayed by one year due to the COVID-19 pandemic. The buoy was deployed in the Main Lake off Burlington, VT during May-October 2021 (Fig. 5.1) with assistance from University of Vermont crew and specialists from the Coastal Data Information Program (CDIP). Real-time wave data (wave height, period and direction) were reported on the web pages for CDIP (https://cdip.ucsd.edu/m/products/?stn=251p1) and the National Data Buoy Center (NDBC) (https://www.ndbc.noaa.gov/station_page.php?station=45195). Example of Waverider buoy data displayed on CDIP web page in 2021 is shown in Fig. 5.2.

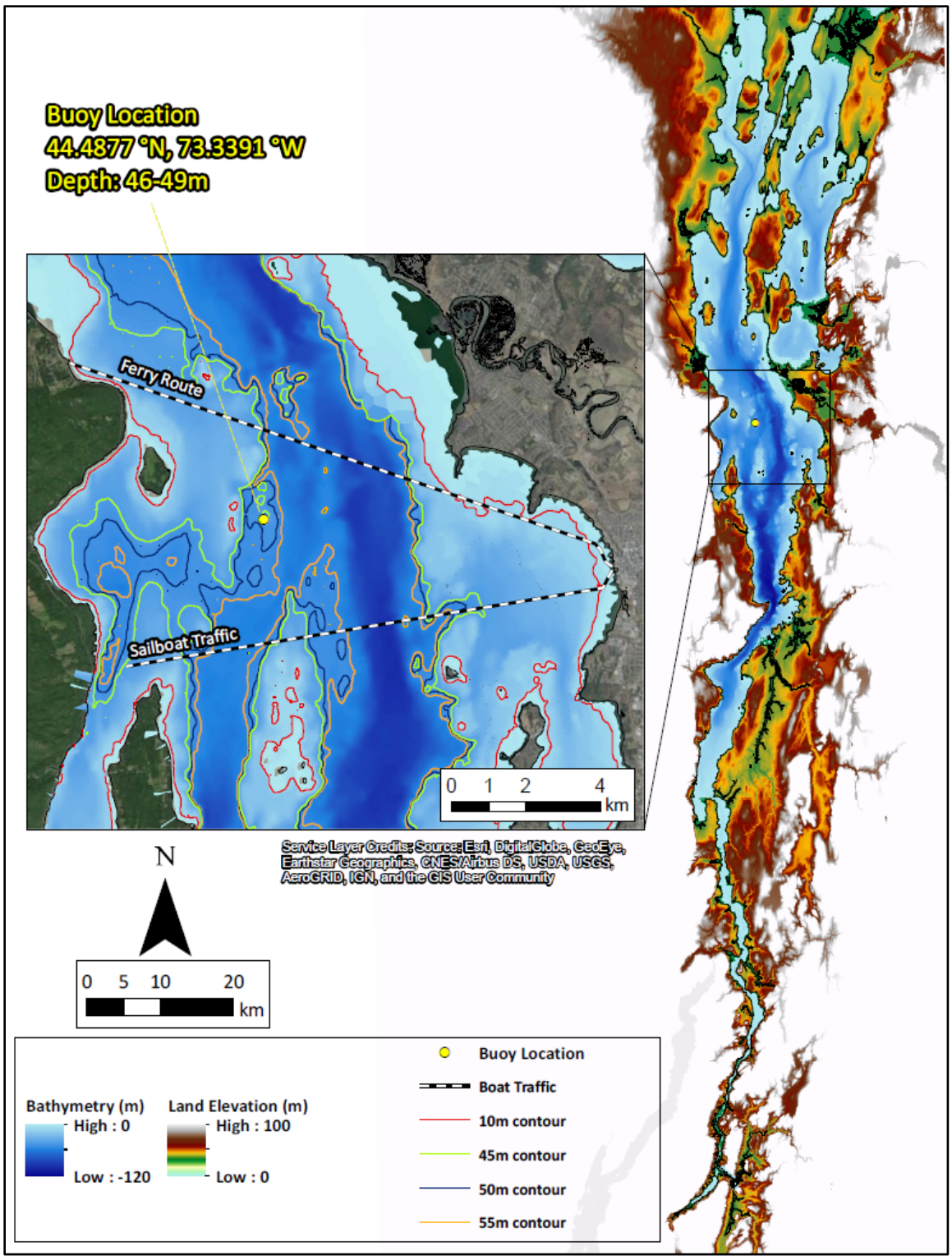

Figure 5.1 Location of Waverider buoy in 2021.

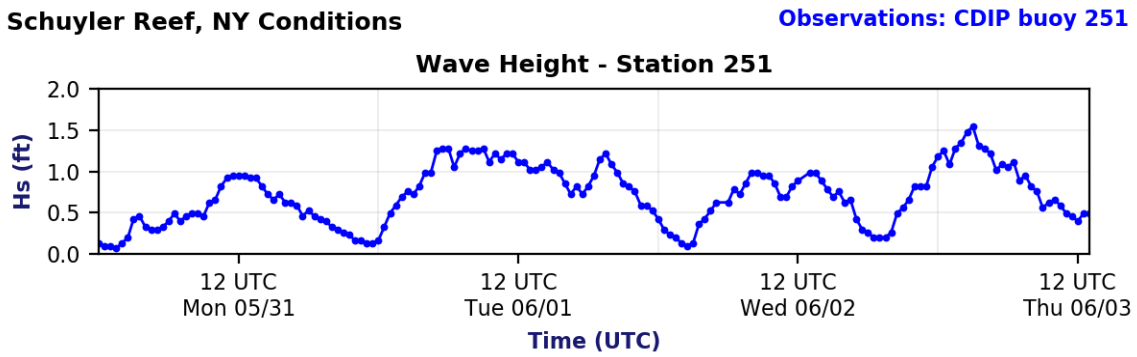

Figure 5.2 Significant wave height observations (ft) in Lake Champlain during one week in 2021; Waverider data.

5.2 FVCOM

5.2.1 Bottom Roughness

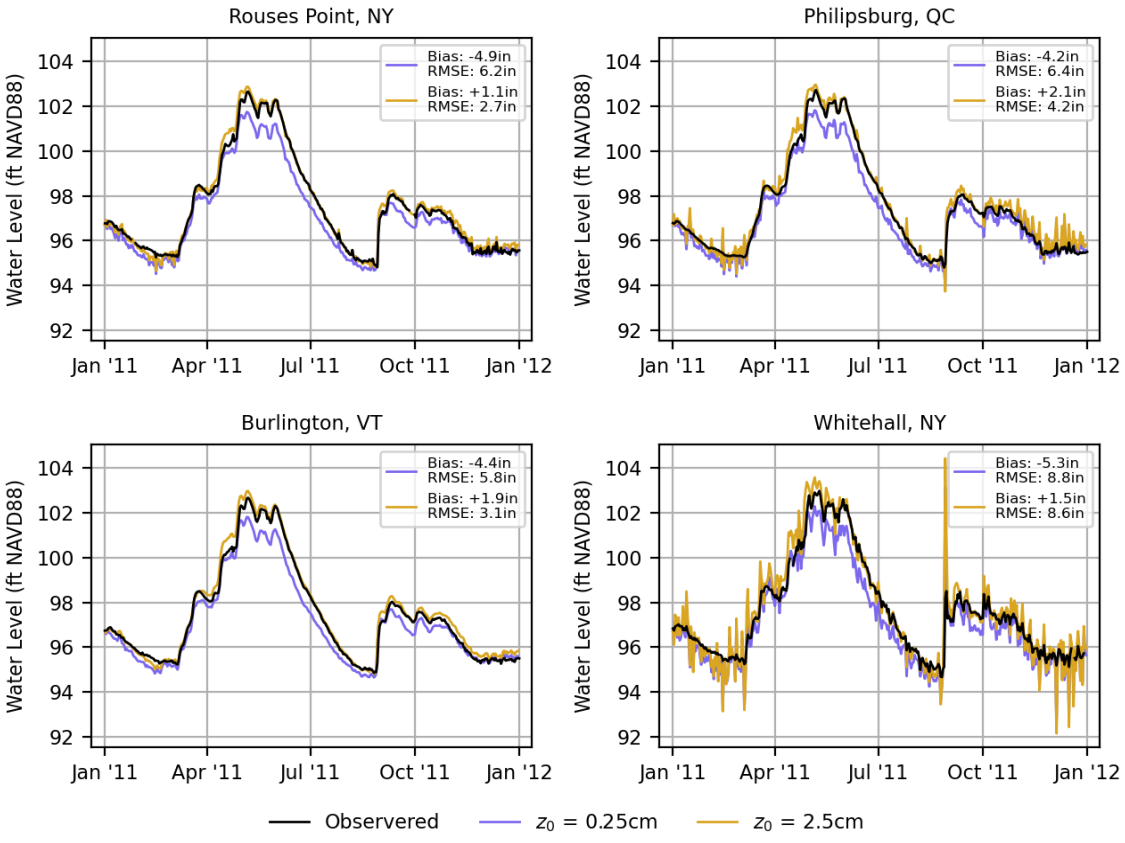

Figure 5.3 FVCOM bottom roughness calibration results.

Model hindcasts for the record flood year of 2011 showed a sensitivity to bottom roughness parameterization. Sensitivity runs were setup using the FVCOM mesh with 5 uniform sigma depth levels, wind forcing from the FEMC Colchester Reef station, river inflow forcing from available USGS and ECCC gauge observations, and with the Richelieu River outflow forced with elevation observations from the St Jean QC ECCC water level gauge; daily instantaneous water levels were output. It was found that when the default FVCOM bottom roughness length scale of 0.25 cm (0.0984 in) was used, water levels throughout the yearlong hindcast run were lower than observed. Based on results of the sensitivity testing, a bottom roughness length scale of 2.5 cm (0.984 in) was chosen for use in the model. The 2.5 cm (0.984 in) length scale was found to have the best agreement with observations in terms of both bias and RMSE at all four water level gauges analyzed (Figure 5.3).

Results from sensitivity testing found that while the lakewide water level is sensitive to bottom roughness over seasonal scales, the increased bottom roughness had minimal effect on the magnitude of localized wind-driven storm surges in the lake. It is possible that modeled water level results are particularly sensitive to bottom roughness within the Richelieu River portion of the domain, because that stretch constrains the amount of water leaving the lake. A length scale of 2.5 cm (0.984 in) is more representative of what may typically be found in a riverine setting, and may explain why the use of this bottom roughness parameterization yields more accurate water level predictions.

5.2.2 Storm Surges

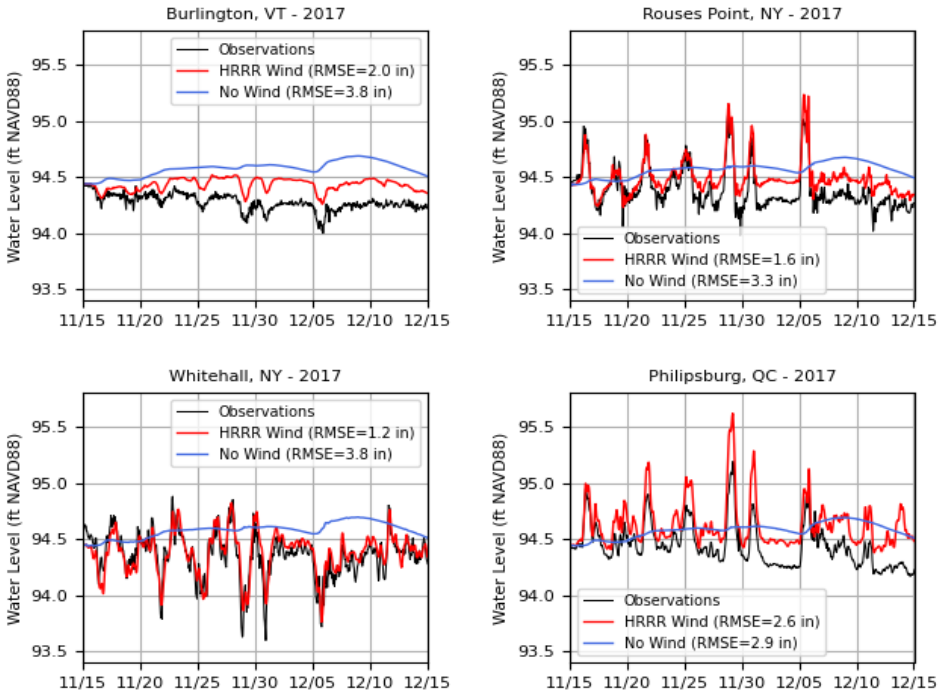

Figure 5.4 Comparison of FVCOM water level results with and without wind forcing

To validate the model's ability to simulate localized wind-driven storm surges, short-term hindcasts were run for two periods with strong wind events: April 15 to May 1, 2017 and November 15 to December 15, 2017. Simulations were run with and without HRRR wind forcing so that the influence of wind on model results could be quantified. The simulations used the FVCOM mesh with 21 uniform sigma depth levels, river inflow forcing from available ECCC and USGS gauges, and with the Richelieu River outflow forced with elevation observations from the St Jean QC ECCC water level gauge; hourly instantaneous water level results were output.

Results from the period November 15 to December 15, 2017 are shown to demonstrate the improvement in model skill when wind is included (Figure 5.4). Both the timing and magnitude of short-term wind-driven fluctuations are well-characterized by the model. Bias and RMSE are reduced at all four stations analyzed when the model is forced with HRRR wind, relative to when no wind forcing is used; this is true for both the April 2017 and November-December, 2017 hindcasts. These results demonstrate the importance of characterizing spatially-variable wind-driven effects on water levels when producing local flood forecasts.

5.2.3 NWM Coupling

River inflow estimates from the NWM were incorporated into the FVCOM model through a one-way coupling setup. Information from the NWM is used to inform conditions in the FVCOM model, but there is no feedback from FVCOM into the NWM. There are a total of 73 inflow features in the NWM that feed into Lake Champlain, which range in size from major inflows to small unnamed tributaries. All 73 of these NWM inflows were incorporated into FVCOM as volumetric flow rates, applied on cell edges at the boundary of the domain.

The 14 largest river inflows in the domain are spatially resolved in the topobathymetric mesh (Section 2.1). Remaining inflows are too small to be resolved at the spatial scales of the model. In addition, FVCOM requires that rivers be applied at the outer boundary of the model domain, and inflow characteristics are best preserved in the model when inflows are applied to a wet area of the grid. Due to these limitations, flows from the 59 inflows that are too small to be resolved in the model are added to the nearest of the 14 spatially-resolved major inflow features (Figure 4. 1). The thalwegs of these 14 major river inflows were extended to the outer boundary of the model domain, such that the upstream nodes of the rivers reliably meet the above-mentioned FVCOM criteria for river inflows. In addition, adding each smaller tributary to the nearest major river will help preserve sub-basin-scale hydrology within the domain.

Operational NWM output is downloaded, subset, and archived locally prior to initiating the corresponding FVCOM nowcast/forecast run. Externally, the NWM analysis model is updated hourly, with a delay in availability of approximately 1 hour; the NWM short-range forecast model is initiated hourly, with a delay in availability of approximately 2 hours; and the NWM medium-range forecast model is initiated every 6 hours, with a delay in availability of approximately 6 hours. FVCOM runs are delayed relative to their nominal runtime to account for these delays in NWM data availability. The FVCOM nowcast model is delayed by 80 minutes,

to ensure the availability of corresponding NWM analysis data. The FVCOM forecast model is delayed by 140 minutes, and uses the NWM analysis model for hours 0-1 of the forecast, the NWM short-range forecast for hours 2-18 of the forecast, and hours 24-126 of the 6-hour-old NWM medium-range forecast for the remainder of the FVCOM forecast. These delays were chosen to balance the timeliness of results with the accuracy of forcing.

5.2.4 Handling Ponding Effects

Due to spatial discretization in the FVCOM model grid, an unrealistic "ponding" effect can occur under scenarios where inadequately-resolved coastal regions undergo wetting and drying. When, for example, a low-lying coastal area is represented in the model grid, but a smaller hydrologic connection to the main lake is not resolved, the low-lying area can become unrealistically disconnected from the main lake in the model. Such ponded areas can be associated with localized model inaccuracies, including unrealistic estimates of water level and other output parameters.

While ponding is normal and expected in hydrodynamic models that include wetting and drying, care was taken to minimize the negative impacts of ponding on model results and visualizations. Processes were developed to dynamically identify wet areas that are connected to the main lake versus those that are disconnected ponds. When applying precipitation forcing, either as realistic overlake precipitation (Section 4.1) or as a systematic water level nudge (Section 5.2.5), precipitation is not applied to disconnected ponds. This is done to avoid exacerbating any unrealistic water level difference between these ponds and the main body of the lake. In addition, disconnected ponds are not plotted on visualizations of model results, because results in ponded areas are understood to be misleading.

5.2.5 Water Level Nudge

In order to keep errors in water level predictions from compounding over time, a water level nudging method was implemented into the nowcast/forecast system. After each 6-hourly nowcast run, modeled water level results are compared to water level observations from available gauges, and any difference between modeled and observed water level is accounted for by adding commensurate precipitation or evaporation over the subsequent model run. This method keeps the modeled lake level from drifting from the observed water level over time, and results in 5-day forecasts being initiated from a state that more-closely matches realistic conditions. There is no specific parameterization for domain-wide water level adjustment in FVCOM, so this precipitation and evaporation scheme is implemented to adjust the model to observations.

Five water level gauges are used in the comparison of model results to observations, and they are reasonably evenly distributed around the lake. The gauges used in the comparison are the ECCC gauge in Philipsburg QC, and the USGS gauges in Whitehall NY, Port Henry NY, Burlington VT, and Rouses Point NY (Figure 4.2). The median difference between the modeled and observed water level among these five stations at the end of each nowcast run is the value used to determine the water level nudge. The median difference is used instead of the mean in order to

help mitigate errors in the difference calculation that may arise from erroneous data being present in the real time gauge data. The real time gauge data are preliminary, and have not yet gone through full quality control procedures at the time of the comparison.

Overlake precipitation or evaporation is applied over the first 6 hours of the subsequent model run to shift the water level by this calculated difference. The overlake precipitation/evaporation is only applied in areas of the domain with water at least one-meter deep, because it was found that instabilities in the model can arise when precipitation or evaporation change the wet/dry state of a grid node. In addition, no water level nudge is applied in ponded areas that are disconnected from the main lake (Section 5.2.4). In order to prevent the system from applying unexpectedly high precipitation or evaporation rates as a result of the water level nudging process, a nudge limit of 6 cm (2.36 in) per model run is applied in nowcast runs, and a limit of 12 cm (4.72 in) per model run is applied in forecast runs. Based on initial testing, the magnitude of the water level nudge is typically much below these values, so it is expected that these limits will rarely be reached.

While the nudge is conceptually applied as either precipitation or evaporation, it is forced into FVCOM as positive or negative evaporation. Review of the FVCOM code found that the precipitation and evaporation variables are interchangeable within the modules used in the Lake Champlain system, and that applying negative evaporation is functionally equivalent to applying precipitation. By utilizing only the FVCOM evaporation variable when applying the nudge, it allows the precipitation variable to be used solely for realistic overlake precipitation, as intended. Because realistic overlake precipitation is incorporated in the Lake Champlain model (Section 4.1), it is desirable to keep it separate from the nudge in the model forcing, as conflating the two would possibly complicate or confound interpretation of data produced by the modeling system.

5.2.6 Water Level Skill Assessment

Hourly nowcast and forecast guidance of water levels from GLERL's semi-operational FVCOM-based Lake Champlain forecast system for the period January 1 to December 31, 2021 were compared to hourly observations recorded at U.S. and Canadian gauges. The evaluation used the standard NOS suite of skill assessment statistics (Hess et al., 2003). The statistics were calculated for hourly water levels. A description of statistics is given below followed by a brief description of the verification sites.

5.2.6.1 Description of NOS Suite of Skill Assessment Statistics

The NOS suite of skill assessment statistics include Mean Error, or more commonly referred to as Mean Algebraic Error (MAE) or bias; Root Mean Squared Error (RMSE); Central Frequency (CF); Positive Outlier Frequency (POF); Negative Outlier Frequency (NOF); Maximum Duration of Positive Outliers (MDPO); and Maximum Duration of Negative Outliers (MDNO). These statistics are described briefly in Table 5.1. The comparisons were done using the NOS standard skill assessment software (Zhang et al., 2010 and Zhang et al., 2013).

The calculation of the target frequency of skill statistics, CF, POF, MDPO and MDNO, required the assignment of 1) acceptable magnitude errors for water level amplitudes, 2) acceptable timing error for water levels, and 3) maximum allowable time durations for consecutive positive and negative water level outliers. The acceptable magnitude errors for water levels were set at +/- 15 cm (0.5 ft) and the acceptable timing error was set at +/- 1.5 hours. In addition, for the calculation for the MDPO and MDNO statistics, a maximum allowable time duration of consecutive occurrences with an error greater than the acceptable amplitude or timing error was specified at 24 hours.

The resulting values for each statistic were then judged against the NOS Acceptance Criteria (Table 5.1) for that statistic. These criteria include target frequencies for CF, NOF, and POF and limits on the duration of errors (i.e. maximum length of time of consecutive) for MDPO and MDNO. Any new or upgraded NOS operational oceanographic modeling system is expected to meet or exceed most of the NOS Acceptance Criteria (targets) in order to be implemented operationally.

Table 5.1 Description of NOS skill assessment statistics (Modified from Hess et al., 2003) along with NOS Acceptance Criterion (targets) used to evaluate nowcasts and forecast guidance.

Statistic	Units	Description	NOS Acceptance Criterion
Mean Algebraic Error (MAE)	Inches or Hours	The error is defined as the predicted value, p, minus the reference (observed value)	NA
SD	Inches or Hours	Standard Deviation	NA
RMSE	Inches or Hours	Root Mean Square Error	NA
SM	Inches or Hours	Series Mean. The mean value of a series y	NA
CF(X)	%	Central Frequency. Fraction (percentage) of errors that lie within the limits $\pm$X.	≥ 90%
POF(X)	%	Positive Outlier Frequency. Fraction (percentage) of errors that are greater than X.	≤ 1%
NOF(X)	%	Negative Outlier Frequency. Fraction (percentage) of errors that are less than -X.	≤ 1%
MDPO(2X)	Hours	Maximum Duration of Positive Outliers. A positive outlier event is two or more consecutive occurrences of an error greater than +2X. MDPO is the length of time in hours (based on the number of consecutive occurrences) of the longest positive outlier event.	≤ L
MDNO(2X)	Hours	Maximum Duration of Negative Outliers. A negative outlier event is two or more consecutive occurrences of an error less than -2X. MDNO is the length of time in hours (based on the number of consecutive occurrences) of the negative outlier longest event.	≤ L
NOS Standard Criteria		where X = acceptable error magnitude (cm or minutes) X = +- 5.9 in. (15 cm) for water level amplitude errors X = +- 1.5 hours (90 minutes) for water level timing errors	where L=time limit or max. allowable duration L=24 hours

5.2.6.2 Description of Verification Data

The water level time series from hourly hindcasts were compared to observed hourly water levels recorded at United States Geological Survey (USGS) and Environment and Climate Change Canada (ECCC) gauges along the shores of Lake Champlain (Fig. 5.5). Information about these stations is given in Table 5.2. The water level observations from the USGS gauges were obtained

from the USGS National Water Information System API (https://nwis.waterdata.usgs.gov/nwis). The water levels from the ECCC gauges were obtained from the ECCC's Meteorological Service of Canada (MSC) HTTPS Open Data Server (https://dd.weather.gc.ca/).

Discrepancies in the elevation datums for lake gage and stream gauge data were observed at the border of Canada and the United States for the Canadian Geodetic Vertical Datum of 1928 (CGVD 28), North American Vertical Datum of 1988 (NAVD 88), and National Geodetic Vertical Datum of 1929 (NGVD 29), requiring geospatial datum harmonization for consistency and continuity (Flynn et al., 2016).

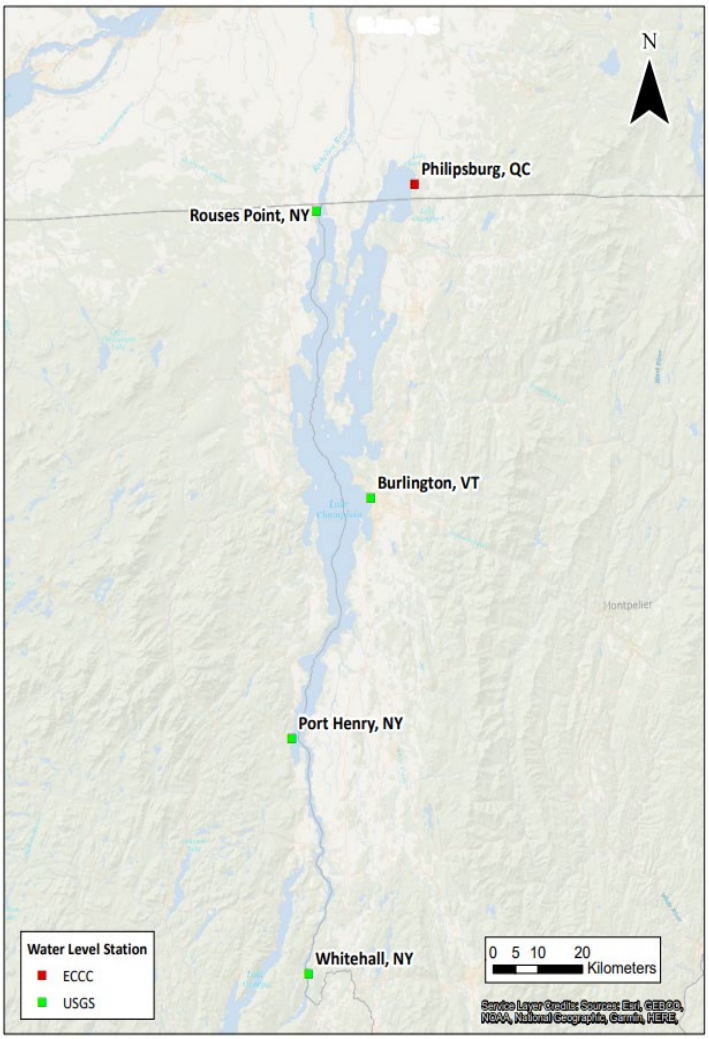

Figure 5.5 Locations of USGS and ECCC water-level gauges used to evaluate Lake Champlain water level nowcasts and forecast guidance.

Table 5.2 Information on USGS and ECCC stations whose water level observations were used to evaluate the Lake Champlain nowcasts and forecasts.

Station Name	State or Prov.	Station ID	Agency	Coordinates		Vertical Datum	Conversion to NAVD88 (ft)
				Lat. (deg N)	Lon. (deg W)		
Burlington	VT	04294500	USGS	44.476	73.222	NGVD29	-0.522
Port Henry	NY	04294413	USGS	44.053	73.453	NGVD29	-0.600
Rouses Point	NY	04295000	USGS	44.996	73.360	NGVD29	-0.430
Whitehall	NY	04279085	USGS	43.622	73.419	NAVD88	-0.269
Philipsburg	QC	02OH001	ECCC	45.040	73.080	Arbitrary (CGVD28 - 24.384m)	79.787

5.2.6.3 Skill Assessment Results

The results of the skill assessment of the nowcasts and forecast guidance for Lake Champlain during 2021 will be presented in this section starting with the nowcasts.

5.2.6.3.1 Assessment of Water Level Nowcasts

The standard suite of skill assessment statistics evaluated the ability of the nowcasts to simulate hourly water levels at USGS and ECCC gauges. The nowcasts were compared to the adjusted hourly water level observations discussed previously.

The hourly water level time series plots at the five water level gauges are shown in Fig. 5.8. The MAE (or bias) and RMSE of the nowcast are highlighted on each time series. The complete set of skill statistics for each gauge are available in Table 5.3.

The time series plots indicate that the nowcasts simulated the yearly cycle of lake levels very well, including the peak in April and May at all gauges which is associated with snowmelt and runoff. The nowcasts did very well simulating the sudden rise in water levels around July 19th (Day 200). The rise was due to 2–3 in. (5–7.6 cm) of rainfall that fell over the Lake Champlain Watershed from an extratropical cyclone which passed slowly through New York State and New England from July 17–20 (Fig. 5.6). The nowcasts also did very well simulating the sudden rise in water levels around November 1st (Day 305) from the +2 in. (+5 cm) of rain that fell in the watershed from an extra-tropical cyclone which moved from the Ohio River Valley into Maine during October 30–31 (Fig. 5.7). Overall, the most energetic level changes of the five gauges occurred at the Whitehall gauge and to a lesser extent at the Philipsburg gauge, located at the south and north ends of the lake.

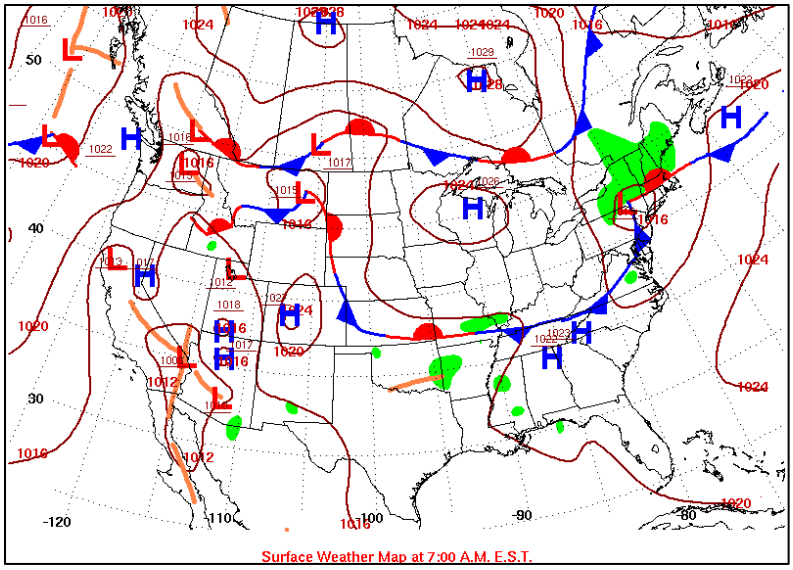

Figure 5.6 Surface weather map valid at 7 AM EST, July 18, 2021. Green indicates areas of precipitation.

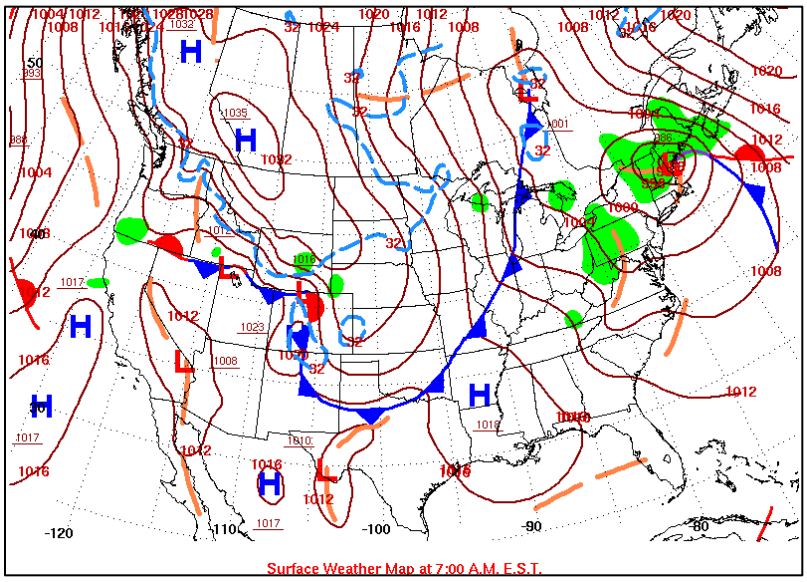

Figure 5.7 Surface weather map valid at 7 AM EST, October 31, 2021. Green indicates regions of precipitation.

Based on the MAE values, the nowcasts underpredicted water levels at Rouses Point, Port Henry, and Burlington between 0.08–0.51 in. (0.2–1.3 cm), but overpredicted water levels at Philipsburg and Whitehall between 0.20–0.35 in. (0.61–0.9 cm). The greatest RMSEs were at the gauges at the two ends of the lake, with 0.83 in. (2.1 cm) at Rouses Point and 0.87 in. (2.21 cm) at Philipsburg in the north, and 1.93 in. (4.9 cm) at Whitehall in the south. The nowcasts passed all the NOS criteria for NOF, CF, POF, MDNO and MDPO.

There is a noticeable 24-hour periodicity in the skill assessment statistics, particularly at stations toward the northern and southern ends of the lake, where the effects of storm surges are greatest. Preliminary analysis indicates that this periodicity is associated with a 24-hour periodicity in meridional wind velocity, which is not perfectly replicated in the model. This periodicity in wind is believed to be orographic in nature, though the mechanisms driving it are not fully understood, and additional analysis and characterization may be warranted.

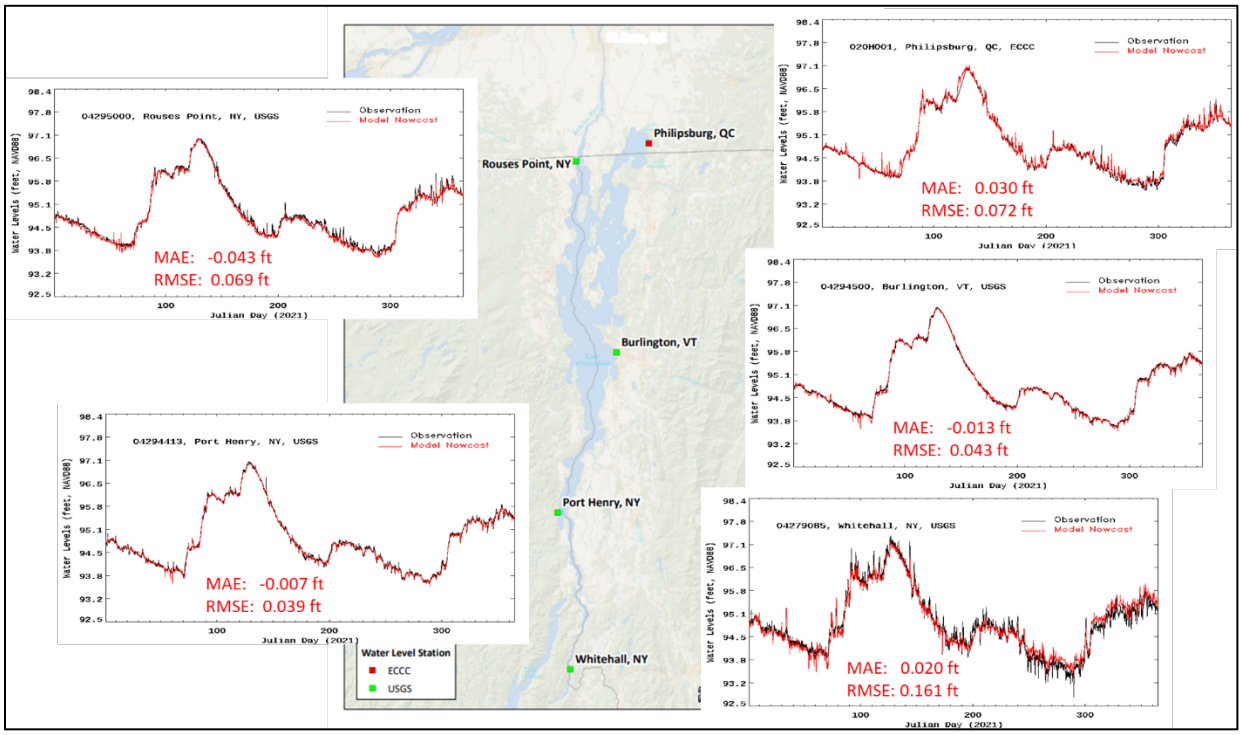

Figure 5.8 Time series plots of hourly Lake Champlain nowcasts of water level (red) vs. observations (black, converted to NAVD88 (ft)) at USGS and ECCC gauges (From north to south: 1. Philipsburg, QC, ECCC, 2. Rouses Point, NY, USGS, 3. Burlington, VT, USGS, 4. Po

Since April and May are the months when the lake levels are the highest and the threat for lake shore flooding is the greatest due high winds, waves, and rainfall from strong extratropical cyclones, a few high-water level events were examined from mid-March to early June 2021 by comparing the nowcasts to the observations at gauges in the southern and northern parts of the lake, Whitehall, NY and Philipsburg, QC, respectively. Figures 5.9–5.11 depict the water levels at Whitehall from Day 70 to 80 (Mar. 11–21), Day 90 to 100 (Mar. 31–Apr.10), and Day 140–155 (May 20–Jun. 4) and Figures 5.12–5.14 show the nowcasts vs. observations at Philipsburg for the same time periods. The nowcasts did very well in simulating the high-water levels at both locations during these periods, generally being within 0.33–0.49 ft (0.1–0.15 m) of the observed value.

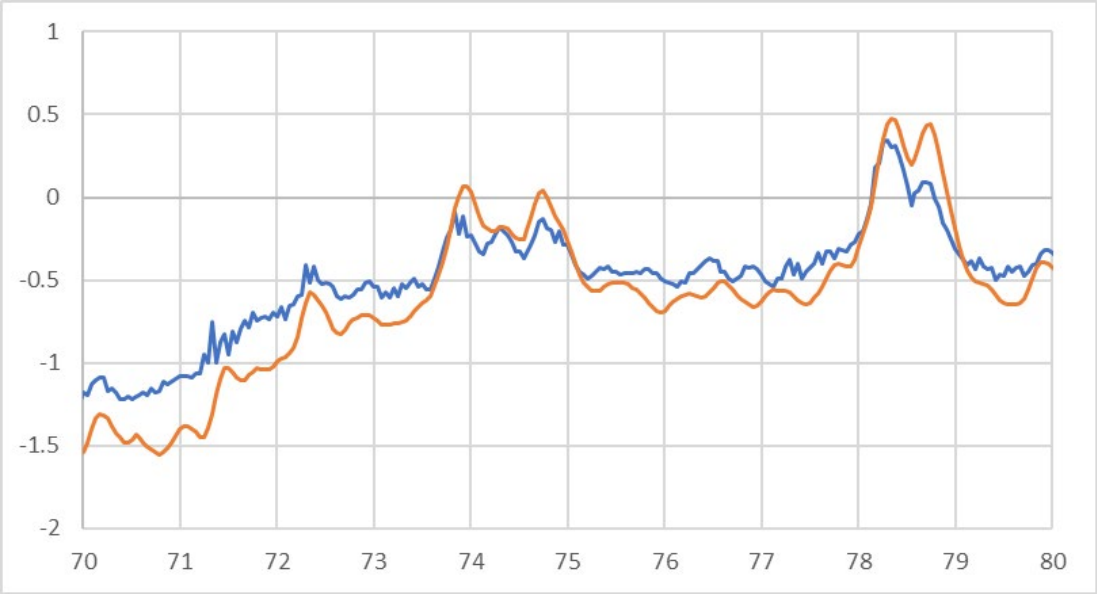

Figure 5.9 Time series plots of hourly Lake Champlain nowcasts of water level (red) vs. observations (blue) referenced to model datum of 95.1184 ft at the USGS gauge at Whitehall, NY from March 11 (Day 70) to March 21 (Day 80) in 2021.

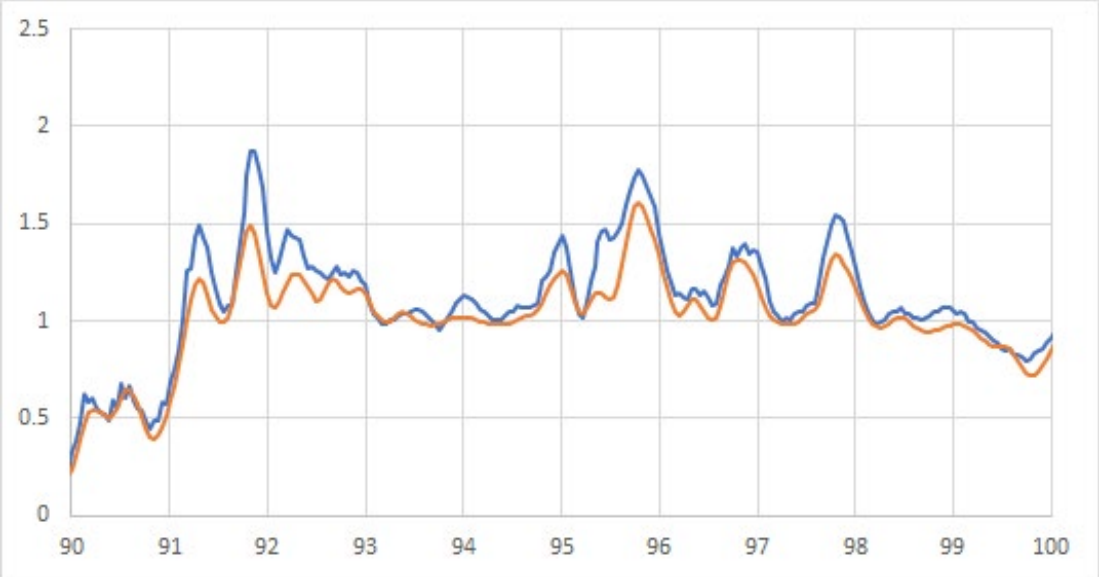

Figure 5.10 Same as Fig. 5.9 but for the period from March 31 (Day 90) to April 10 (Day 100) in 2021.

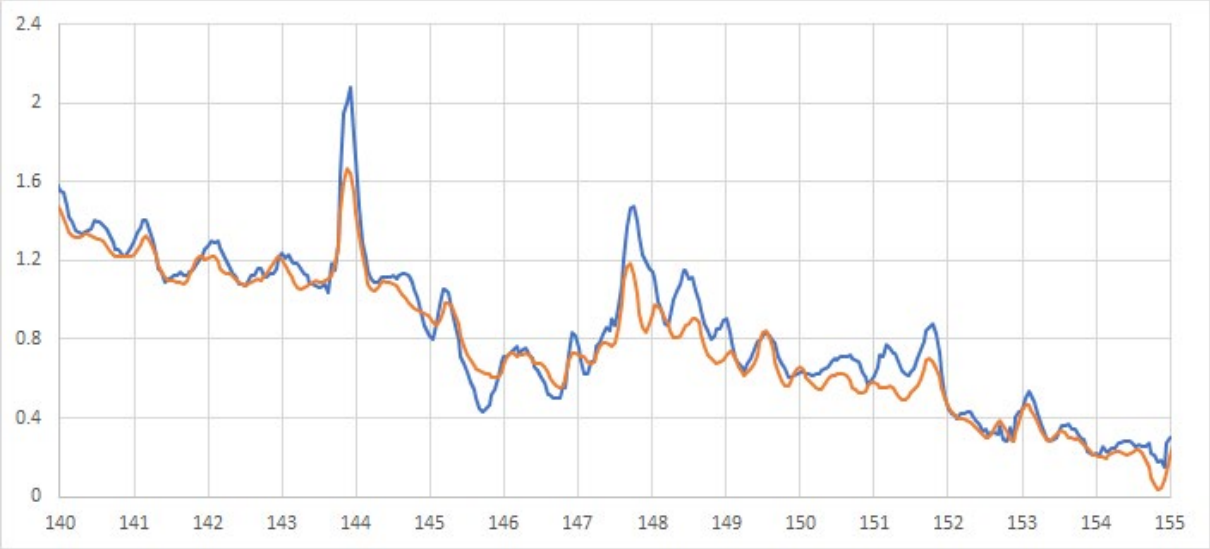

Figure 5.11 Same as Fig. 5.9 but for the period from May 20 (Day 140) to June 4 (Day 155) in 2021.

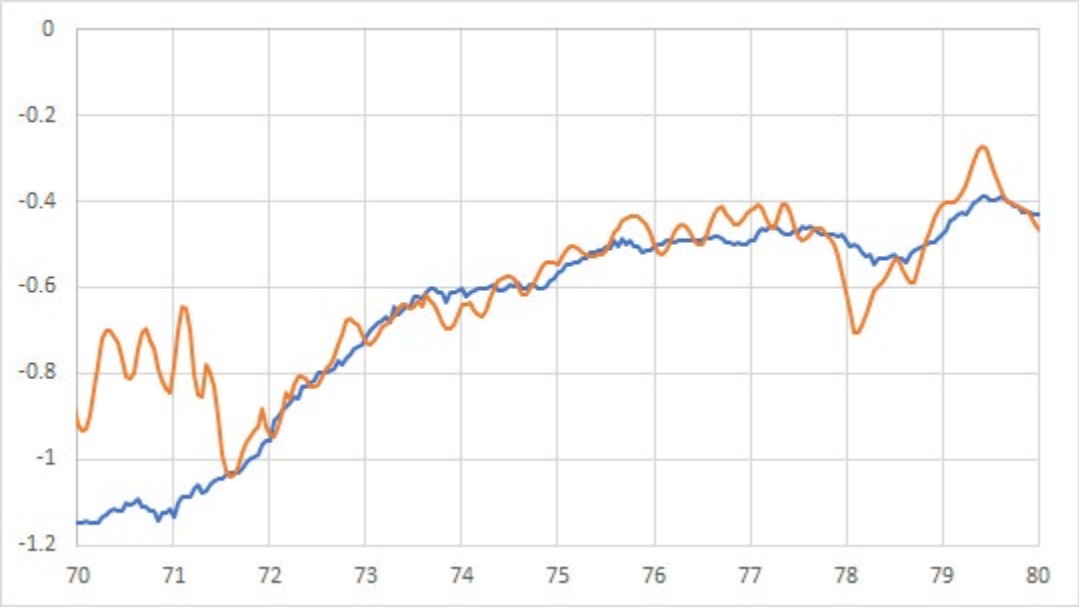

Figure 5.12 Time series plots of hourly Lake Champlain nowcasts of water level (red) vs. observations (blue) referenced to model datum of 95.1184 ft at the ECCC gauge at Philipsburg, QC from March 11 (Day 70) to March 21 (Day 80) in 2021.

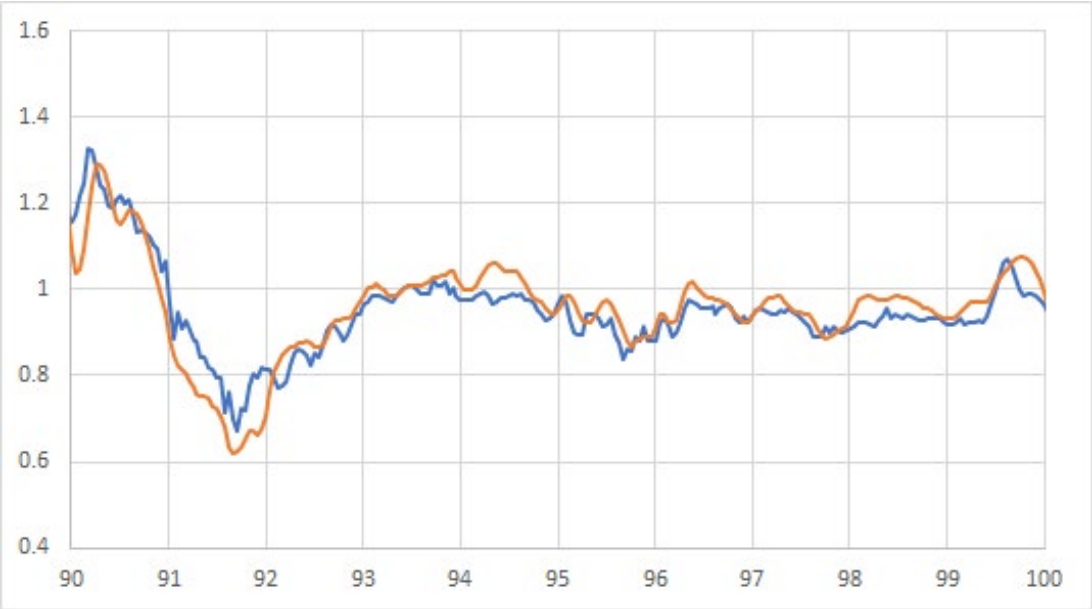

Figure 5.13 Same as Fig. 5.12 but for the period from March 31 (Day 90) to April 10 (Day 100) in 2021.

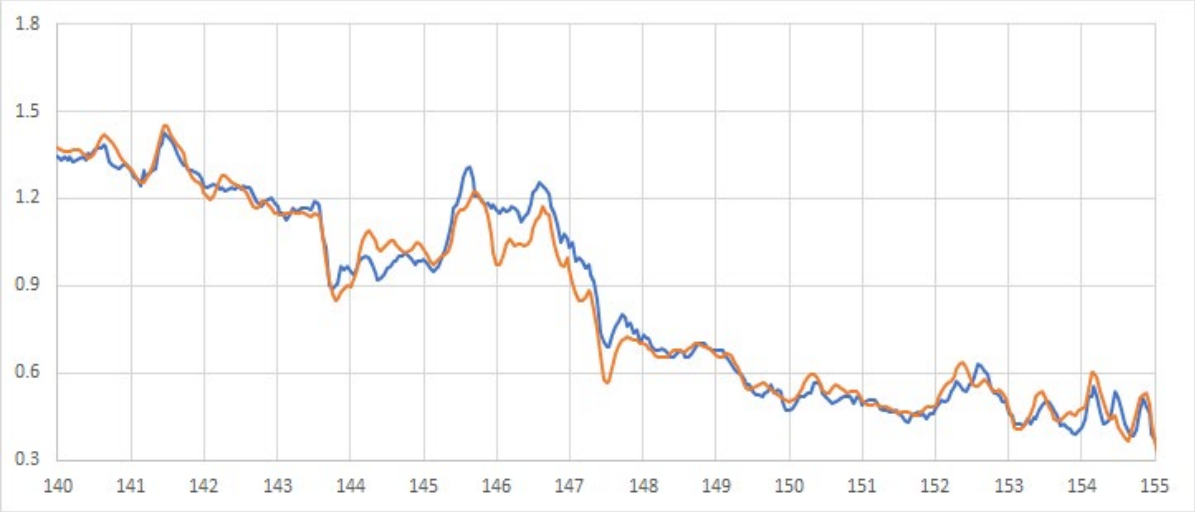

Figure 5.14 Same as Fig. 5.12 but for the period from but for the period from May 20 (Day 140) to June 4 (Day 155) in 2021.

Table 5.3 Summary of skill assessment statistics evaluating the ability of the Lake Champlain nowcasts to predict hourly water levels at USGS and ECCC gauges in Lake Champlain during 2021. Gray shading, if present, indicates that it did not meet the NOS acceptance criteria.

Statistic, Acceptable Error [ ], and Units ( )	04294500 Burlington USGS	04294413 Port Henry USGS	04295000 Rouses Point USGS	04279085 Whitehall USGS	02OH001 Philipsburg ECCC
N	8759	8759	8759	8759	8539
Mean Alg. Error (in)	-0.157	-0.079	-0.512	0.197	0.354
RMSE (in)	0.512	0.472	0.827	1.929	0.866
SD (in)	0.472	0.472	0.630	1.890	0.827
NOF [5.9 in] (%)	0.0	0.0	0.0	0.0	0.0
CF [5.9 in] (%)	100.0	100.0	100.0	99.8	100.0
POF [5.9 in] (%)	0.0	0.0	0.0	0.0	0.0
MDNO [2x5.9 in] (hr)	0.0	0.0	0.0	0.0	0.0
MDPO [2x5.9 in] (hr)	0.0	0.0	0.0	0.0	0.0

5.2.6.3.2 Assessment of Water Level Forecast Guidance

The same NOS standard suite of skill assessment statistics were also used to evaluate the ability of the forecast guidance to predict hourly water levels at USGS and ECCC gauges. Similarly, the guidance was compared to the adjusted hourly water level observations.

Time series plots of the MAE (bias) at different forecast projections from 6 to 120 hours at each gauge are shown in Figure 5.15. The plots for the RMSE at different forecast projections at the gauges are given in Figure 5.16. The complete skill statistics for the five gauges are available in Appendix Table A1–A5.

The MAE plots indicate that underprediction occurred at three of the gauges (Rouses Point, Port Henry, and Burlington), at all forecast projections. At these three gauges there was a noticeable increase of MAEs with the forecast projection. At Rouses Point, the MAE increased from -0.512 in. (1.30 cm) at +6 hours to -0.866 in. (2.20 cm) by +120 hours with an average MAE of -0.675 in. (1.71 cm) for the entire forecast period. At Port Henry, the MAEs ranged from -0.079 in. (0.20 cm) at +6 hours to -0.512 in. (1.30 cm) at +120 hours with an average MAE of -0.264 in. (0.671 cm). At Burlington, the MAE started at -0.157 in. (0.399 cm) and increased to -0.591 in. (1.50 cm) by +120 hours. The average MAE for the period was -0.346 in. (0.88 cm).

At Philipsburg, the forecasts overpredicted at all forecast projections with skill slightly decreasing from 0.354 in. (0.90 cm) at +6 hours to 0.118 in. (0.30 cm) at +120 hours. The average MAE for the forecast period was 0.252 in. (0.64 cm).

At the Whitehall gauge, the forecast slightly overpredicted up to +60 hours (except at +24 and +48 hours) between 0.315 and 0.118 in (0.80 to 0.30 cm). It then generally underpredicted from +66 to +120 hours between -0.118 in. (0.30 cm) and -0.551 in. (-0.118 to -1.40 cm). The average MAE at Whitehall for the entire forecast period was -0.047 in. (-0.12 cm).

The RMSE plots for all five gauges indicate a similar pattern as exhibited by forecast guidance from other forecast systems, the RMSE increased with the forecast projection hour. The difference across the different projections (+6 to +120 hours) was about 0.13–0.16 in. (0.34-0.41 cm) at the five gauges. For the entire forecast period, the average RMSEs at Rouses Point, Port Henry, and Burlington were 1.42 in. (3.6 cm), 1.20 in. (3.0 cm), and 1.21 in. (3.1 cm), respectively. The average RMSEs at Whitehall and Philipsburg were 2.5 in. (6.4 cm) and 1.5 in. (3.8 cm), respectively.

The forecast guidance passed all the NOS criteria for NOF, CF, POF, MDNO and MDPO.

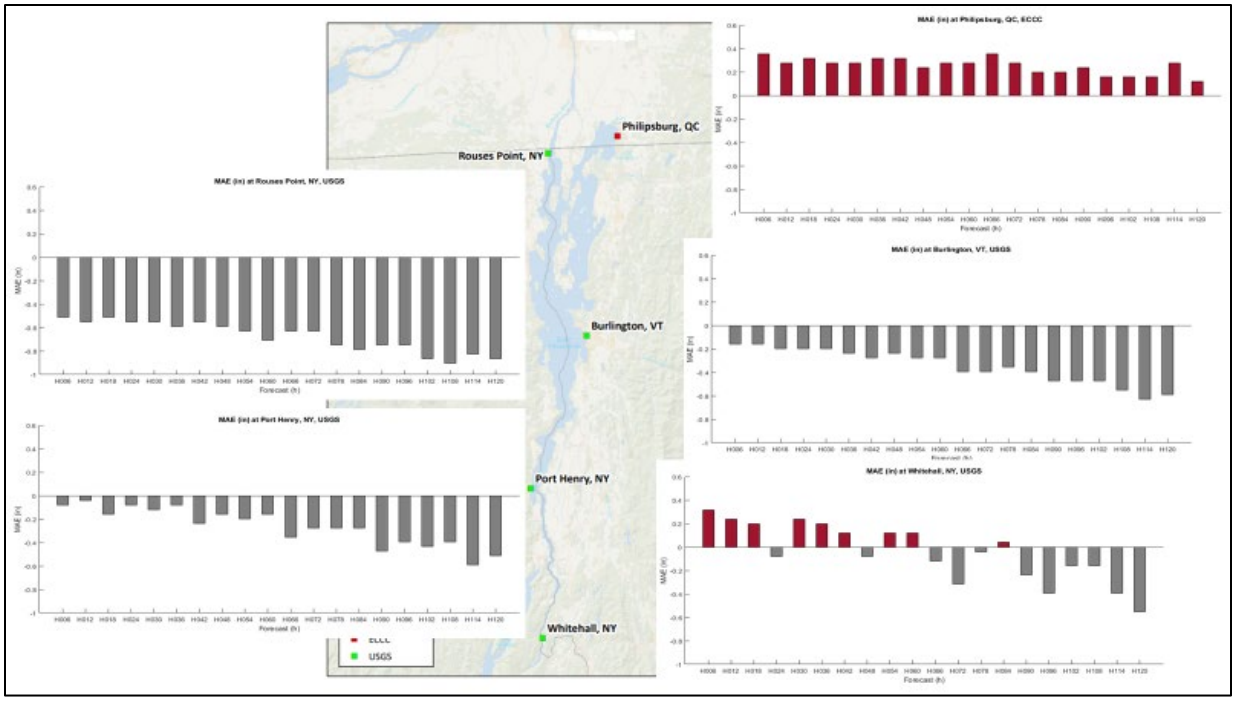

Figure 5.15 Water level MAE or bias (in, negative values gray, positive values red) by forecast projections at USGS and ECCC gauges (From north to south: 1. Philipsburg, QC, ECCC, 2. Rouses Point, NY, USGS, 3. Burlington, VT, USGS, 4. Port Henry, NY, USGS, and 5. Whitehall, NY, USGS), Lake Champlain during 2021.

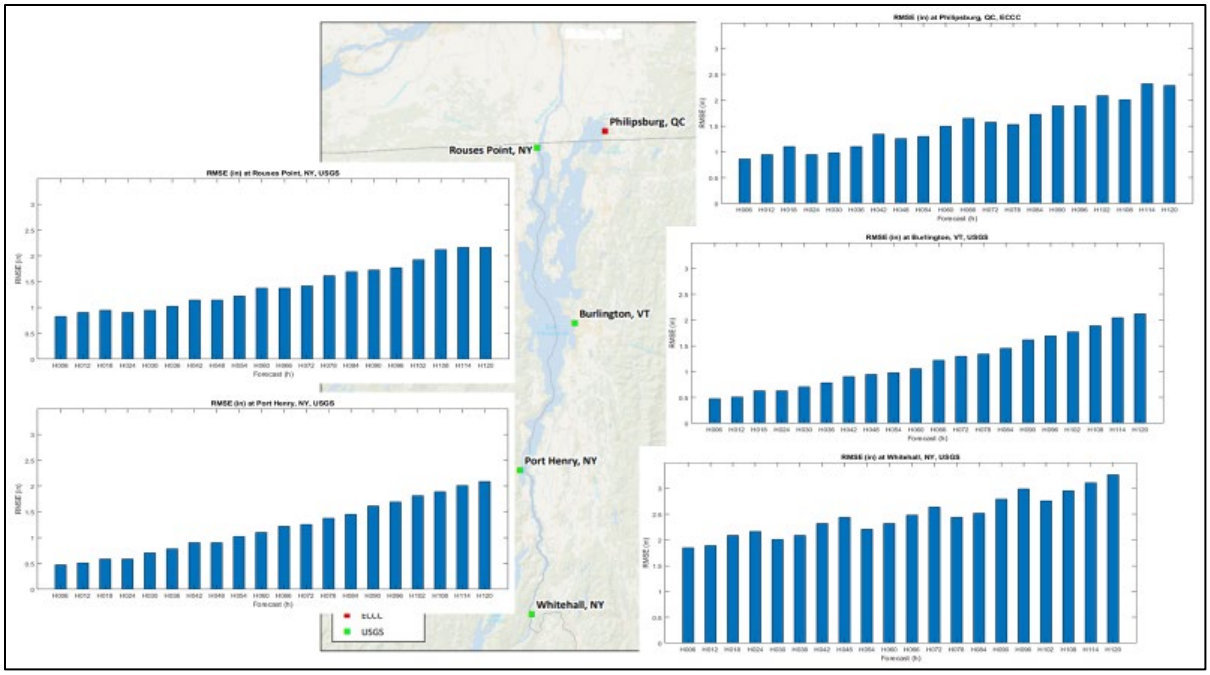

Figure 5.16 Same as Fig. 5.15 but for water level RMSE (in, blue) by forecast projections.

5.2.7 Baroclinic Temperature Testing

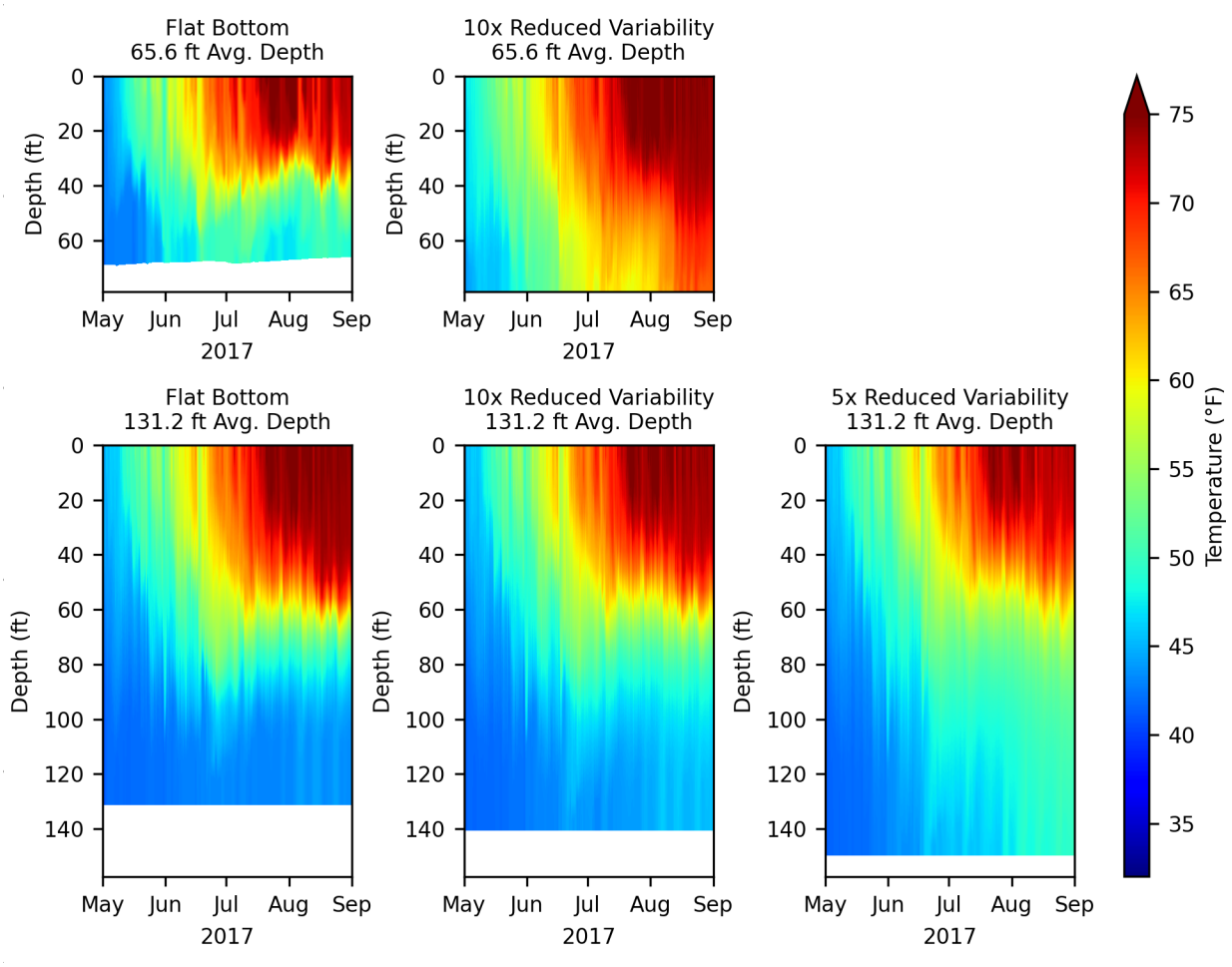

Figure 5.17 FVCOM thermal structure results using bathymetry with reduced depth-variability.

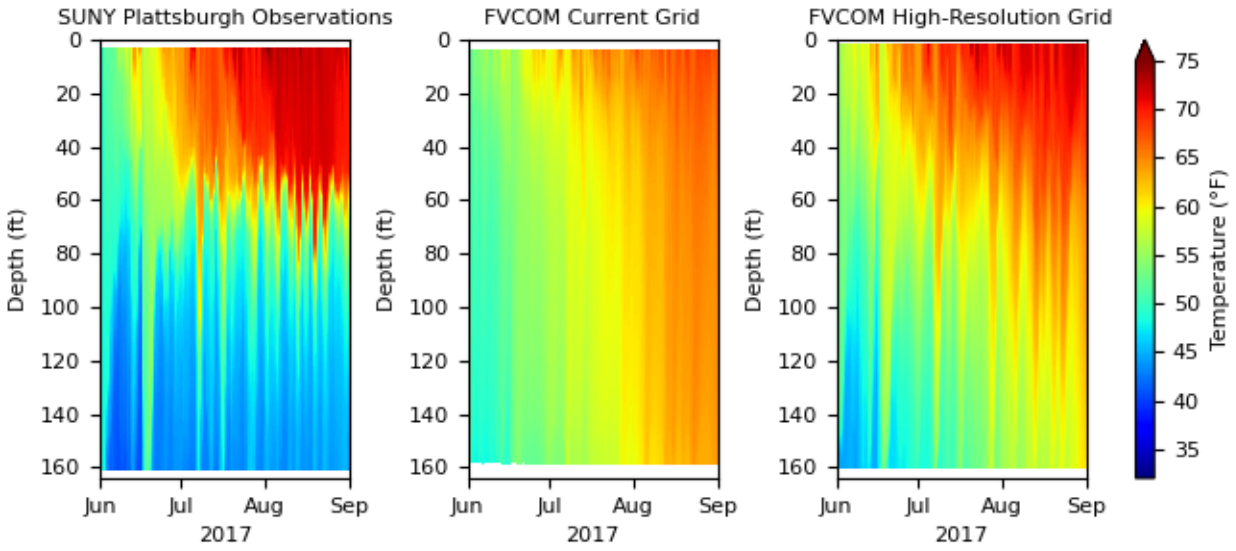

Figure 5.18 FVCOM thermal structure results at Valcour Island using a high-resolution grid.

Attempts were made to run FVCOM in a 3D baroclinic mode to predict water temperature; however, it was ultimately found that the parameterization of FVCOM in combination with the naturally steep bathymetry of Lake Champlain result in unrealistically-high vertical mixing, and preclude the accurate formation of a stable thermal structure. Extensive testing was done to attempt to debug this issue, including smoothing the grid, increasing the horizontal and vertical grid resolutions, reducing the model time step, using FVCOM's hybrid vertical coordinate system, turning off wetting and drying, and turning off meteorology and river forcing, among other configurations. Results of these tests found that smoothing the grid and increasing the horizontal resolution each result in better thermocline stability, but require trade-offs that are untenable for the Lake Champlain modeling system.

Figure 5.17 shows a time-series of modeled thermal structure near Valcour Island under various scenarios of reduced depth variability. Observations at this location show a stable thermocline at a depth of approximately 50 feet (Figure 5.18). To setup these model configurations with reduced depth variability, the following smoothing function was applied to the bathymetry:

$$z_{smooth} = c_1(z - \bar{z}) + c_2$$

Where:

z_{smooth} is the smoothed depth

z is the original (realistic) depth

c_1 is the constant smoothing factor

c_2 is the desired average bottom depth for the smoothed bathymetry

Runs with smoothing factors of 0 (flat bottom), 0.2 (5x reduced variable), and 0.1 (10x reduced variability) were tested along with average bottom depths of 65.6 feet and 131.2 feet. The models were run with HRRR meteorological forcing, and the FVCOM solar heating algorithm was used to calculate surface heat flux in the model (Chen et al 2013). Results of this testing shows that when the model is run with a flat bottom, a stable thermocline forms at a depth that is roughly consistent with observations (Figure 5.17). When even 10% of the original depth variability is reintroduced into the system, the stability of the thermocline is impacted, and these impacts are more severe as depth variability is further increased.

Following these results, attempts were made to mitigate the unrealistically-high vertical mixing by increasing the horizontal resolution of the model grid. A model grid was developed with a horizontal resolution of 164 feet, which increased the number of triangular grid cells to 1,318,193 from 61,332. Results of these tests (Figure 5.18) found that increasing the horizontal resolution of the grid does improve thermocline stability, but that there is still unrealistic decay in thermal stratification over the course of the season. This results in a more diffuse thermal structure than was observed at this location. In addition, the computational requirements associated with modeling the lake at the higher resolution are unlikely to be feasible in a real time operational environment, which is a requirement of the Lake Champlain nowcast/forecast system.

It was concluded from these baroclinic tests that the configuration and parameterization of FVCOM produces unrealistically-high vertical mixing in the naturally-steep Lake Champlain domain, which degrades the modeled thermal structure and precludes the use of the model for simulating lake temperature. As a result of these findings, it was determined that the Lake Champlain nowcast/forecast system will operate FVCOM in a 3D barotropic mode.

Preliminary testing was also conducted with the SCHISM hydrodynamic model (Zhang 2016) for the summer of 2017, using the same grid and atmospheric forcing as the FVCOM model. Results from this testing found that SCHISM showed improvement over FVCOM in simulating Lake Champlain thermal structure. Thermal stratification was present in the preliminary SCHISM results throughout the main basin of the lake during the summer stratified season. This thermal stratification was present in the SCHISM results when using a configuration with 20 uniform vertical sigma layers, and was strengthened when using a hybrid sigma and z-level

configuration. Additional evaluation of the SCHISM hydrodynamic model is outside the scope of the project, but may be warranted for any future improvements to the Lake Champlain modeling system.

5.3 WAVEWATCH III

5.3.1 Coupling with FVCOM Water Levels

An initial water level coupling test was set up for the period of February 20 to April 20, 2017. The purpose of this test was to validate the methods by which spatially-variable water level results can be conveyed from the FVCOM hydrodynamic model to the WAVEWATCH III wave model (Section 2.4). The period of February to April, 2017 was chosen as a period with substantial change in water levels, with a rise in lake level of over one meter during the two-month run.

After running WAVEWATCH III with the water level results from FVCOM, it was found that the extent of inundation was identical between the two models at each hourly output time step. This demonstrates the ability to convey water level information from FVCOM to WAVEWATCH III using the one-way coupling process that was developed. It is beneficial to accurately model the extent of inundation in WAVEWATCH III such that wave heights are predicted in flooded regions of the domain, which has direct implications on the severity of flood impacts.

5.3.2 Sensitivity to Water Currents

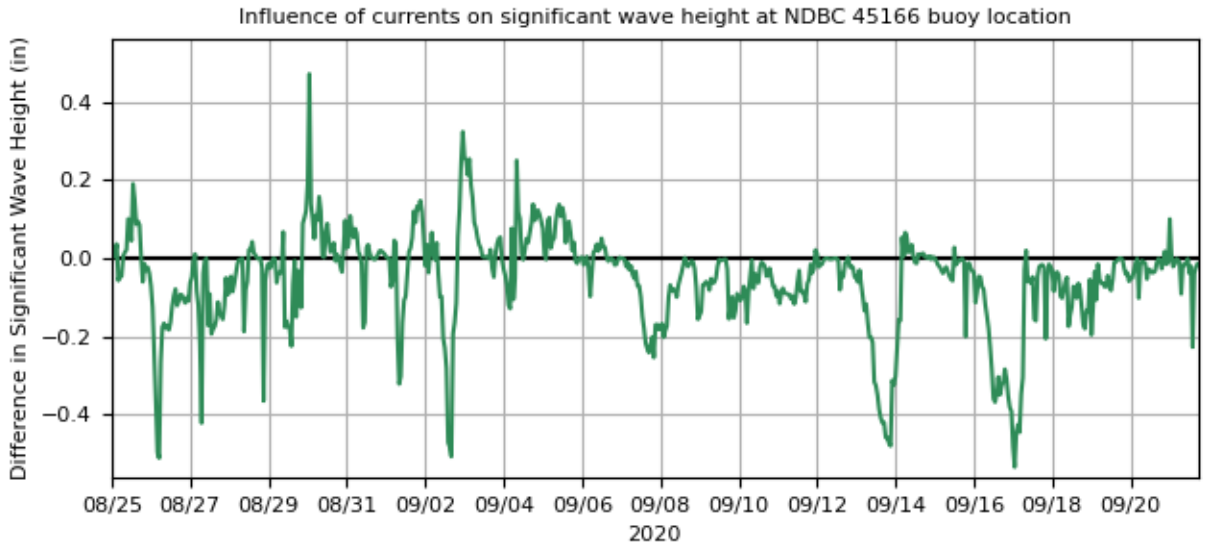

Figure 5.19 Sensitivity of modeled wave heights to water currents at the location of NDBC Buoy 45166 (difference between model runs with and without current forcing).

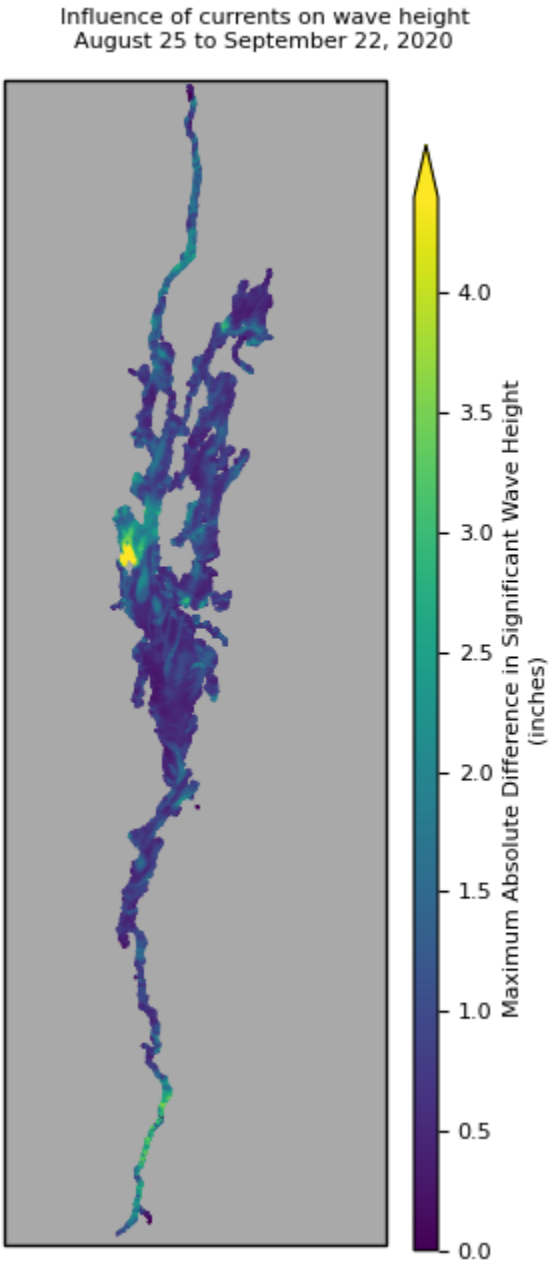

Figure 5.20 Spatial differences in sensitivity of modeled wave heights to water currents (runs with and without current forcing).

Sensitivity tests were conducted to evaluate the influence of water currents on wave height results. Tests were run for the period of August 25 through September 21, 2020, which is a period with several strong wind events. In these tests, FVCOM was first run to produce spatially variable water level and water current results over the test period. WAVEWATCH III was then

run with and without FVCOM water current forcing to quantify the sensitivity of wave height results to realistic water currents in the lake.

Water currents were coupled from FVCOM to WAVEWATCH III using the same general process as was used for water levels (Section 2.4), and both models were run using the same unstructured mesh. However, because water currents are defined on the center of triangular grid elements in FVCOM and on the vertices of the elements in WAVEWATCH III, spatial interpolation and extrapolation were necessary to process FVCOM output into WAVEWATCH III input. Bilinear interpolation was used to map data from mesh element centers to mesh element vertices. In addition, minimal extrapolation was necessary in areas such as the outer boundary of the grid mesh, where element vertices may be present outside the convex hull of surrounding element centers. Nearest neighbor extrapolation was used in these cases.

Results from these sensitivity tests demonstrate that incorporating water currents has minimal impact on wave height results. Comparisons of wave height results with and without water current forcing were produced at the location of the Inland Sea Buoy, NDBC 45166 (Figure 5.19). During the analysis period, there was a maximum effect of less than 0.5 inches in significant wave height when currents were incorporated, compared to when they were not. These largest differences generally occurred during periods when observed significant wave heights were above 4 feet. Resulting wave heights at this location were generally slightly smaller when currents were included, on top of a general trend of low bias in the model during large wave events (Section 5.3.5).

Spatial analysis of the model results generated as part of these sensitivity runs showed a similarly small influence of water currents on modeled wave heights throughout the majority of the domain (Figure 5.20). However, some areas of the domain showed differences in significant wave heights of approximately 2-3 inches when currents were included, including in the narrow Richelieu River and South Lake portions of the domain and the channel west of Grande Isle, and the largest differences occur in around the northern portion of Valcour Island.

Results of these sensitivity tests found that the influence of water currents on wave heights is minimal under most conditions and throughout most locations of the lake. When currents are included, significant wave height results during high wave events are typically reduced, exacerbating an existing low bias in the model. Based on these results, it was determined that FVCOM water currents would not be incorporated as forcing in the wave model.

5.3.3 Incorporating Ice Cover

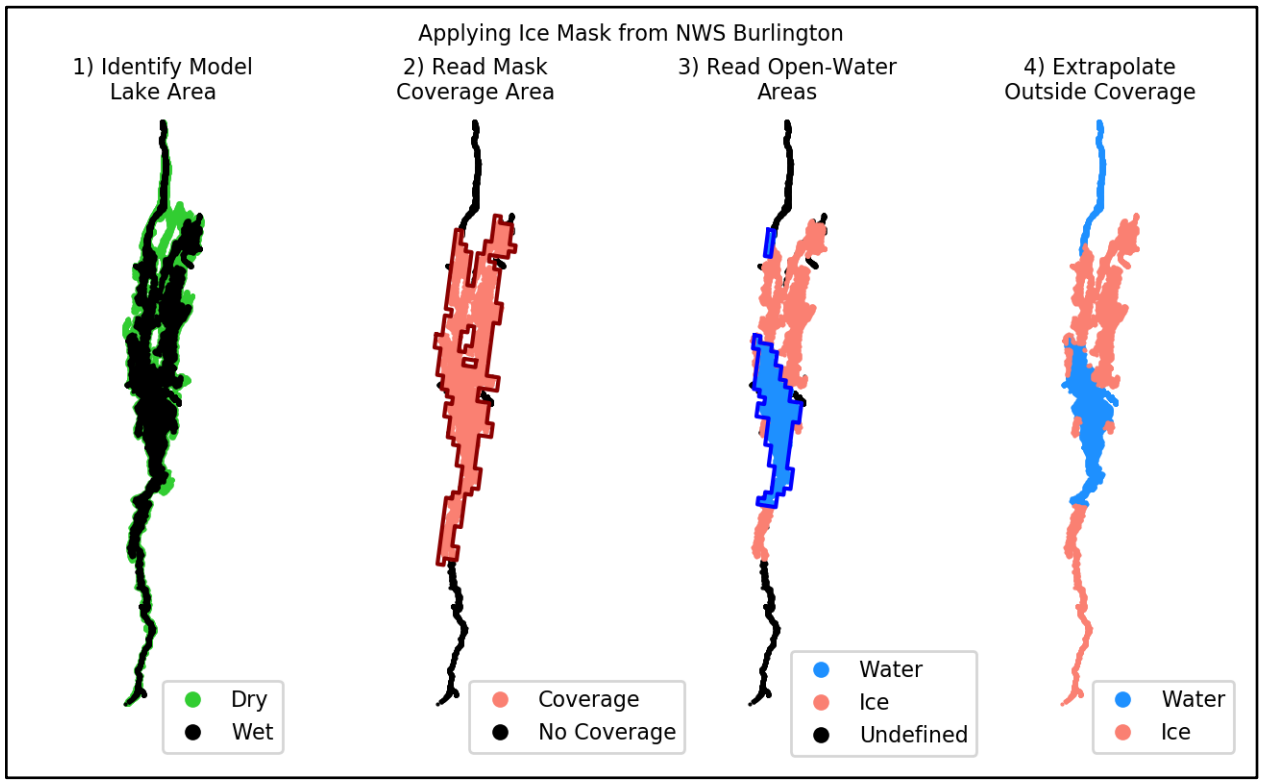

Figure 5.21 Creating ice forcing from an ice mask.

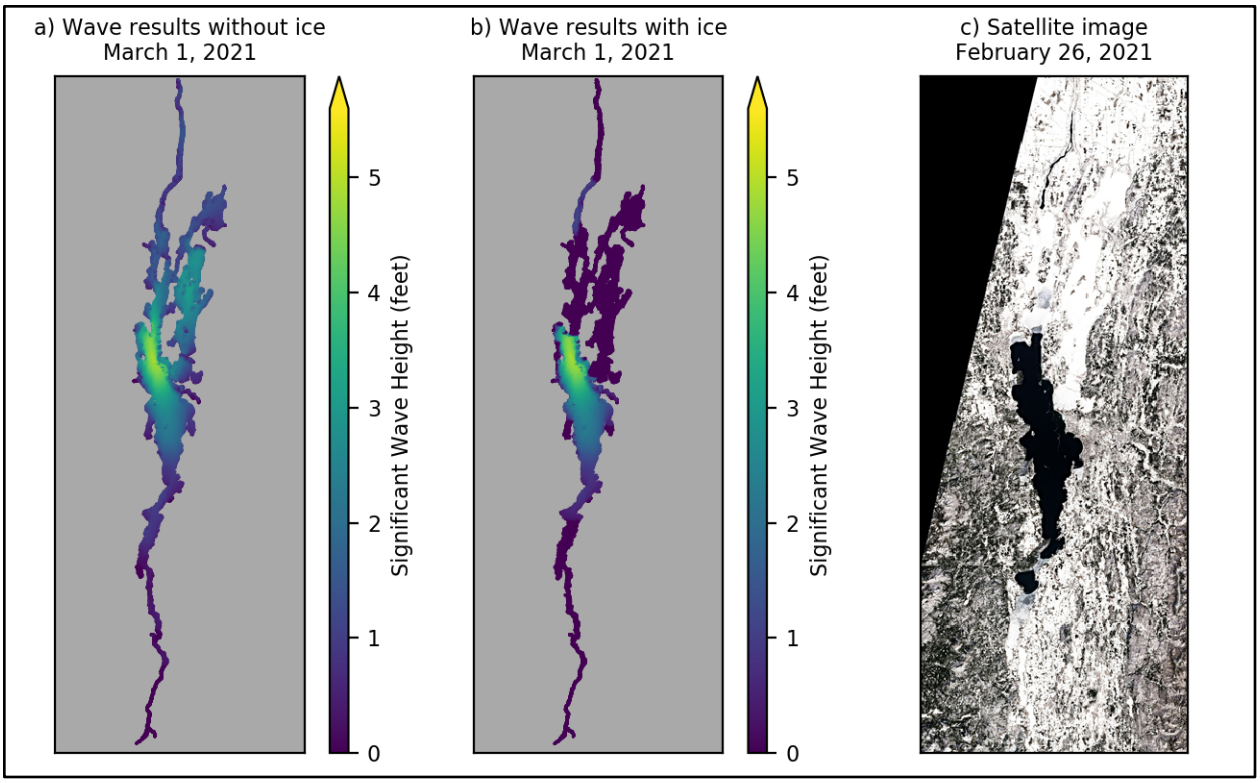

Figure 5.22 Influence of ice forcing on modeled wave height results.

Because Lake Champlain experiences ice cover during winter, and ice cover inhibits wave formation where present, it is critical to represent ice cover in the WAVEWATCH III wave model in order to accurately depict the distribution of waves during the winter.

Availability of ice cover data for Lake Champlain is limited. After reviewing available data sources, it was determined that the best available source of ice cover data is an ice mask produced by the NOAA National Weather Service Weather Forecast Office in Burlington, VT (WFO Burlington). These ice masks are manually produced by a technician from clear-sky satellite imagery, and uploaded to a webserver from which they are automatically downloaded and processed for use in the Lake Champlain forecast system. The ice masks are binary, showing presence or absence of ice, and have spatial resolution of approximately 2.5 km. Because they are based on clear-sky satellite imagery, temporal availability of the data is irregular, and there may be periods of multiple weeks between updates. Ice cover in the model is persisted from the last available ice mask update. This ice cover dataset is not operational, and the format and distribution of data was established through an informal agreement between WFO Burlington and the CIGLR/GLERL Lake Champlain model development team.

The ice mask covers only the Main Lake and Restricted Arm portions of the domain, and does not include South Lake or the Richelieu River. Ice cover in these areas is estimated using nearest neighbor extrapolation. However, ice cover in the Richelieu River is extrapolated separately,

based on ice values at the northwest boundary of the ice mask coverage area, at the outlet of the Main Lake near Rouses Point, NY. This is done because some portions of the Richelieu River are nearest to Missisquoi Bay by straight distance, but ice cover at the lake's outlet to the Richelieu River is expected to be more representative of ice conditions in the Richelieu River, due its hydrologic proximity (Figure 5.21).

Data from the National Ice Center Ice Mapping System operational daily 1 km ice product was also considered as a source of ice forcing data. However, the 1-km ice product uses a 4-km land mask, and after review, it was determined that the dataset has inadequate accuracy and spatial precision within Lake Champlain to serve as an ice forcing data source in the modeling system. In addition, while FVCOM has the capability to dynamically predict ice cover, the inability of the model to accurately represent thermal structure in Lake Champlain precludes the use of an FVCOM ice model as a source of ice forcing data in the wave model (Section 5.2.7).

Ice cover is incorporated into WAVEWATCH III using a simple blocking parameterization. This parameterization utilizes a binary presence or absence treatment of ice cover, with any ice-covered portions of the model domain treated as land in model calculations. These pseudo-land boundaries mask wave formation within the ice-covered area, as well as influencing wave dynamics in surrounding areas just as a land boundary would. In the WAVEWATCH III model output, ice-covered areas are indistinguishable from land areas, and no results are produced in ice-covered areas of the domain. When post-processing data for use in analyses or visualizations, significant wave height values in ice-covered areas of the domain are manually set to zero, which is believed to be a reasonable estimate of wave height in ice-covered areas (Figure 5.22).

5.3.4 Implicit/Explicit Solver Testing

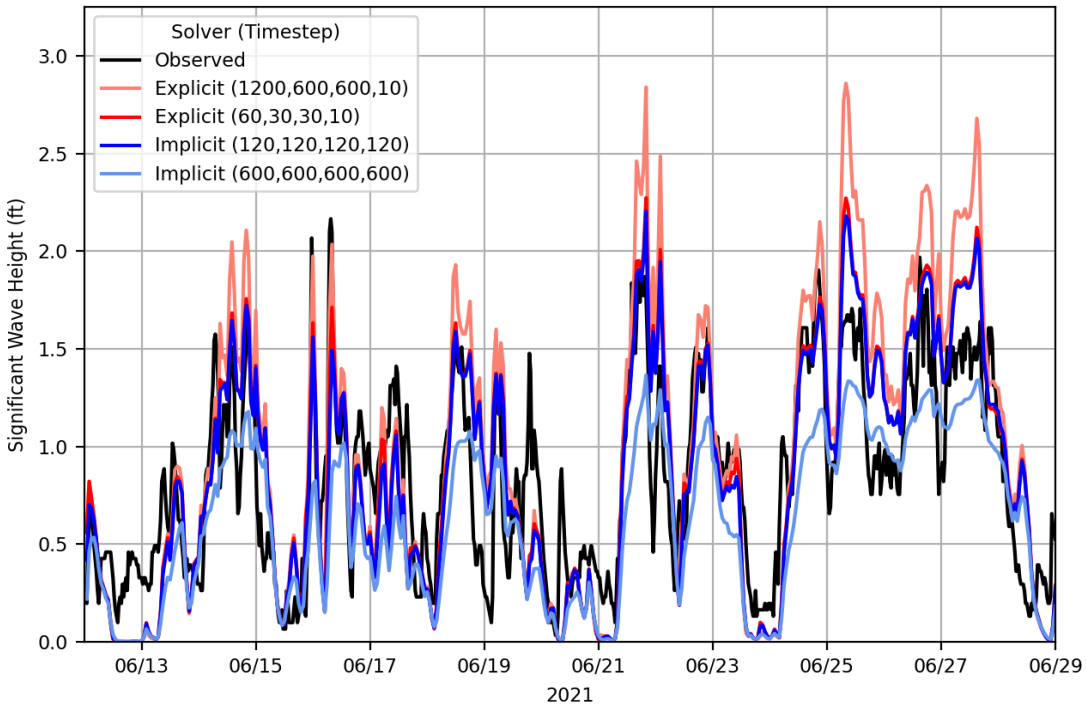

Figure 5.23 WAVEWATCH III explicit and implicit solver convergence.

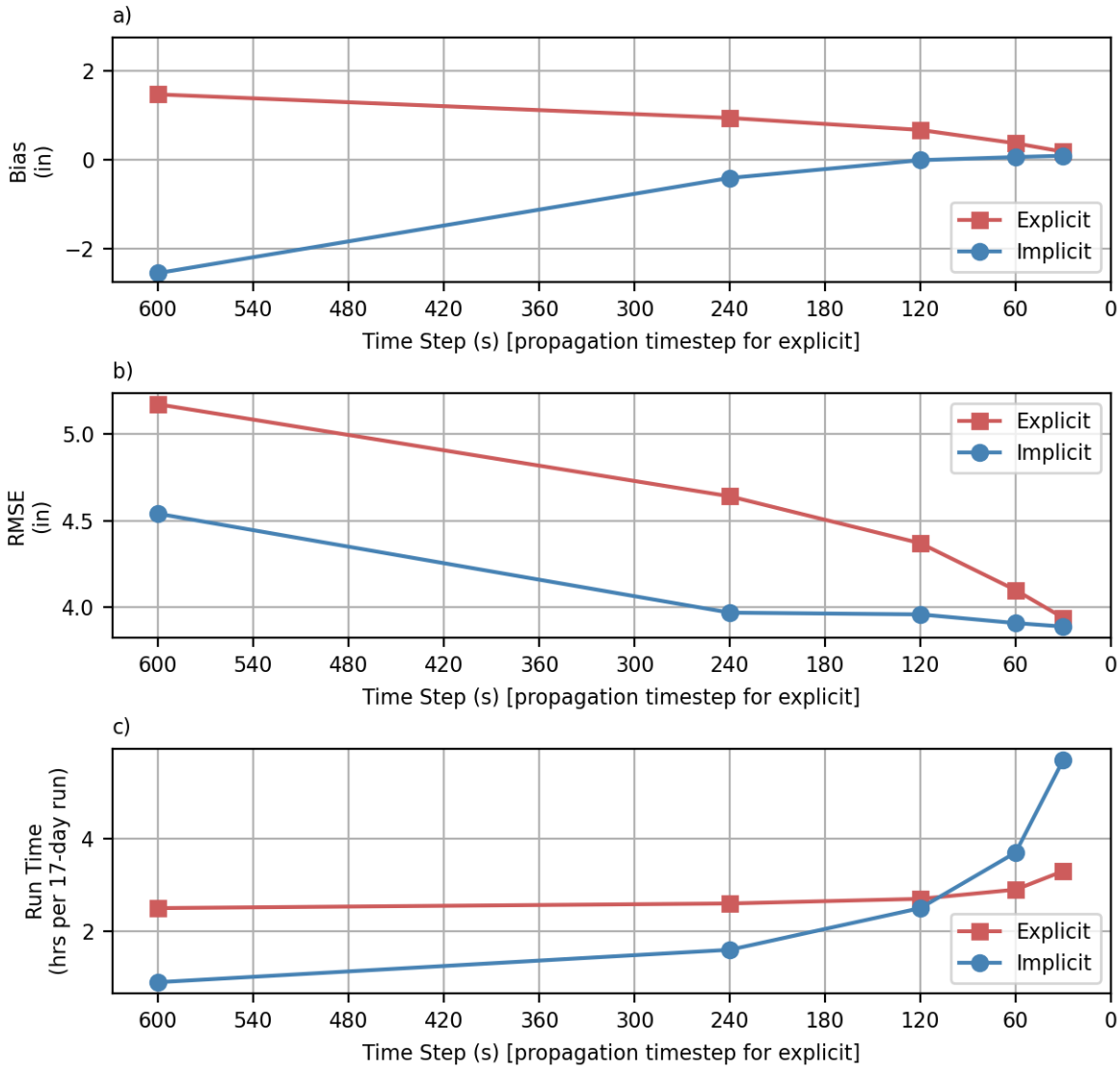

Figure 5.24 WAVEWATCH III model configuration optimization.

Testing was conducted for the WAVEWATCH III model to evaluate the optimal solver and time step configuration. Model runs were conducted using both the implicit and explicit solver with different time step settings to assess model convergence and model run times (Figure 5.23). All models were run on the same HPC system using 256 cores. Model results were compared between runs to assess convergence, and were compared to buoy results from the GLERL Waverider buoy (Section 5.1) to assess model skill. A period of June 12-29, 2021 was chosen for these tests, because it is a period with multiple wave events with significant wave heights on the order of 2 feet, which includes the maximum wave heights observed at the Waverider buoy at the time the tests were conducted.

All model runs used version 6.07 of WAVEWATCH III, and included HRRR wind and spatially variable FVCOM water levels. Explicit runs were conducted with spatial propagation (CFL x-y) time steps of 600s, 240s, 120s, 60s, and 30s; all runs used global time steps of twice the CFL x-y time step, refraction time steps equal to the CFL x-y time step, and minimum source term time steps of 10s. The relative sizing of these time steps is consistent with the ranges outlined in the WAVEWATCH III user manual (WW3DG 2019). Implicit runs were conducted with time steps of 600s, 240s, 120s, 60s, and 30s. Time-series of significant wave height results were extracted at the location of the Waverider buoy, and corresponding skill statistics (RMSE, Bias) were calculated.

Time-series and skill statistic results suggest that approximate model convergence is achieved at time steps at or below approximately 120s when using the implicit solver (Figure 5.24). Model runs using the explicit solver do not appear to fully converge, even at the 30s CFL x-y time step. Models run with the explicit solver have an increasing high bias when increasingly longer time steps are used, while models run with the implicit solver have an increasing low bias when time steps longer than 120s are used. Results from each the implicit and explicit solver runs converge toward a common result at increasingly smaller time steps (Figure 5.23).

Results from these optimization tests also demonstrate the penalty in run time when smaller time steps are used. An implicit time step of 60s resulted in a 52% increase in run time over a time step of 120s, and an implicit step of 30s resulted in a 134% increase in run time over a time step of 120s. Based on the convergence and run time results of these optimization tests, the implicit solver with a time step of 120s was determined to be the optimal configuration.

5.3.5 Skill Assessment at Buoy

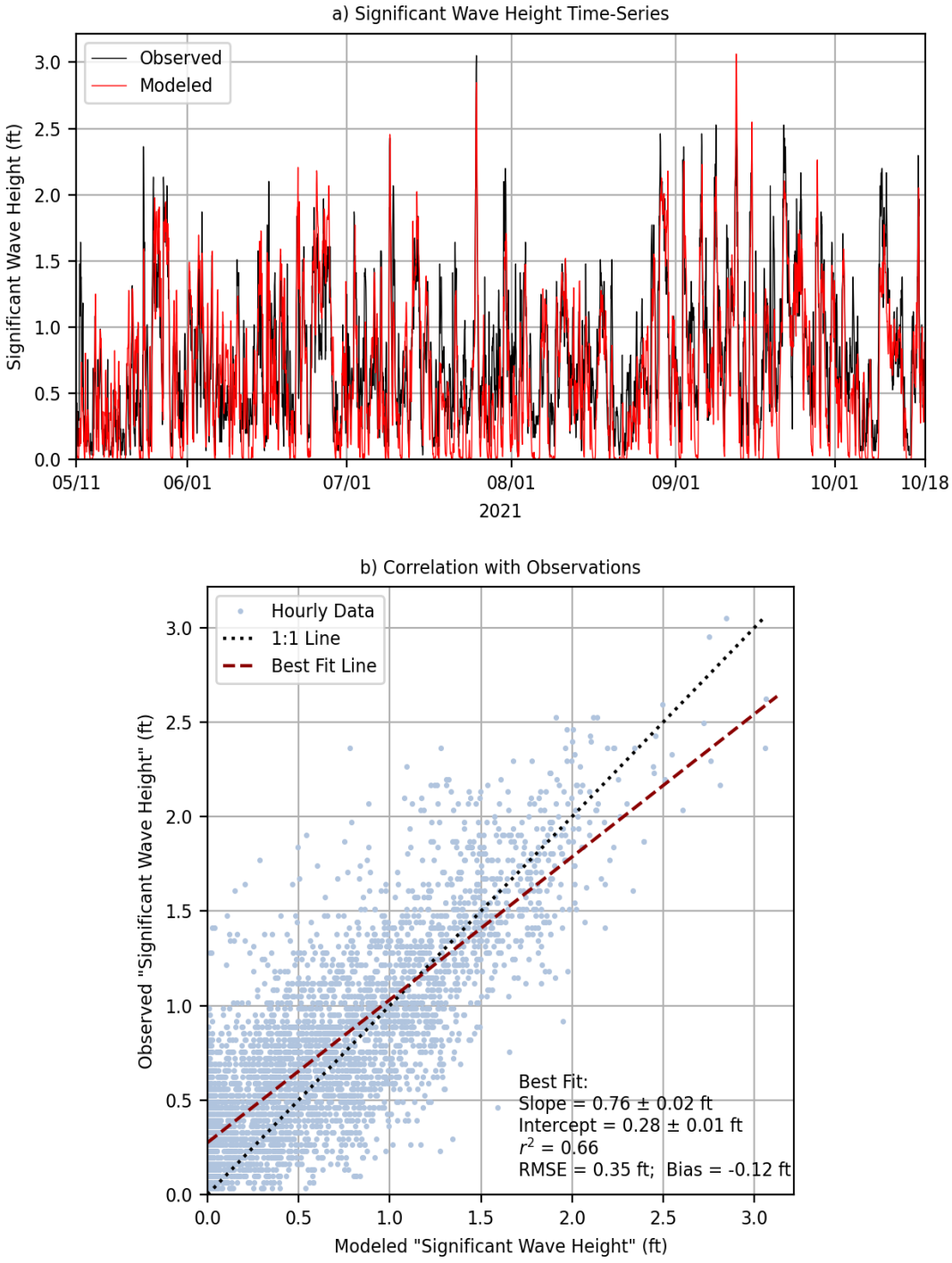

Figure 5.25 Skill assessment of modeled wave height.

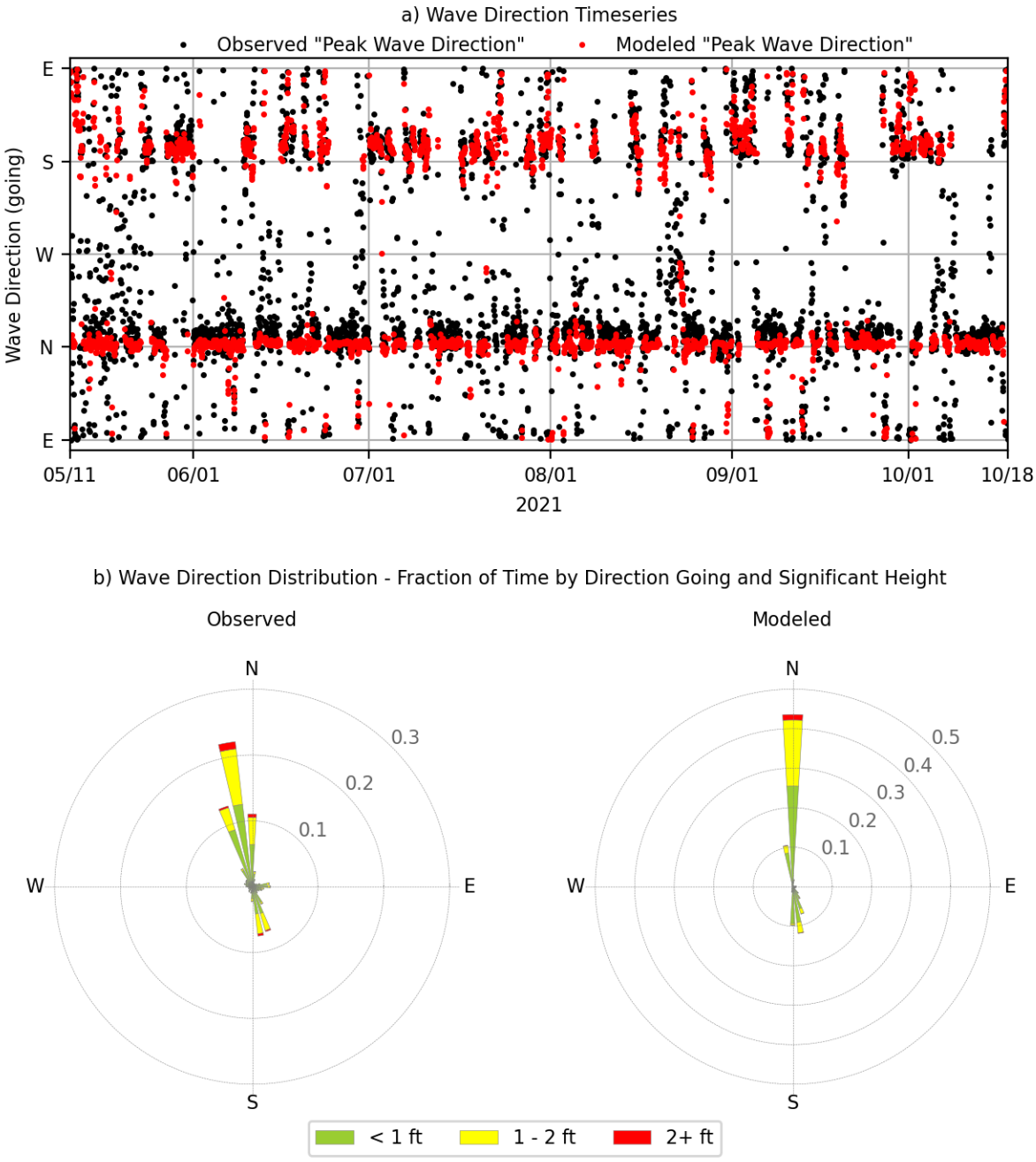

Figure 5.26 Skill assessment of modeled wave direction.

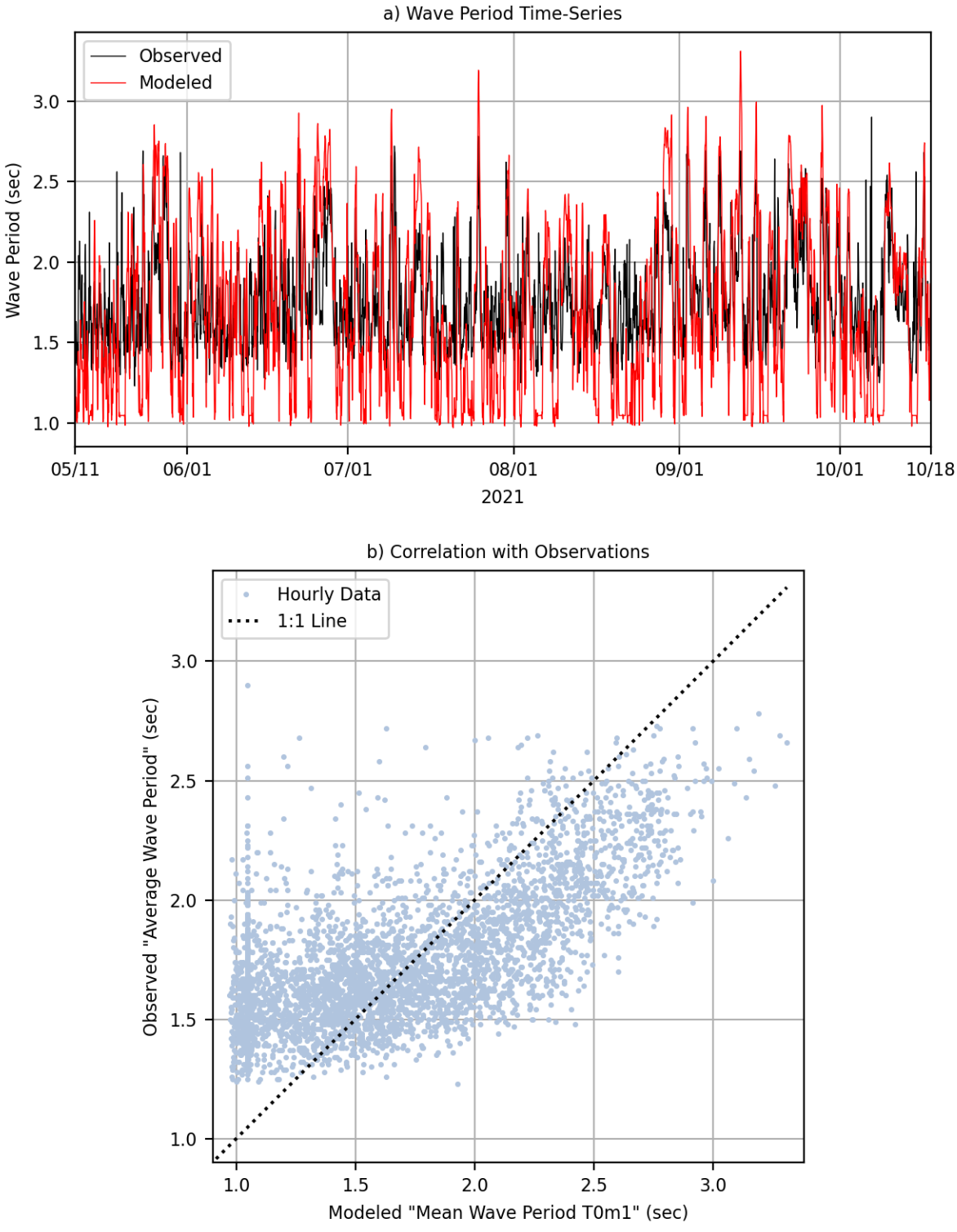

Figure 5.27 Skill assessment of modeled wave period.

A skill assessment was conducted at the Waverider buoy location for the deployment period of May 11 to October 18, 2021. A hindcast simulation was run for this period using the WAVEWATCH III nowcast model configuration, which uses the implicit solver with a time step of 2 seconds, HRRR winds, and spatially variable water level information from FVCOM. Wave height, wave direction, and wave period results were extracted at this location and compared to Waverider buoy observations.

Modeled significant wave height results show an overall agreement with significant wave height observations from the Waverider buoy, both in terms of the timing and magnitude of events (Figure 5.25). There is a tendency for the model to under-predict wave heights by several inches during periods with bigger waves, though this is not universally true. The model has an overall bias of -0.12 inches in significant wave height over the skill assessment period. Lake Champlain is known to experience waves on the order of 10 feet (Section 1); however, the highest waves observed on the lake during the deployment period were only approximately 3 feet in significant wave height, so no comparison could be made for these especially large wave events. Lake Champlain often experiences large waves as a result of strong winds in the late fall period before ice formation (i.e. November, December), but logistical restraints required that the buoy be recovered in October. An additional deployment of the Waverider buoy is planned for the 2022 ice-free season.

Modeled wave direction results show similar dynamics to observed wave direction, with waves most commonly moving northward at the buoy location (Figure 5.26). Modeled waves most commonly move more-directly north, while observed wave directions have a slight 10 to 20 degree westward component. Modeled wave periods do not show good agreement with observations, and have a nonlinear relationship (Figure 5.27). It should be noted that in the case of wave period, derived parameters available for comparison are not identical, and may account for some of these discrepancies. Additional analysis of these results is planned, and results of these analyses may result in additional modifications to the WAVEWATCH III model configuration.

6 NOWCAST/FORECAST SYSTEM DESCRIPTION

6.1 WORKFLOW

The Lake Champlain nowcast/forecast system is a real time implementation of the Lake Champlain modeling system, configured to produce 5-day forecasts of spatially variable, water level, water currents, and waves. The nowcast/forecast system is designed to run in a near-real time operational environment, and at the time of this report is running in an experimental pseudo-operational state. The nowcast model updates to the present every 6 hours, nominally at 00:00, 06:00, 12:00, and 18:00 UTC. 5-day forecasts are generated once per day, nominally from 00:00 UTC.

The workflow for the modeling system was developed in Python 3, and consists of forcing data archiving, forcing data pre-processing, and data post-processing components. The data archiving

processes are maintained and run independently from the model processes. In order to allow for necessary forcing data to be posted and subsequently archived, initiation of nowcast and forecast runs are delayed by approximately 80 minutes and 140 minutes, respectively. The delay is imposed primarily due to a delay in availability of NWM results (Section 5.2.3). Because FVCOM water level results are used as an input for WAVEWATCH III, the FVCOM run for a given time must run before the corresponding WAVEWATCH III run (Section 2.4).

Model preprocessing consists of reading archived forcing data and processing it into the formats used as input in FVCOM and WAVEWATCH III. Forcing is generally prepared on an hourly input time grid, and 2D input fields are prepared on the models' spatial grid. Any temporal upscaling is done using linear interpolation, and any temporal downscaling is done through aggregation and averaging. Spatial re-gridding is done through bilinear interpolation, and any extrapolation is based on the nearest neighbor. If one or more forcing data sources is unavailable at the time that pre-processing for a run has initiated, the system will resort to backup data sources or processing methods (Section 6.2).

Post-processes are run after all models for a given time have completed. Post-processing includes extracting and visualizing model output and forcing, and posting the current nowcast and forecast results online. Currently, time-series of nowcast and forecast water levels, wave heights, total river inflows, and wind velocity are produced, as well as 2D plots and forecast animations of wind velocity, water level, surface currents, and wave heights.

6.2 BACKUP FORCING

Table 6.1 Backup forcing methods.

Forcing Type	Data Source	Interpolation Method	Alternate Source(s) / Method(s)
Wind	HRRR (Nowcast) HRRR / GFS (Forecast)	Linear up to 12 hours	Recent HRRR forecast Recent GFS forecast Recent NDFD forecast Revert to no-wind model (fade to calm over 12 hours)
Overlake Precipitation	HRRR (Nowcast) HRRR / GFS (Forecast)	Linear up to 4 hours	Revert to no overlake precip
River Inflow	NWM	Linear up to 2 days	Extrapolate flows up to 2 days Revert to climatology/average
Water Level Nudge	USGS / ECCC Water Level Gauges (5)	Linear up to 1 day	Revert to no-nudge model

Downstream Water Level	ECCC St Jean Water Level Gauge (1)	Linear up to 1 day	Extrapolate up to 1 day (nowcast) or 6 days (forecast) Estimate from Rouses Point USGS gauge Estimate from Burlington USGS gauge Abort system
Ice Cover	NWS Burlington	Linear up to 60 days	Extrapolate up to 60 days Revert to ice free

If primary forcing for a parameter is missing at the time that model pre-processing occurs, attempts are made to estimate the values of that parameter using the next-best available data source and/or estimation method. Planning for backup forcing is an important component of the nowcast/forecast system, because the system is designed to become operational, and therefore to function without interruption. Backup forcing allows the system to continue operating when primary forcing is unavailable for any reason, albeit in a sub-optimal state.

Before reverting to backup forcing, attempts are made to fill any gaps in data through time-interpolation. Limits to time-interpolation vary by parameter, and were chosen with typical decorrelation timescales in mind. If data gaps cannot be filled through interpolation, backup estimation methods are used. These include the use of alternate data sources for forcing when available, simple data extrapolation methods, and/or reverting to a conservative constant field that allows the modeling to continue running without the influence of that forcing parameter. Backup forcing methods for each parameter are listed in Table 6.1.

7 FUTURE PLANS

7.1 WAVEWATCH III OPERATIONAL TRANSITION

In accordance with the project plan, the WAVEWATCH III component developed during this study has been transitioned to NWS/NCEP/Environmental Modeling Center for operational implementation as part of the Great Lakes Wave Model (GLWU). At present, the operational GLWU v1.0 features a single unstructured mesh describing the five Great Lakes. As part of this operational transition, the Lake Champlain domain mesh will be integrated with that of the existing five lakes, and run as a single unstructured wave model.

Similar to the existing operational GLWU, the extended GLWU model will be run with hourly cycling - out to 144 hours every 6 hours (at 01Z, 07Z, 13Z, and 19Z) and out to 48 hours for the remaining cycles. The Lake Champlain portion of this model will be forced with HRRR fields out to 18 hours, similar to what was done during the present study. For forecast hours 19 to 84, this domain will be forced with the North American Mesoscale Model (NAM), and for hours 85 to 144 it will be forced by the Global Forecast System (GFS). Lake ice forcing over Lake Champlain will initially be provided by the WFO Burlington Ice Desk, and in future potentially by the Winter Hydrology and Remote Sensing Desk at the National Water Center. In this initial

implementation, the lake levels will be taken as constant in space and time (no surge effects). In future versions, when dynamic water levels from FVCOM become available operationally, these will be included in order to determine the effect of inundation on wave heights at the lake coastline.

The current implementation timeline of the above-mentioned scope calls for all model changes to be integrated and frozen by May 15, 2022. This will be followed by a period of extensive testing and field evaluation, including by WFO Burlington, planned for May 15 to June 30, 2022. Upon successful testing and evaluation, the upgraded GLWU v2.0, including Lake Champlain, is planned to be implemented operationally by FY23Q1.

7.2 FVCOM OPERATIONAL TRANSITION

The FVCOM component developed in this study is expected to be transitioned to NOAA operations to provide forecast guidance for the NWS GLWU-Lake Champlain, NWS Weather Forecast Office in Burlington, Vermont, the NWS Northeast River Forecast Center in Norton, MA, Environmental Canada, other users (e.g. U.S. Coast Guard), and the general public. As mentioned earlier in this report, FVCOM's numerics cannot accurately predict the thermocline due to the steep bathymetry in the almost fjord-like Lake Champlain and thus is presently run at GLERL in 3D barotropic model. In this mode, FVCOM provides forecast guidance of water levels and barotropic driven currents, but not water temperatures. Thus, the configuration of FVCOM used for operations will also be 3D barotropic.

NOS/CO-OPS in collaboration with GLERL and NOS/CSDL will develop a transition plan to move the FVCOM component into NOAA operations. The initial vision is to have FVCOM run on NOAA WCOSS operated by NWS/NCEP Central Operations, the same location where GLWU-Lake Champlain will be run and operated in a similar manner as NOS Great Lakes Operational Forecast System. The transition plan is expected to be completed before the end of FY22.

Although the exact details of how FVCOM would run in operation will be ironed out in the transition plan, it is anticipated that FVCOM would be run every six hours (e.g. 0, 6, 12, and 18Z) to provide forecast guidance out to 120 or 144 hours. It would likely be forced in a similar manner as GLWU-Lake Champlain using meteorological predictions from HRRR for the first 18 hours and NAM, and for hours 85 to 120 or 144 be forced by the GFS. Predictions of river inflow would be provided by the NWS National Water Model. The forecast guidance from FVCOM would be available on its unstructured grid in netCDF and possibly interpolated to the NDFD 2.5 km regular grid. The forecast points would also be made available at specified forecast locations (e.g. USGS and ECCC gauges) in both netCDF and NWS Standard Hydrometeorological Exchange Forecast (SHEF).

No year has been specified yet on when the FVCOM would be implemented operationally.

8 CONCLUSIONS

An experimental flood forecasting system was developed for the Lake Champlain-Richelieu River basin. Flood forecasting system addresses one objective of the IJC study: developing improved forecasts in Lake Champlain. The system resolves wind-driven spatial variability in water levels, surface waves, and the associated extent of coastal inundation, thus improving upon an existing one-dimensional model that is currently used for forecasting by the NWS NERFC. This is the first lake flood forecasting system that uses NWM inflows. For accurate prediction of water level in Lake Champlain, NWM domain was expanded across the Richelieu River portion of the Lake Champlain basin.

FVCOM hydrodynamic model runs in a 3D barotropic mode without ice, driven by meteorological forcing (wind and overlake precipitation), river flows, and single outflow (Richelieu River). Floodplain is included in the model domain to predict wetting/drying due to seasonal and event-driven water level variations. The current version of the FVCOM uses HRRR model surface wind and precipitation predictions in the nowcast mode. In the forecast, HRRR forecast guidance is used in the first 48 hours, followed by GFS forecast guidance for the rest of the 5-day forecast period. Water level observations at St. Jean, QC ECCC gauge are used as downstream boundary conditions. In addition, spatially-uniform water level adjustment is used in the nowcast mode to keep water level from drifting over time. Model results show strong agreement with water level observations.

Wind waves in the lake are predicted by the WAVEWATCH III wave model, with wetting/drying in floodplain areas informed by FVCOM. This is the first Lake Champlain wave model capable of predicting waves in flood areas. Model grid and wind forcing is identical to that of FVCOM. Wave model is validated with observations collected at Waverider buoy deployed in summer of 2021. Results showed that wave model predictions are well-correlated with buoy observations but modeled wave heights are slightly lower than observed.

The forecast system automatically processes model input to generate model forcing: hydrologic inflows, meteorological forcing and saves model output for post processing. A nowcast/forecast cycle was implemented on NOAA/GLERL's research infrastructure to provide experimental predictions: nowcast runs 4 times per day, 5-day forecast runs once per day. Lake Champlain predictions as generated for water levels, currents, and waves and data is available online: www.glerl.noaa.gov/res/champlain. Webpage presents nowcast and forecast results for key outputs from the FVCOM and WAVEWATCH III models and intended to be a resource for both forecasters and the public. Updates are provided in near-real time, after each nowcast/forecast run. An experimental real-time application of the forecasting system began operation in 2020 at NOAA GLERL and the system exhibited a high level of robustness during two years of operations.

9 ACKNOWLEDGEMENTS

We would like to thank Kaelan Weiss for his assistance in wind forcing skill assessment, ECCC for providing topobathymetric data and Burlington WFO for providing an ice mask. This is GLERL Contribution No. 2014. This project was funded by the International Joint Commission (IJC). Funding was awarded to the Cooperative Institute for Great Lakes Research (CIGLR) through the NOAA Cooperative Agreement with the University of Michigan (NA17OAR4320152). This is CIGLR contribution number is 1202.

10 REFERENCES

Anderson, E. J, D. J. Schwab, and G. A. Lang. 2010. Real-time hydraulic and hydrodynamic model of the St. Clair River, Lake St. Clair, Detroit River System. *Journal of Hydraulic Engineering (ASCE)* 136: 507-518

Bjerklie, D.M., Trombley, T.J., and Olson, S.A., 2014, Assessment of the spatial extent and height of flooding in Lake Champlain during May 2011, using satellite remote sensing and ground-based information: U.S. Geological Survey Scientific Investigations Report 2014–5163, 18 p.

Chen, C., H. Liu, and R. C. Beardsley. 2003. An unstructured grid, finite-volume, three-dimensional, primitive equations ocean model: application to coastal ocean and estuaries, *Journal of Atmospheric and Oceanic Technology*, 20: 159-86.

Chen, C., R. Beardsley, G. Cowles, J. Qi, Z. Lai, G. Gao, D. Stuebe, Q. Xu, P. Xue, J. Ge, S. Hu, R. Ji, R. Tian, H. Huang, L. Wu, H. Lin, Y. Sun, L. Zhao. 2013. An Unstructured Grid, Finite-Volume Community Ocean Model: FVCOM User Manual. Fourth Edition. SMAST/UMASSD-13-0701.

Environment Canada (ECCC). 2015. Development of an experimental 2D hydrodynamic model of Lake Champlain using existing bathymetric data (Task 1-2). Technical report prepared by Environment Canada for the International Lake Champlain - Richelieu River Technical Working Group.

Gochis, D.J., M. Barlage, A. Dugger, K. FitzGerald, L. Karsten, M. McAllister, J. McCreight, J. Mills, A. RafieeiNasab, L. Read, K. Sampson, D. Yates, W. Yu. 2018. The WRF-Hydro modeling system technical description, (Version 5.0). NCAR Technical Note. 107 p.

Gochis, D.J., B. Cosgrove, A. RafieeiNasab, A. Dugger, 2019.Status Update and Regional Performance Evaluation of the National Water Model. American Geophysical Union Fall Meeting, San Francisco, CA.

Hunkins, K., Manley, T.O., Manley, P., Saylor, J., 1998. Numerical studies of the 4-day oscillation in Lake Champlain. *J. Geophys. Res. Oceans* 103, 18425–18436.

Hunkins, K.L., Mendelsohn, D., Isaji, T., 1999. Numerical hydrodynamic models of Lake Champlain. In: Manley, T.O., Manley, P.L. (Eds.), Lake Champlain in Transition; From Research toward Restoration. American Geophysical Union, Washington, DC, United States (USA), United States (USA), pp. 117–134.

Mellor, G.L., and T. Yamada. 1982. Development of a turbulence closure model for geophysical fluid problems. *Rev. of Geophysical Space Physics* 20(4):851-875.

Manley, T.O., 2004. Hydrodynamics of the South Main Lake and South Lake, Lake Champlain. In: Manley, T.O., Manley, P.L., Mihuc, T.B. (Eds.), Lake Champlain; Partnerships and Research in the New Millennium. Kluwer Academic/Plenum Publishers, New York, NY, United States (USA), pp. 349–384.

Manley, T.O., Hunkins, K.L., Saylor, J.H., Miller, G.S., Manley, P.L., 1999. Aspects of summertime and wintertime hydrodynamics of Lake Champlain. In: Manley, T.O., Manley, P.L. (Eds.), Lake Champlain in Transition; From Research toward Restoration. American Geophysical Union, Washington, DC, United States (USA), United States (USA), pp. 67–116.

Manley, T.O., M. McCormick, J-C. Gascard, P. Tillier; K. L Hunkins, P. L. Manley, 2012. An Initial View of Subsurface Lagrangian Observations in Lake Champlain; General Patterns, Cross-lake Flow and Coastal Currents. *J. Great Lakes Res*. 38, 76-87

McCormick, M.J., Manley, T.O., Beletsky, D., Foley III, A.J., Fahnenstiel, G.L., 2008. Tracking the surface flow in Lake Champlain. *J. Great Lakes Res*. 34, 721–730.

Myer, G.E., Gruendling, G.K., 1979. Limnology of Lake Champlain. Lake Champlain Basin Study, New England River Basins Commission.

Saylor, J.H., Miller, G.S., Hunkins, K.L., Manley, T.O., Manley, P.L., 1999. Gravity currents and internal bores in Lake Champlain. In: Manley, T.O., Manley, P.L. (Eds.), Lake Champlain in transition; From Research toward Restoration. American Geophysical Union, Washington, DC, United States (USA), United States (USA), pp. 135–156.

Shanley J.B. and J.C, Denner, 1999. The hydrology of the Lake Champlain Basin. Aspects of summertime and wintertime hydrodynamics of Lake Champlain. In: Manley, T.O., Manley, P.L. (Eds.), Lake Champlain in Transition; From Research toward Restoration. American Geophysical Union, Washington, DC, United States (USA), United States (USA), pp. 41-66.

Smagorinsky, J., General circulation experiments with the primitive equations, I. The basic experiment. *Monthly Weather Review*, 91:99-164, 1963.

The WAVEWATCH III® Development Group (WW3DG), 2019: User manual and system documentation of WAVEWATCH III® version 6.07. Tech. Note 333, NOAA/NWS/NCEP/MMAB, College Park, MD, USA, 326 pp. + Appendices.

Zhang, Y., Ye, F., Stanev, E.V., Grashorn, S. (2016) Seamless cross-scale modeling with SCHISM, *Ocean Modelling*, 102, 64-81.

APPENDIX

Table A. 1. Summary of skill assessment statistics evaluating the ability of the Lake Champlain forecast guidance to predict hourly water levels out to 120 hours at the USGS gauge at Burlington, Vermont during 2021. Gray shading, if present, indicates that it did not meet the NOS acceptance criteria.

USGS Gauge at Burlington, VT											
Observed data time period from: 1/ 1/2021 to 12/31/2021											
Variable & Forecast Projection	X (in)	N (hr)	IMAX	MAE (in)	RMSE (in)	SD (in)	NOF <1%	CF >90%	POF <1%	MDNO <N	MDPO <N
H06-h06	5.9	24	365	-0.157	0.472	0.433	0.0	100.0	0.0	0.0	0.0
H12-h12	5.9	24	365	-0.157	0.512	0.472	0.0	100	0.0	0.0	0.0
H18-h18	5.9	24	365	-0.197	0.630	0.591	0.0	100	0.0	0.0	0.0
H24-h24	5.9	24	365	-0.197	0.630	0.591	0.0	100	0.0	0.0	0.0
H30-h30	5.9	24	364	-0.197	0.709	0.669	0.0	100	0.0	0.0	0.0
H36-h36	5.9	24	364	-0.236	0.787	0.748	0.0	100	0.0	0.0	0.0
H42-h42	5.9	24	364	-0.276	0.906	0.866	0.0	100	0.0	0.0	0.0
H48-h48	5.9	24	364	-0.236	0.945	0.906	0.0	100	0.0	0.0	0.0
H54-h54	5.9	24	363	-0.276	0.984	0.945	0.0	100	0.0	0.0	0.0
H60-h60	5.9	24	363	-0.276	1.063	1.024	0.0	100	0.0	0.0	0.0
H66-h66	5.9	24	363	-0.394	1.220	1.142	0.0	99.4	0.0	0.0	0.0
H72-h72	5.9	24	363	-0.394	1.299	1.220	0.0	99.7	0.0	0.0	0.0
H78-h78	5.9	24	362	-0.354	1.339	1.299	0.0	99.2	0.0	0.0	0.0
H84-h84	5.9	24	362	-0.394	1.457	1.417	0.0	98.9	0.0	0.0	0.0
H90-h90	5.9	24	362	-0.472	1.614	1.535	0.0	98.6	0.0	0.0	0.0
H96-h96	5.9	24	362	-0.472	1.693	1.654	0.0	98.1	0.0	0.0	0.0
H102-h102	5.9	24	361	-0.472	1.772	1.732	0.0	97.8	0.0	0.0	0.0

H108-h108	5.9	24	361	-0.551	1.890	1.811	0.0	97.5	0.0	0.0	0.0
H114-h114	5.9	24	361	-0.630	2.047	1.929	0.0	96.7	0.0	0.0	0.0
H120-h120	5.9	24	361	-0.591	2.126	2.047	0.0	96.7	0.0	0.0	0.0
Average	5.9	24	363	-0.346	1.205	1.152	0.0	99.1	0.0	0.0	0.0

Table A. 2. Summary of skill assessment statistics evaluating the ability of the Lake Champlain forecast guidance to predict hourly water levels out to 120 hours at the USGS gauge at Port Henry, New York during 2021. Gray shading, if present, indicates that it did not meet the NOS acceptance criteria.

USGS Gauge at Port Henry, NY											
Observed data time period from: 1/ 1/2021 to 12/31/2021											
Variable & Forecast Projection	X (in)	N (hr)	IMAX	MAE (in)	RMSE (in)	SD (in)	NOF <1%	CF >90%	POF <1%	MDNO <N	MDPO <N
H06-h06	5.9	24	365	-0.079	0.472	0.472	0.0	100.0	0.0	0.0	0.0
H12-h12	5.9	24	365	-0.039	0.512	0.512	0.0	100.0	0.0	0.0	0.0
H18-h18	5.9	24	365	-0.157	0.591	0.591	0.0	100.0	0.0	0.0	0.0
H24-h24	5.9	24	365	-0.079	0.591	0.591	0.0	100.0	0.0	0.0	0.0
H30-h30	5.9	24	364	-0.118	0.709	0.709	0.0	100.0	0.0	0.0	0.0
H36-h36	5.9	24	364	-0.079	0.787	0.748	0.0	100.0	0.0	0.0	0.0
H42-h42	5.9	24	364	-0.236	0.906	0.866	0.0	100.0	0.0	0.0	0.0
H48-h48	5.9	24	364	-0.157	0.906	0.906	0.0	100.0	0.0	0.0	0.0
H54-h54	5.9	24	363	-0.197	1.024	1.024	0.0	100.0	0.0	0.0	0.0
H60-h60	5.9	24	363	-0.157	1.102	1.063	0.0	100.0	0.0	0.0	0.0
H66-h66	5.9	24	363	-0.354	1.220	1.142	0.0	100.0	0.0	0.0	0.0
H72-h72	5.9	24	363	-0.276	1.260	1.220	0.0	99.7	0.0	0.0	0.0
H78-h78	5.9	24	362	-0.276	1.378	1.339	0.0	99.4	0.0	0.0	0.0
H84-h84	5.9	24	362	-0.276	1.457	1.457	0.0	99.4	0.0	0.0	0.0
H90-h90	5.9	24	362	-0.472	1.614	1.535	0.0	98.9	0.0	0.0	0.0
H96-h96	5.9	24	362	-0.394	1.693	1.654	0.0	98.3	0.0	0.0	0.0
H102-h102	5.9	24	361	-0.433	1.811	1.732	0.0	97.5	0.0	0.0	0.0
H108-h108	5.9	24	361	-0.394	1.890	1.850	0.0	97.2	0.0	0.0	0.0

H114-h114	5.9	24	361	-0.591	2.008	1.929	0.0	97.2	0.0	0.0	0.0
H120-h120	5.9	24	361	-0.512	2.087	2.008	0.0	97.0	0.0	0.0	0.0
Average	5.9	24	363	-0.264	1.201	1.167	0.0	99.23	0.0	0.0	0.0

Table A. 3. Summary of skill assessment statistics evaluating the ability of the Lake Champlain forecast guidance to predict hourly water levels out to 120 hours at the ECCC gauge at Philipsburg, QC during 2021. Gray shading, if present, indicates that it did not meet the NOS acceptance criteria.

ECCC Gauge at Philipsburg, QC											
Observed data time period from: 1/ 1/2021 to 12/31/2021											
Variable & Forecast Projection	X (in)	N (hr)	IMAX	MAE (in)	RMSE (in)	SD (in)	NOF <1%	CF >90%	POF <1%	MDNO <N	MDPO <N
H06-h06	5.9	24	357	0.354	0.866	0.787	0.0	100.0	0.0	0.0	0.0
H12-h12	5.9	24	356	0.276	0.945	0.906	0.0	100.0	0.3	0.0	0.0
H18-h18	5.9	24	355	0.315	1.102	1.024	0.0	99.7	0.0	0.0	0.0
H24-h24	5.9	24	355	0.276	0.945	0.906	0.0	100.0	0.0	0.0	0.0
H30-h30	5.9	24	356	0.276	0.984	0.945	0.0	100.0	0.0	0.0	0.0
H36-h36	5.9	24	355	0.315	1.102	1.063	0.0	99.4	0.0	0.0	0.0
H42-h42	5.9	24	354	0.315	1.339	1.299	0.0	99.4	0.0	0.0	0.0
H48-h48	5.9	24	354	0.236	1.260	1.220	0.0	99.4	0.0	0.0	0.0
H54-h54	5.9	24	355	0.276	1.299	1.260	0.0	99.7	0.0	0.0	0.0
H60-h60	5.9	24	354	0.276	1.496	1.496	0.0	99.4	0.0	0.0	0.0
H66-h66	5.9	24	353	0.354	1.654	1.654	0.0	98.6	0.0	0.0	0.0
H72-h72	5.9	24	353	0.276	1.575	1.575	0.0	99.4	0.0	0.0	0.0
H78-h78	5.9	24	354	0.197	1.535	1.535	0.0	100.0	0.0	0.0	0.0
H84-h84	5.9	24	353	0.197	1.732	1.732	0.0	99.2	0.0	0.0	0.0
H90-h90	5.9	24	352	0.236	1.890	1.890	0.0	98.0	0.3	0.0	0.0
H96-h96	5.9	24	352	0.157	1.890	1.890	0.0	98.0	0.0	0.0	0.0
H102-h102	5.9	24	353	0.157	2.087	2.087	0.0	97.7	0.0	0.0	0.0
H108-h108	5.9	24	352	0.157	2.008	2.008	0.0	98.0	0.0	0.0	0.0

H114-h114	5.9	24	351	0.276	2.323	2.323	0.0	96.3	0.3	0.0	0.0
H120-h120	5.9	24	351	0.118	2.283	2.283	0.0	96.9	0.0	0.0	0.0
Average	5.9	24	354	0.252	1.516	1.494	0.0	98.96	0.0	0.0	0.0

Table A. 4. Summary of skill assessment statistics evaluating the ability of the Lake Champlain forecast guidance to predict hourly water levels out to 120 hours at the USGS gauge at Rouses Point, NY during 2021. Gray shading, if present, indicates that it did not meet the NOS acceptance criteria.

USGS Gauge at Rouses Point, NY											
Observed data time period from: 1/ 1/2021 to 12/31/2021											
Variable & Forecast Projection	X (in)	N (hr)	IMAX	MAE (in)	RMSE (in)	SD (in)	NOF <1%	CF >90%	POF <1%	MDNO <N	MDPO <N
H06-h06	5.9	24	365	-0.512	0.827	0.669	0.0	100.0	0.0	0.0	0.0
H12-h12	5.9	24	365	-0.551	0.906	0.709	0.0	100.0	0.0	0.0	0.0
H18-h18	5.9	24	365	-0.512	0.945	0.787	0.0	100.0	0.0	0.0	0.0
H24-h24	5.9	24	365	-0.551	0.906	0.748	0.0	100.0	0.0	0.0	0.0
H30-h30	5.9	24	364	-0.551	0.945	0.748	0.0	100.0	0.0	0.0	0.0
H36-h36	5.9	24	364	-0.591	1.024	0.866	0.0	100.0	0.0	0.0	0.0
H42-h42	5.9	24	364	-0.551	1.142	1.024	0.0	100.0	0.0	0.0	0.0
H48-h48	5.9	24	364	-0.591	1.142	0.984	0.0	100.0	0.0	0.0	0.0
H54-h54	5.9	24	363	-0.630	1.220	1.063	0.0	100.0	0.0	0.0	0.0
H60-h60	5.9	24	363	-0.709	1.378	1.181	0.0	99.7	0.0	0.0	0.0
H66-h66	5.9	24	363	-0.630	1.378	1.220	0.0	99.7	0.0	0.0	0.0
H72-h72	5.9	24	363	-0.630	1.417	1.299	0.0	99.7	0.0	0.0	0.0
H78-h78	5.9	24	362	-0.748	1.614	1.417	0.0	99.2	0.0	0.0	0.0
H84-h84	5.9	24	362	-0.787	1.693	1.496	0.0	99.2	0.0	0.0	0.0

H90-h90	5.9	24	362	-0.748	1.732	1.535	0.0	98.9	0.0	0.0	0.0
H96-h96	5.9	24	362	-0.748	1.772	1.575	0.0	98.3	0.0	0.0	0.0
H102-h102	5.9	24	361	-0.866	1.929	1.732	0.0	98.1	0.0	0.0	0.0
H108-h108	5.9	24	361	-0.906	2.126	1.890	0.0	97.0	0.0	0.0	0.0
H114-h114	5.9	24	361	-0.827	2.165	2.008	0.0	96.7	0.0	0.0	0.0
H120-h120	5.9	24	361	-0.866	2.165	2.008	0.0	96.1	0.0	0.0	0.0
Average	5.9	24	363	-0.675	1.421	1.248	0.0	99.13	0.0	0.0	0.0

Table A. 5. Summary of skill assessment statistics evaluating the ability of the Lake Champlain forecast guidance to predict hourly water levels out to 120 hours at the USGS gauge at Whitehall, NY during 2021. Gray shading, if present, indicates that it did not meet the NOS acceptance criteria.

USGS Gauge at Whitehall, NY											
Observed data time period from: 1/ 1/2021 to 12/31/2021											
Variable & Forecast Projection	X (in)	N (hr)	IMAX	MAE (in)	RMSE (in)	SD (in)	NOF <1%	CF >90%	POF <1%	MDNO <N	MDPO <N
H06-h06	5.9	24	365	0.315	1.850	1.811	0.0	99.7	0.0	0.0	0.0
H12-h12	5.9	24	365	0.236	1.890	1.890	0.0	100.0	0.0	0.0	0.0
H18-h18	5.9	24	365	0.197	2.087	2.087	0.0	100.0	0.0	0.0	0.0
H24-h24	5.9	24	365	-0.079	2.165	2.165	0.0	99.2	0.0	0.0	0.0
H30-h30	5.9	24	364	0.236	2.008	2.008	0.0	99.5	0.0	0.0	0.0
H36-h36	5.9	24	364	0.197	2.087	2.087	0.0	99.2	0.0	0.0	0.0
H42-h42	5.9	24	364	0.118	2.323	2.323	0.3	98.6	0.0	0.0	0.0
H48-h48	5.9	24	364	-0.079	2.441	2.441	0.0	97.8	0.0	0.0	0.0
H54-h54	5.9	24	363	0.118	2.205	2.205	0.0	99.4	0.0	0.0	0.0
H60-h60	5.9	24	363	0.118	2.323	2.323	0.0	99.2	0.0	0.0	0.0
H66-h66	5.9	24	363	-0.118	2.480	2.520	0.0	98.9	0.0	0.0	0.0
H72-h72	5.9	24	363	-0.315	2.638	2.638	0.0	97.0	0.0	0.0	0.0
H78-h78	5.9	24	362	-0.039	2.441	2.441	0.0	97.2	0.0	0.0	0.0
H84-h84	5.9	24	362	0.039	2.520	2.520	0.0	97.0	0.0	0.0	0.0
H90-h90	5.9	24	362	-0.236	2.795	2.756	0.0	95.3	0.0	0.0	0.0
H96-h96	5.9	24	362	-0.394	2.992	2.953	0.0	93.4	0.0	0.0	0.0
H102-h102	5.9	24	361	-0.157	2.756	2.756	0.0	95.0	0.0	0.0	0.0

H108-h108	5.9	24	361	-0.157	2.953	2.953	0.0	94.7	0.0	0.0	0.0
H114-h114	5.9	24	361	-0.394	3.110	3.071	0.0	94.5	0.0	0.0	0.0
H120-h120	5.9	24	361	-0.551	3.268	3.228	0.0	92.8	0.0	0.0	0.0
Average	5.9	24	363	-0.047	2.467	2.459	0.0	97.42	0.0	0.0	0.0